
Tectônica e metamorfismo
Renato de Moraes
rmoraes@usp.br
GMG-0332
GEOCIÊNCIAS
USP

1

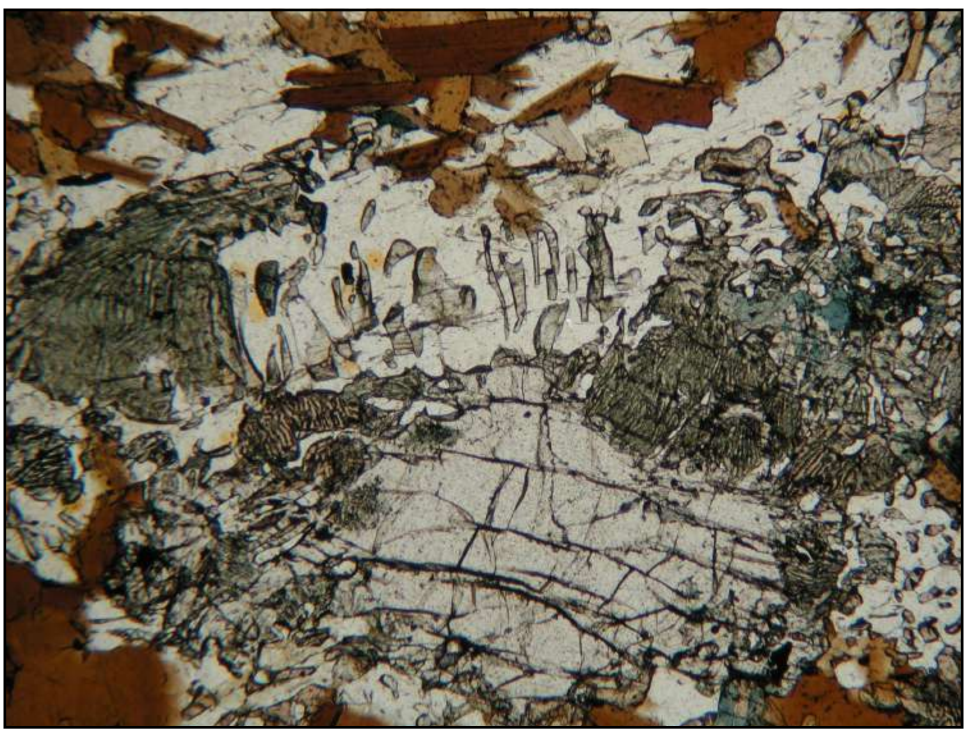

2

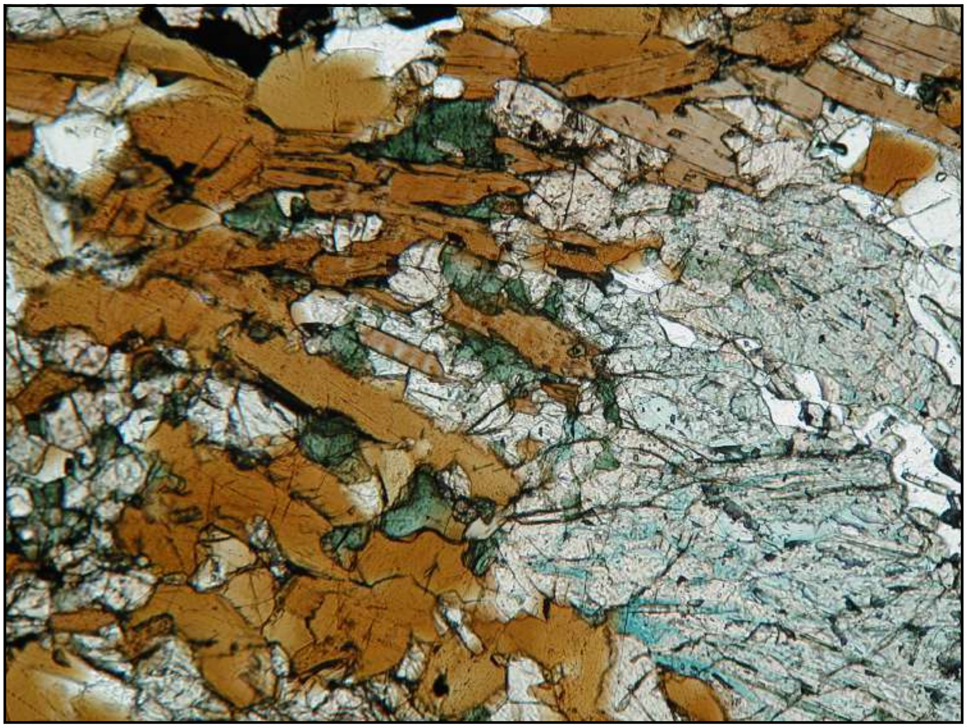

3

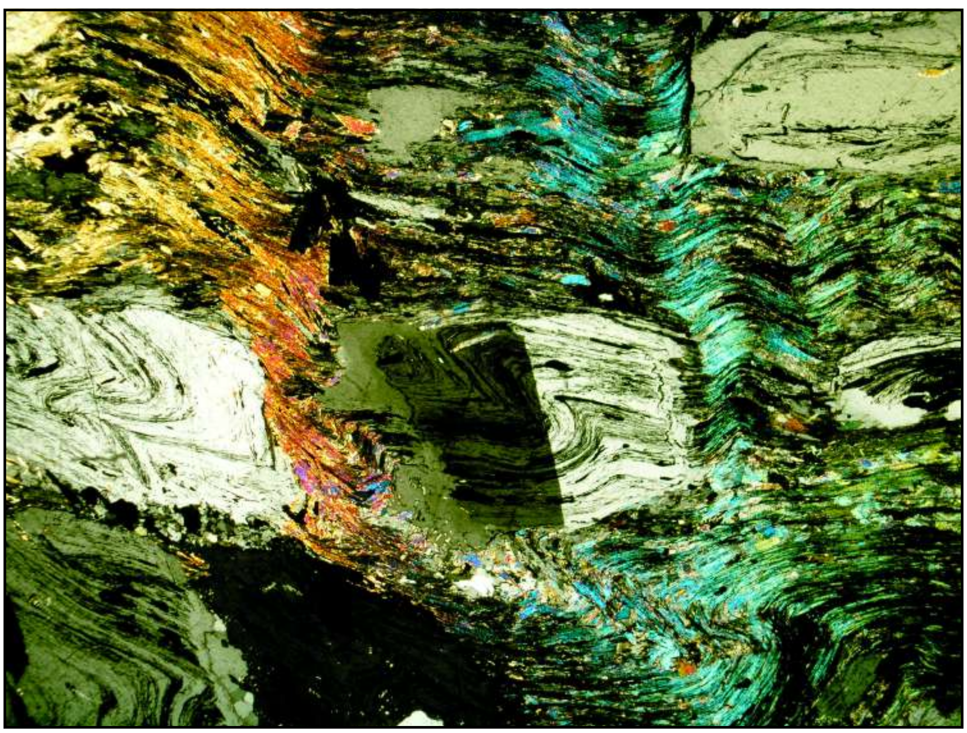

4

5

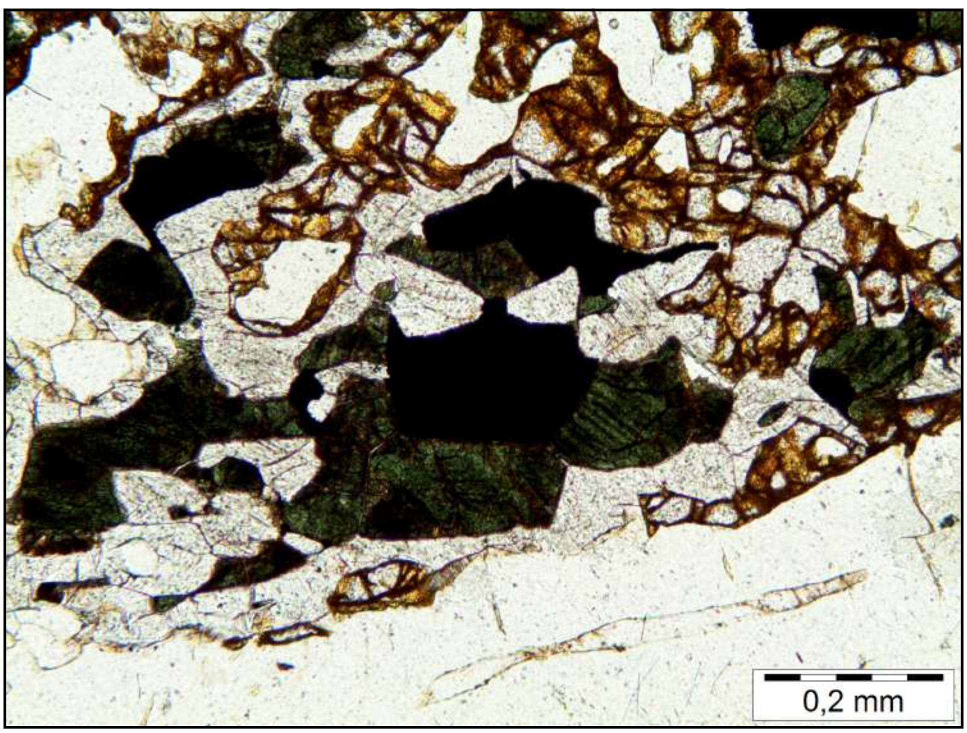

6

7

8

9

Metamorfismo

- Metamorfismo é o conjunto de transformações no estado sólido (mineralógicas e texturais) que as rochas sofrem (ou apreciam) em virtude de mudanças, principalmente, de temperatura e pressão, da composição e quantidade de fluidos e mudança no regime de esforços a que são submetidas após sua formação

10

Perguntas que temos que responder

- Por que ocorre metamorfismo?
- O que controla o metamorfismo?
- O que são trajetórias *P*-*T*-t?
- Em quais ambientes tectônicos ocorre metamorfismo?
  - O metamorfismo é igual em todos ambientes (regimes e trajetórias *P*-*T*-t)?
- Muitas rochas metamórficas são formadas em diversas profundidades. Como elas afloram na superfície do planeta?
- E as rochas de metamorfismo extremo, granulitos e eclogitos, quais são as fontes de calor e como funciona sua exumação?

11

Por que ocorre metamorfismo?

- Metamorfismo é a resposta que as rochas dão à perturbação da geoterma crustal e também à profundidade em que são soterradas (tectonicamente)
- A geoterma continental é perturbada durante a colisão continental, formação de arco magmático ou em *rifts*
- A geoterma oceânica é perturbada nas cadeias oceânicas e em zonas de subducção

12

Fácies e série de fácies

A escala é em GPa

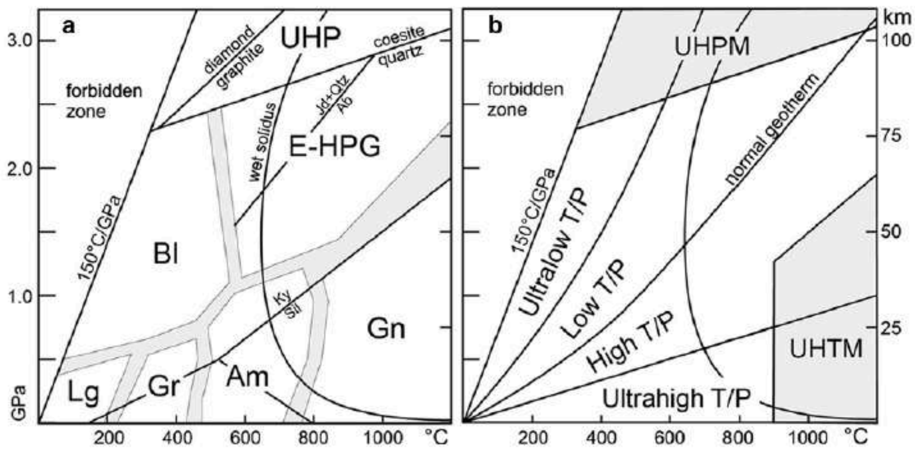

Brown, 2014, Geosciences Frontiers

13

Trajetórias *P-T*-t e gradiente metamórfico de campo

- Trajetória *P-T*-t define o caminho no espaço *P-T* que a rocha traçou dentro da litosfera em relação ao tempo
- Isso nos dá ideia do soterramento, aquecimento, resfriamento e exumação da rocha
- O gradiente metamórfico de campo é a linha definida em campo pelo pico metamófico de rochas de uma coluna metamorfizada em um único evento e indica a série de fácies

Turner, 1981

14

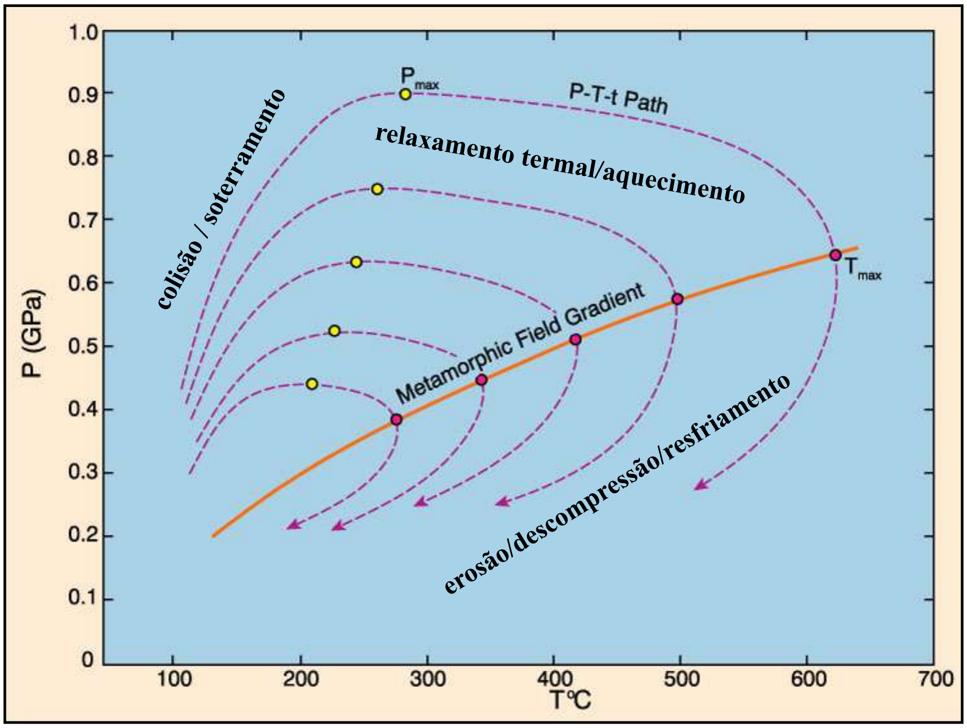

15

gradiente metamórfico de campo indica o tipo de
Série de Fácies (ou tipo bárico) do cinturão metamórfico

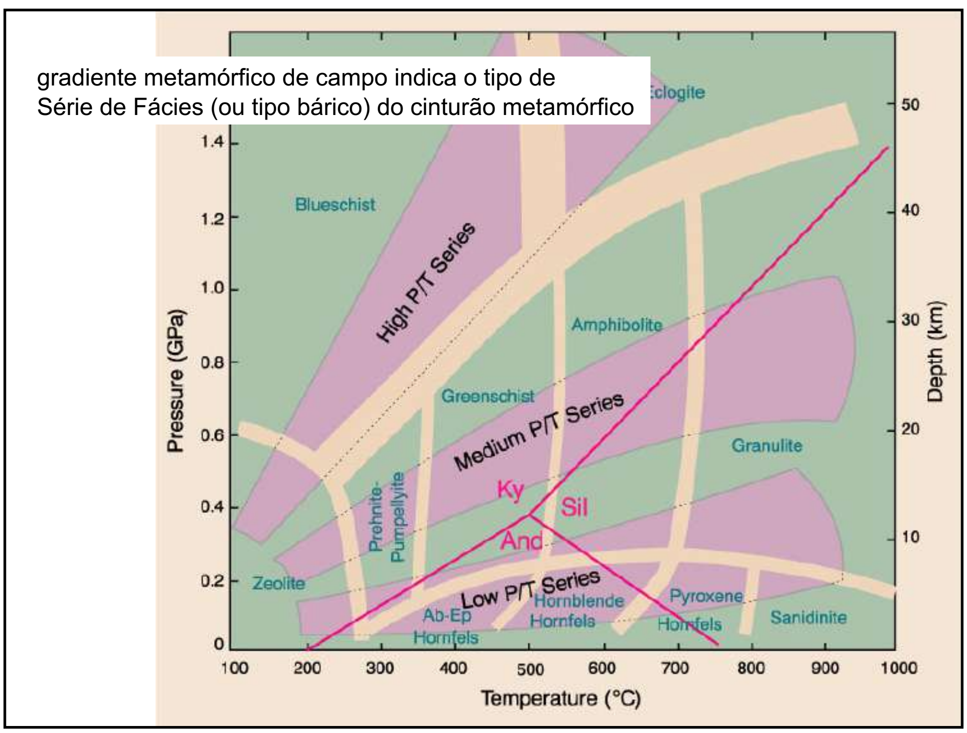

16

Agentes físicos do metamorfismo

- **Temperatura**
- **Pressão**
- Deformação
- Fluidos
- Composição da rocha

17

Por que ocorre metamorfismo?

- Para sabermos porque ocorre metamorfismo, precisamos entender como as duas variáveis intensivas mais importantes para o metamorfismo, *P* e *T*, são controladas tectonicamente
- Precisamos entender:
  - a relação *P vs*. profundidade*, e;
  - o que controla a produção de calor e sua relação com a *T*
  - (ou como as rochas são aquecidas e resfriadas)
  - (ou como as rochas são soterradas e exumadas)

18

Pressão

- Pressão é a segunda variável intensiva mais importante do metamorfismo. Proveniente do peso da coluna de rochas sobrejacente à rocha que esta sendo metamorfizada. Depende da massa e da densidade média das rochas da porção da crosta envolvida

- *P* em kbar ou GPa
- 1 baria = 10^5 Pa
- 1 kbar = 0,1 GPa

19

P em coluna de 1 km (1000m)

rocha	*P* em bars	*P* em kbar
granito	264	0,264
basalto	294	0,294
peridotito	323	0,323

20

Para atingir 1 kbar de *P*

H_2O mar (fossa das Filipinas)	9 – 10 km
rocha	profundidade
granito	3,8 km
basalto	3,4 km
peridotito	3,1 km

21

Pressão *vs* profundidade

Crosta oceânica	5 – 10 km	1,5 a 3 kbar
Crosta continental	35 – 40 km	10 kbar
orógenos	70 – 80 km	20 kbar

Algumas rochas crustais com coesita e diamante indicam *P* > 35 kbar, ~ 120 km ou mais de profundidade (não de espessura crustal)

22

Conclusões sobre *P*

- Basicamente a *P* é uma função da profundidade e da média da densidade da coluna de rochas
- Quanto maior a profundidade da rocha na crosta (ou no manto), durante o metamorfismo, maior será a *P* experimentada pela mesma
- As rochas, na maior parte dos ambientes tectonicamente ativos, são soterradas tectonicamente
- No entanto, a *P* do pico metamórfico (como será visto) não é a *P* máxima que a rocha alcançou

23

Estrutura Termal da Litosfera

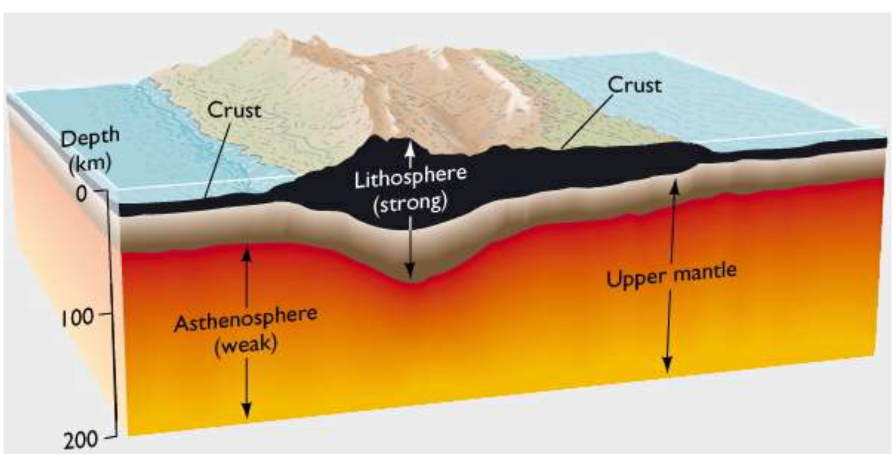

24

Estrutura Termal da Litosfera

- Definição termal da Litosfera
  - A litosfera pode ser definida de forma termal como a camada externa da Terra onde o calor é transportado primariamente por condução
- A litosfera perde calor pela superfície que é dissipado para o espaço por radiação
- Litosfera termalmente estabilizada tem espessura entre 100 e 200 km e apresenta perfil termal (geoterma) estável
- A base da litosfera intersecta a isoterma de ~ 1250 ou 1300 ºC (acima dessas temperaturas o manto começa a fluir – **astenosfera**
- Qual a temperatura na base da crosta continental?

25

Geoterma

- Linha (ou superfície) que descreve a variação de *T* com a profundidade (ou *P*) na Terra
- De onde vem o calor?

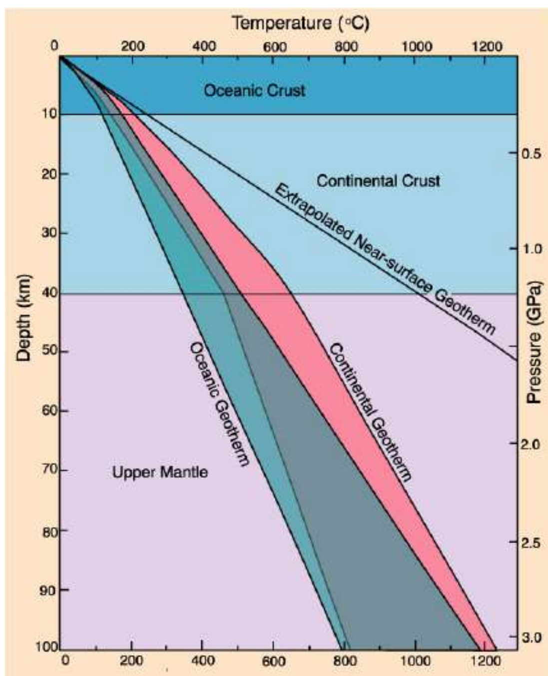

26

De onde vem o calor?

- Radioatividade (60 a 80%)
  - elementos produtores de calor estão concentrados na porção superior da crosta continental e suas concentrações diminuem exponencialmente com a profundidade
- Manto superior transmite calor para a crosta (20 a 40%)

Outros contribuidores

- Astenosfera (pode ter papel muito importante)
- Algumas reações retrometamórficas são exotérmicas
- Calor mecânico (falhas)

27

Tipos de Geoterma

- Geoterma estável (*steady state*) – é formada quando o equilíbrio termal na litosfera é longo (> 100 Ma)
- Geoterma transitória – ocorre em intervalo de tempo determinado (restrito)
- Geoterma perturbada – também é transitória, mas aqui diz respeito à configuração alcançada durante a orogênese

28

Geoterma perturbada

- Quando a geoterma é perturbada ocorre metamorfismo em resposta a variação de *T*
- Para perturbar a geoterma é necessário, de alguma maneira, aumentar o fluxo de calor

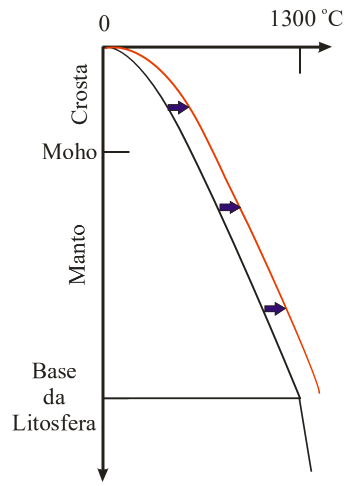

29

Ambientes tectônicos e metamorfismo

- Zonas de subducção – baixa d*T*/d*P*
- Arcos de ilha – alta d*T*/d*P*
- Colisão continental – taxa d*T*/d*P* variável

30

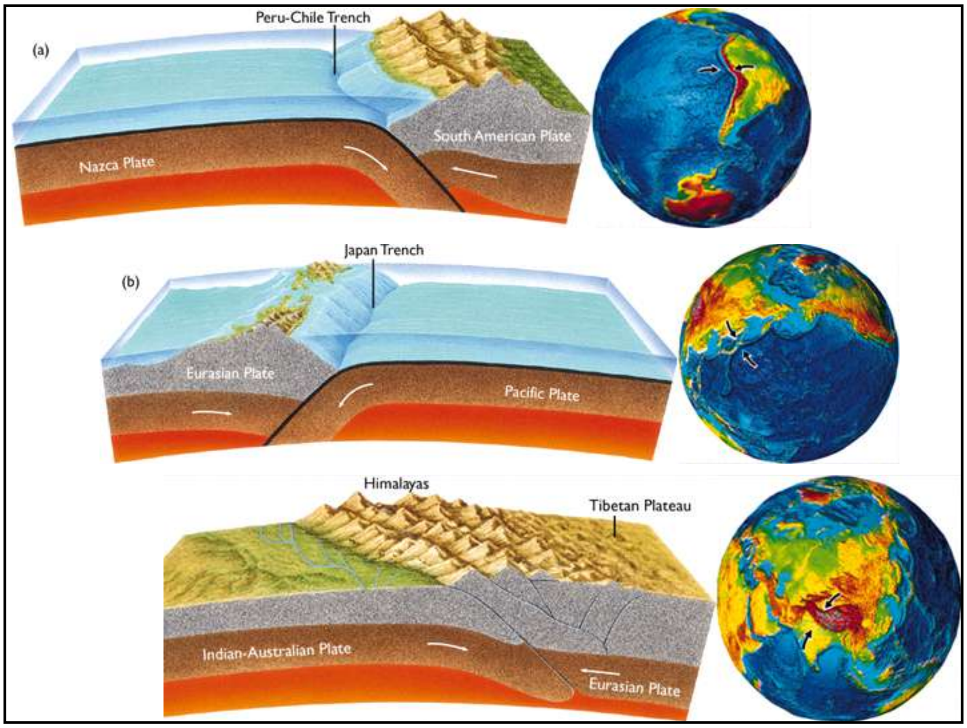

31

Arcos de ilha e zonas de subducção

- Arcos de ilha são formados atrás das zonas de subducção
- Alto fluxo de calor com regimes de pressão relativamente baixos – isotermas são comprimidas
- Comum série de fácies com And-Sil
- Metamorfismo tipo Rioke, Abukuma
  - xisto verde
  - anfibolito (rochas com pouca ou sem Grt e abundante Crd + Sil
  - granulito (fusão em baixa *P*)

32

Evolution of Metamorphic Belts

by AKIHO MIYASHIRO

Geological Institute, Faculty of Science, University of Tokyo, Japan

ABSTRACT

The metamorphic facies series in regional metamorphism may be classified into the following categories according to an order of increasing rock pressure: (1) andalusite–sillimanite type, (2) low-pressure intermediate group, (3) kyanite–sillimanite type, (4) high-pressure intermediate group, and (5) jadeite–glaucophane type.

In Japan and other parts of the circum-Pacific region, a metamorphic belt of the andalusite–sillimanite type and/or low-pressure intermediate group and another metamorphic belt of the jadeite–glaucophane type and/or high-pressure intermediate group run side by side, forming a pair. The latter belt is always on the Pacific Ocean side. They were probably formed in different phases of the same cycle of orogeny. Their origin is discussed.

Regional metamorphism under higher rock pressures appears to have taken place in later geological times.

The metamorphic facies series of contact metamorphism are briefly discussed.

[Journal of Petrology, Vol. 2, Part 3, pp. 277–311, 1961]

0233.8

33

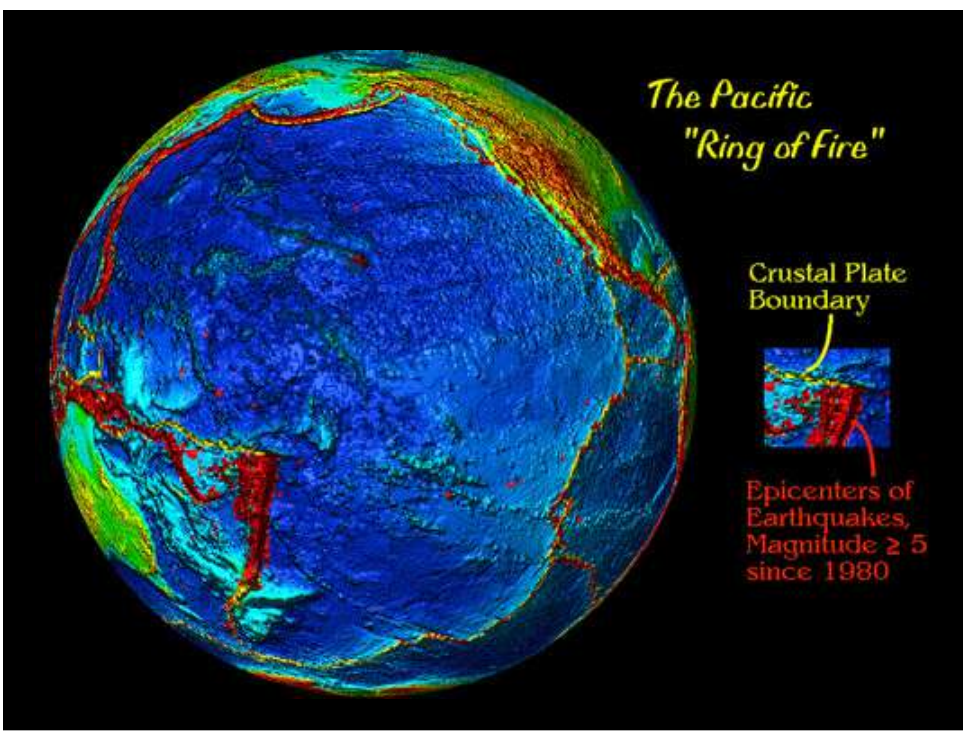

34

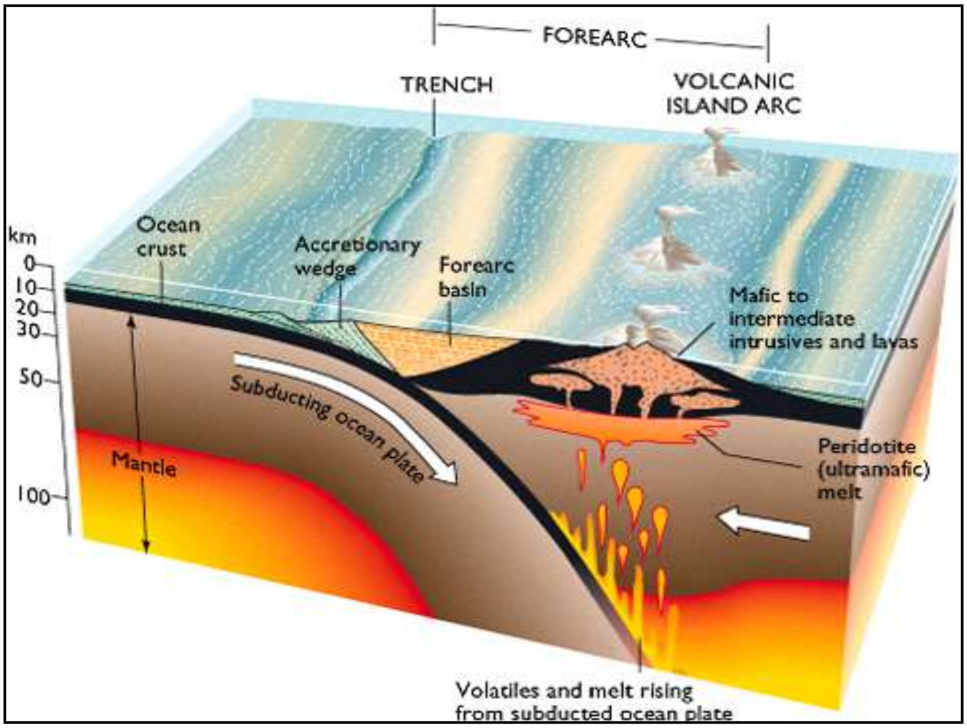

35

Séries de Fácies Metamórficas

- Miyashiro (1961) reconheceu duas séries de fácies metamórficas que eram diferentes das propostas por Barrow
  - zeólita / prehnita-pumpellyita / xisto azul / eclogito
  - xisto verde / anfibolito com And – Sil
- Cinturões metamórficos emparelhados
- Identificou 3 séries de fácies
  - razão *P/T* alta – glaucofano – jadeíta
  - razão *P/T* intermediária – Ky – Sil (barroviano)
  - razão *P/T* baixa – And – Sil

36

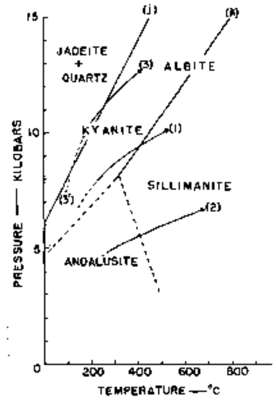

Fig. 4. Stability relations of andalusite, kyanite, and sillimanite and of the jadeite–quartz assemblage and albite. The solid lines (*k*) and (*j*) represent the experimentally determined equilibrium curves for the kyanite–sillimanite transformation, and for the reaction jadeite + quartz = albite, respectively. The arrows (1), (2), and (3) represent typical temperature/rock-pressure relations in regional metamorphism of the kyanite–sillimanite type, andalusite–sillimanite type, and jadeite–glaucophane type, respectively.

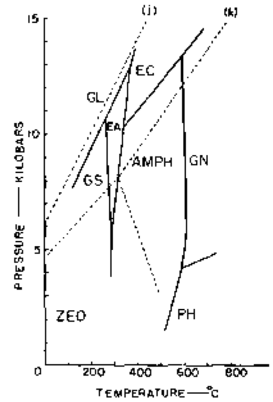

Fig. 5. Estimated temperatures and rock pressures of metamorphic facies. The solid lines (*k*) and (*j*) correspond to those of Fig. 4. GL, glaucophane-schist facies; EC, eclogite facies; GS, greenschist facies, EA, epidote-amphibolite facies; AMPH, amphibolite facies; GN, granulite facies; PH, pyroxene-hornfels facies; ZEO, zeolite facies.

37

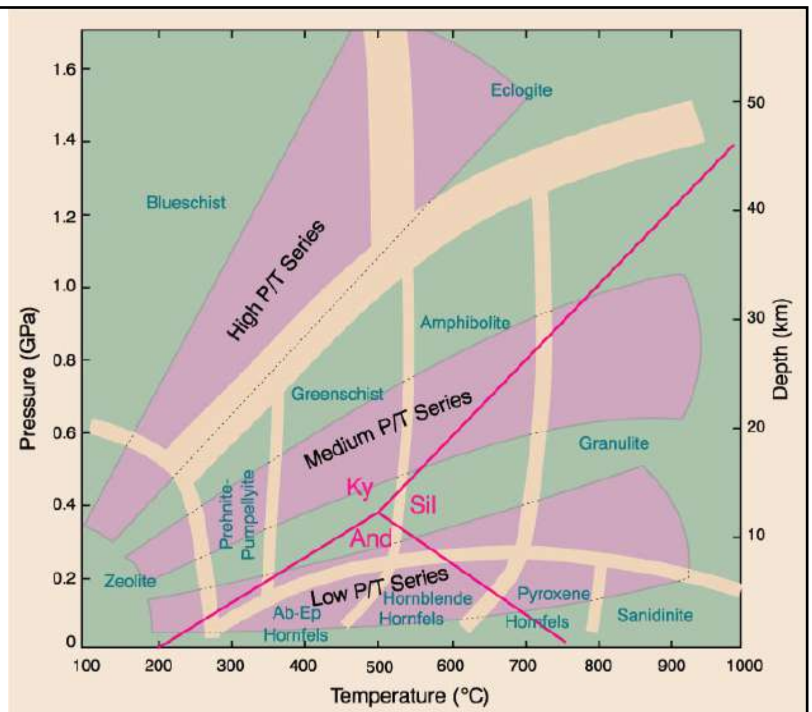

38

Cinturões Metamórficos Emparelhados

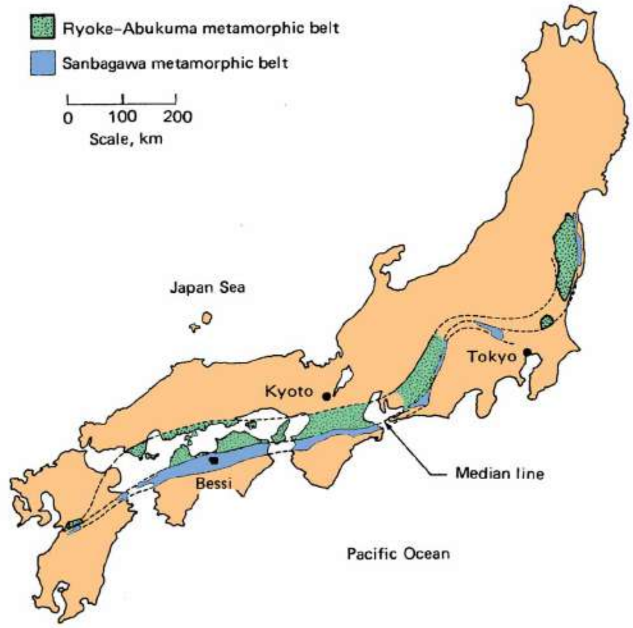

39

Séries de Fácies e Ambientes Tectônicos

- Ambientes colisionais – arcos de ilha e zonas de colisão continental
- Arcos de Ilha - repressão das isotermas em virtude da placa frio descendente e alçamento das mesmas na zona de arco magmático
- Cinturões Metamórficos Emparelhados
  - razão *P/T* alta – glaucofana-jadeita (zona de subducção)
  - razão *P/T* baixa – And-Sil (arcos de ilha)

40

Xisto azul e eclogito

- Rochas típicas de subducção
- As subfáceis dependem da velocidade de subducção e da idade da placa subductada
  - placa antiga – fria – subducção fria ou rápida
    - paragêneses "frias"
  - placa nova – quente – subducção quente ou lenta
    - paragêneses "quentes"

41

JOURNAL OF GEOPHYSICAL RESEARCH, VOL. 108, NO. B1, 2029, doi:10.1029/2001JB001127, 2003

Subduction factory
1. Theoretical mineralogy, densities, seismic wave speeds, and H_2O contents

Bradley R. Hacker
Department of Geological Sciences, University of California, Santa Barbara, California, USA

Geoffrey A. Abers
Department of Earth Sciences, Boston University, Boston, Massachusetts, USA

Simon M. Peacock
Department of Geological Sciences, Arizona State University, Tempe, Arizona, USA

Received 27 August 2001; revised 11 June 2002; accepted 18 July 2002; published 18 January 2003.

[1] We present a new compilation of physical properties of minerals relevant to subduction zones and new phase diagrams for mid-ocean ridge basalt, lherzolite, depleted lherzolite, harzburgite, and serpentinite. We use these data to calculate H_2O content, density and seismic wave speeds of subduction zone rocks. These calculations provide a new basis for evaluating the subduction factory, including (1) the presence of hydrous phases and the distribution of H_2O within a subduction zone; (2) the densification of the subducting slab and resultant effects on measured gravity and slab shape; and (3) the variations in seismic wave speeds resulting from thermal and metamorphic processes at depth. In considering specific examples, we find that for ocean basins worldwide the lower oceanic crust is partially hydrated (<1.3 wt % H_2O), and the uppermost mantle ranges from unhydrated to ~20% serpentinized (~2.4 wt % H_2O). Anhydrous eclogite cannot be distinguished from harzburgite on the basis of wave speeds, but its ~6% greater density may render it detectable through gravity measurements. Subducted hydrous crust in cold slabs can persist to several gigapascals at seismic velocities that are several percent slower than the surrounding mantle. Seismic velocities and V_P/V_S ratios indicate that mantle wedges locally reach 60–80% hydration. *INDEX TERMS:* 3040 Marine Geology and Geophysics: Plate tectonics (8150, 8155, 8157, 8158); 3660 Mineralogy and Petrology: Metamorphic petrology; 3919 Mineral Physics: Equations of state; 5199 Physical Properties of Rocks: General or miscellaneous; 8123 Tectonophysics: Dynamics, seismotectonics; *KEYWORDS:* subduction, seismic velocities, mineral physics, H_2O

Citation: Hacker, B. R., G. A. Abers, and S. M. Peacock, Subduction factory, 1. Theoretical mineralogy, densities, seismic wave speeds, and H_2O contents, *J. Geophys. Res.*, *108*(B1), 2029, doi:10.1029/2001JB001127, 2003.

42

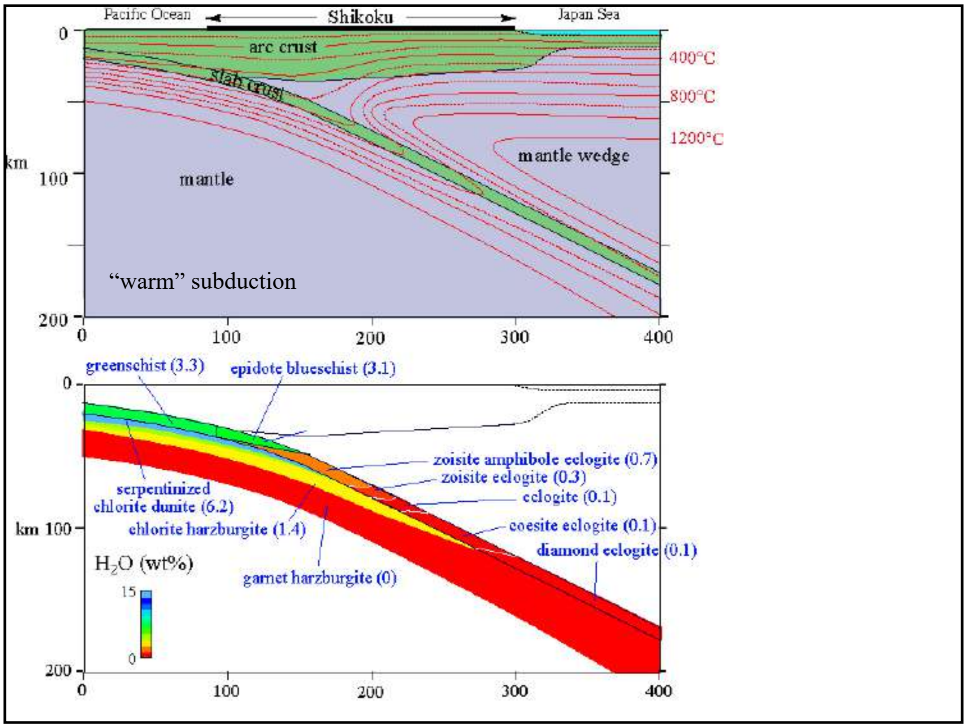
Pacific Ocean
Shikoku
Japan Sea
arc crust
slab crust
400°C
800°C
1200°C
mantle wedge
mantle
km
"warm" subduction
0
100
200
300
400
greenschist (3.3)
epidote blueschist (3.1)
zoisite amphibole eclogite (0.7)
zoisite eclogite (0.3)
eclogite (0.1)
serpentinized chlorite dunite (6.2)
chlorite harzburgite (1.4)
coesite eclogite (0.1)
diamond eclogite (0.1)
garnet harzburgite (0)
H_2O (wt%)
15
0

43

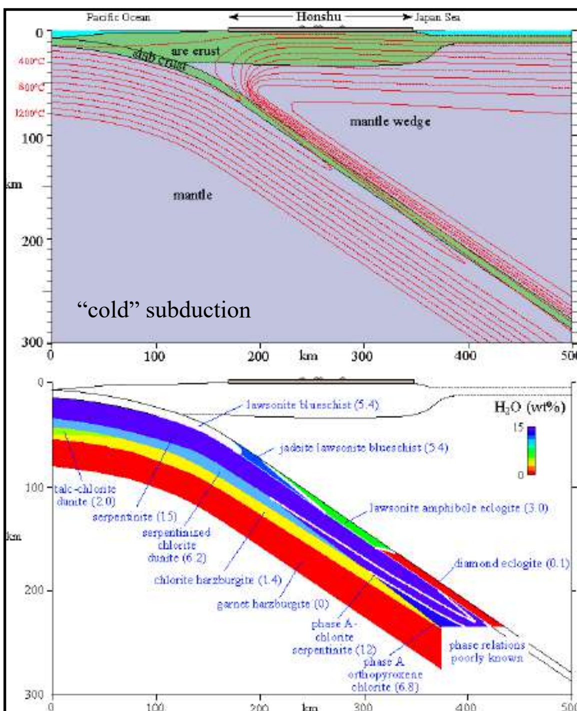
Pacific Ocean
Honshu
Japan Sea
arc crust
slab crust
400°C
800°C
1200°C
mantle wedge
mantle
km
"cold" subduction
0
100
200
300
400
500
lawsonite blueschist (5.4)
jadeite lawsonite blueschist (5.4)
H_2O (wt%)
talc-chlorite dunite (2.0)
serpentinite (15)
serpentinized chlorite dunite (6.2)
lawsonite amphibole eclogite (3.0)
diamond eclogite (0.1)
chlorite harzburgite (1.4)
garnet harzburgite (0)
phase A-chlorite serpentinite (12)
phase A orthopyroxene chlorite (6.8)
phase relations poorly known

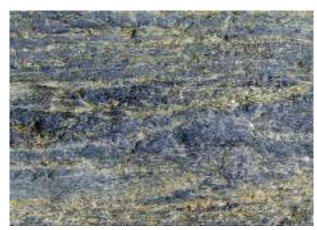

44

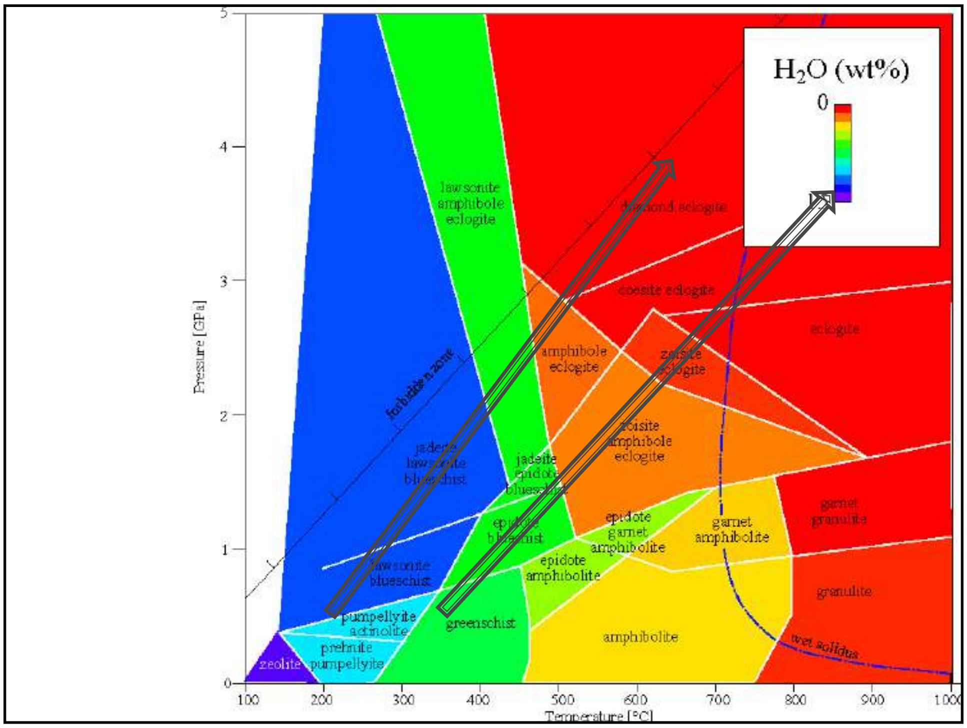
H2O (wt%)
0
lawsonite amphibole eclogite
diamond eclogite
coesite eclogite
eclogite
amphibole eclogite
zoisite eclogite
zoisite amphibole eclogite
forbidden zone
jadeite lawsonite blueschist
jadeite epidote blueschist
epidote blueschist
epidote garnet amphibolite
garnet amphibolite
garnet granulite
lawsonite blueschist
epidote amphibolite
granulite
pumpellyite actinolite
greenschist
amphibolite
wet solidus
prehnite pumpellyite
zeolite
Pressure [GPa]
Temperature [°C]

45

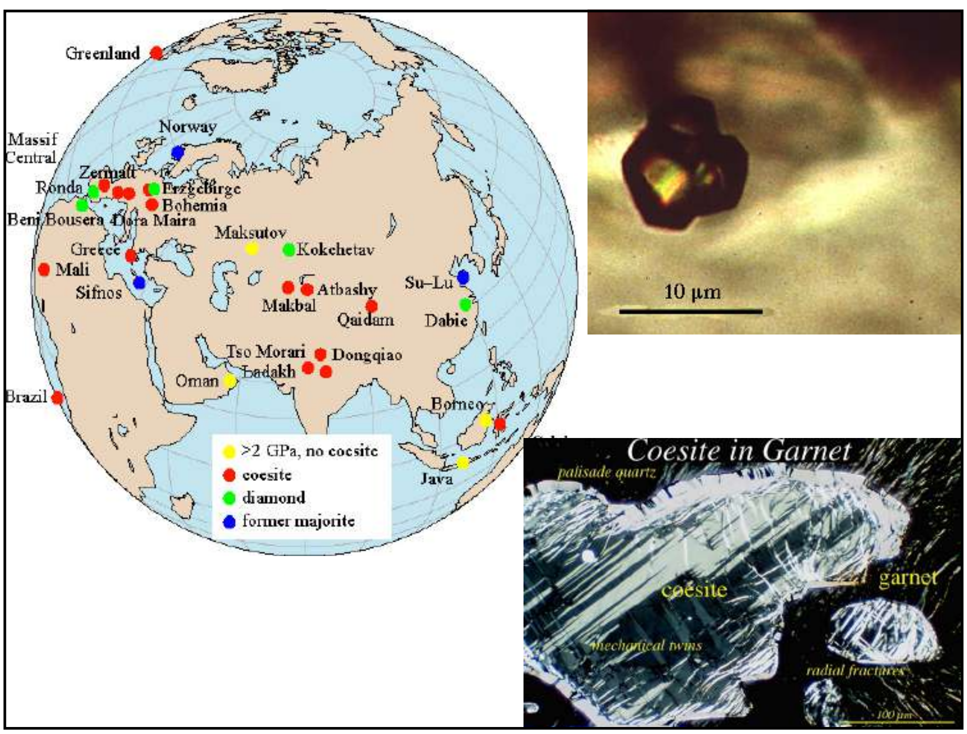
Greenland
Norway
Massif Central
Zermatt
Ronda
Erzgebirge
Bohemia
Beni Bousera
Dora Maira
Maksutov
Kokchetav
Greece
Mali
Sifnos
Atbashy
Makbal
Su-Lu
Qaidam
Dabie
Tso Morari
Dongqiao
Ladakh
Oman
Brazil
Borneo
Java
>2 GPa, no coesite
coesite
diamond
former majorite
10 μm
Coesite in Garnet
palisade quartz
coesite
garnet
mechanical twins
radial fractures

46

Slab break-off

- Evolução e conseqüências semelhantes às que ocorrem com delaminação do manto litosférico

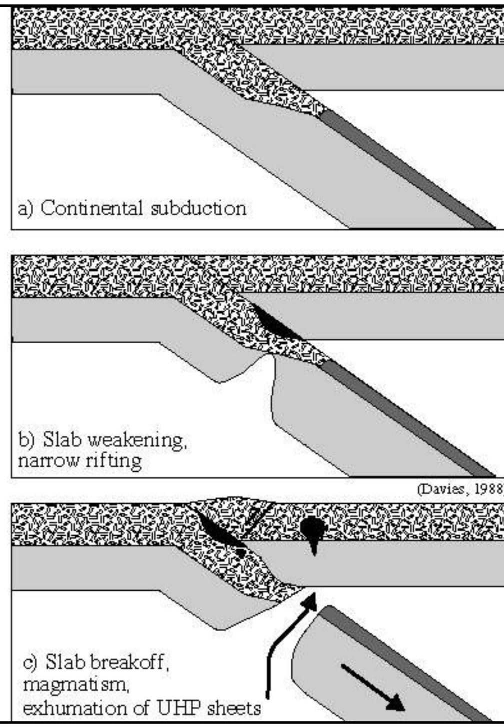

47

Break-off

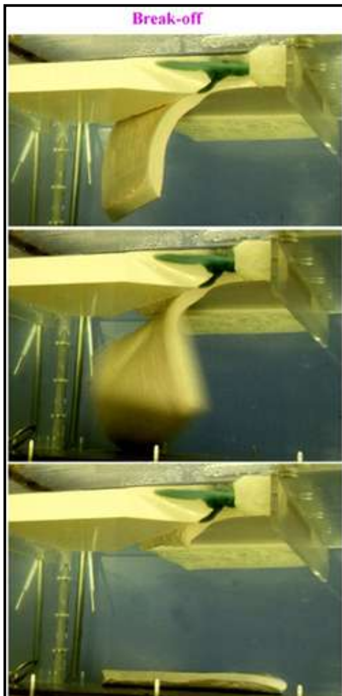

(Chemenda et al.,2000b)

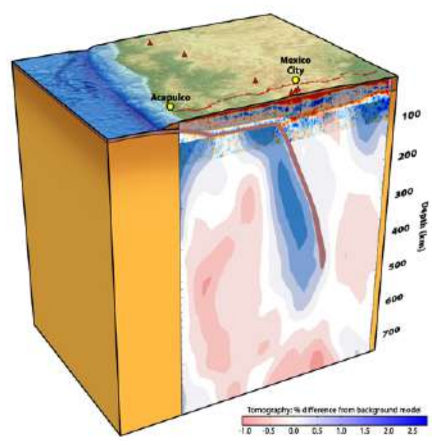

48

Multiple-scale models of slab breakoff and UHP rocks exhumation

Gerya, T.V. (unpublishednumericalresults)

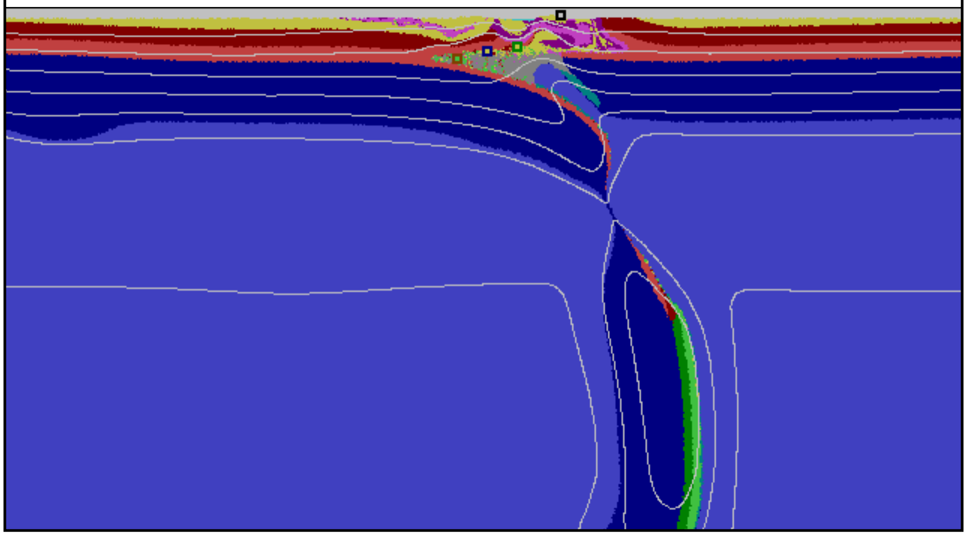

49

Animation 1 "No weak zone"

50

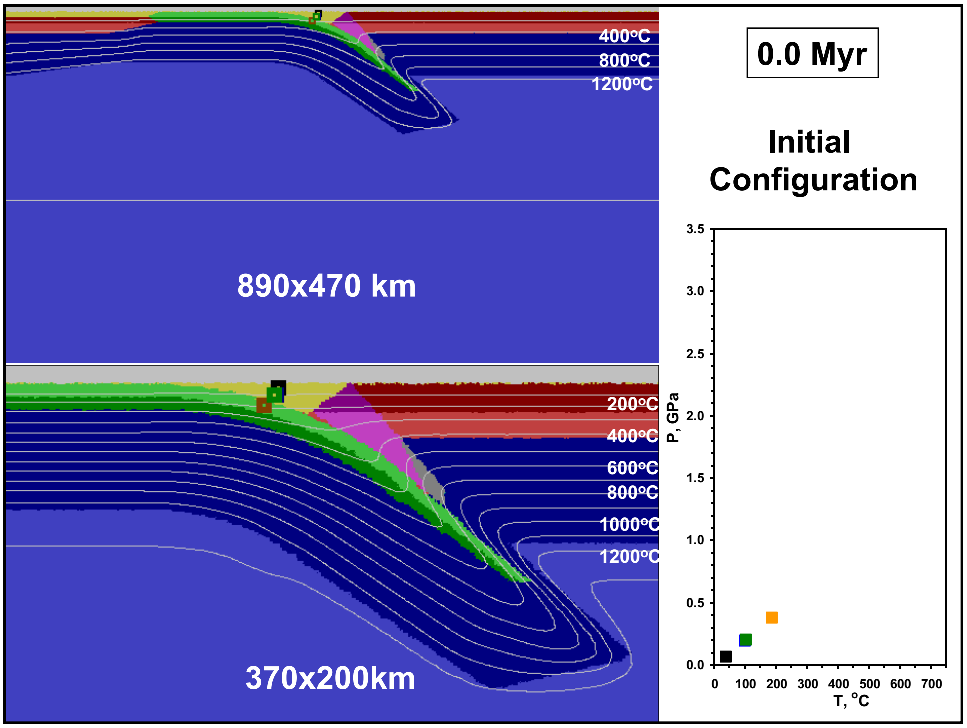

400ºC
800ºC
1200ºC
0.0 Myr
Initial Configuration
890x470 km
200ºC
400ºC
600ºC
800ºC
1000ºC
1200ºC
370x200km
P, GPa
T, °C

51

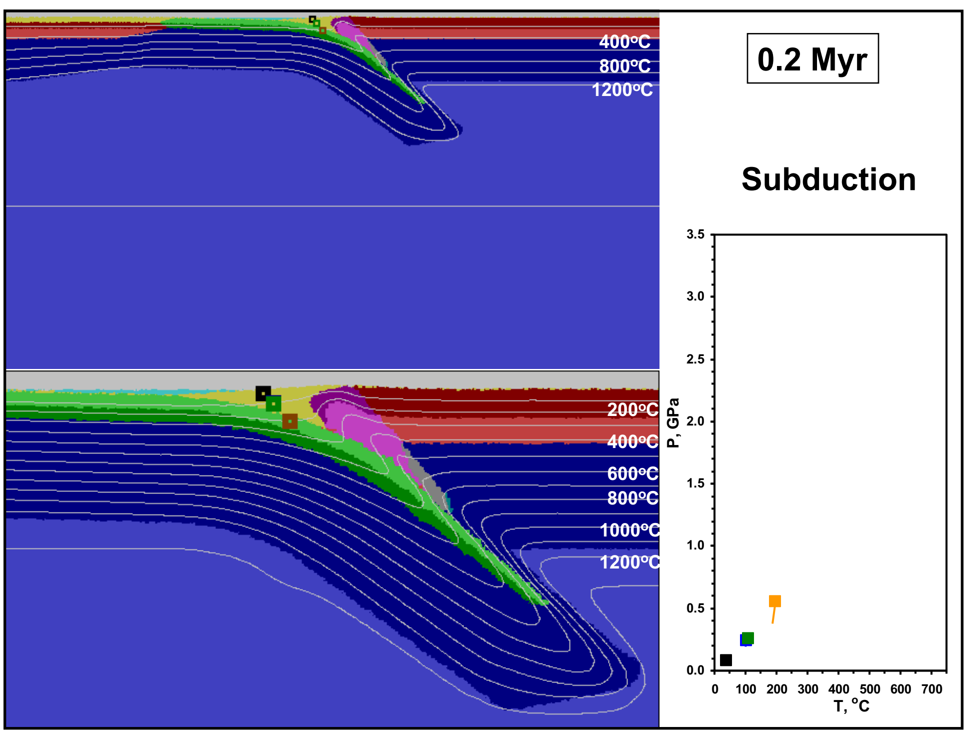

400ºC
800ºC
1200ºC
0.2 Myr
Subduction
200ºC
400ºC
600ºC
800ºC
1000ºC
1200ºC
P, GPa
T, °C

52

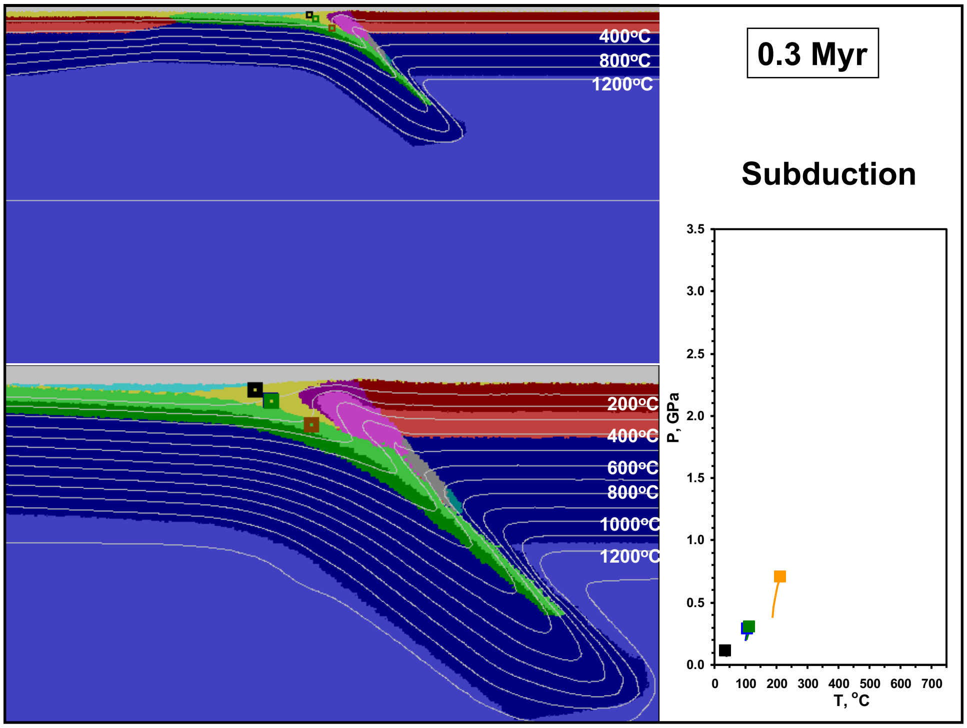
400ºC
800ºC
1200ºC
0.3 Myr
Subduction
200ºC
400ºC
600ºC
800ºC
1000ºC
1200ºC
P, GPa
T, °C

53

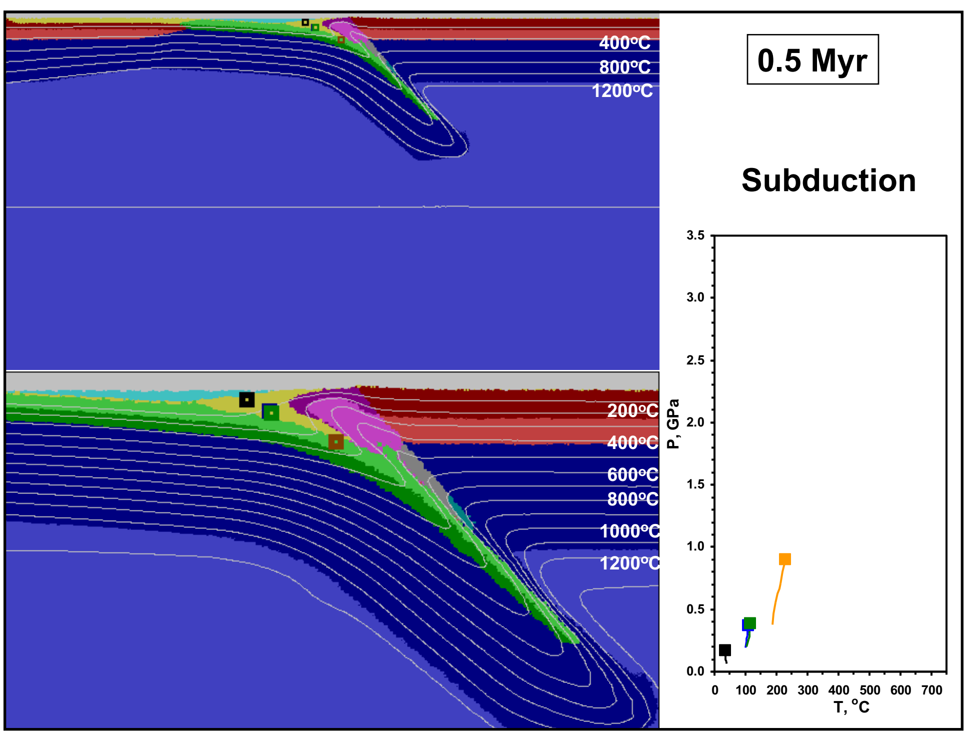
400ºC
800ºC
1200ºC
0.5 Myr
Subduction
200ºC
400ºC
600ºC
800ºC
1000ºC
1200ºC
P, GPa
T, °C

54

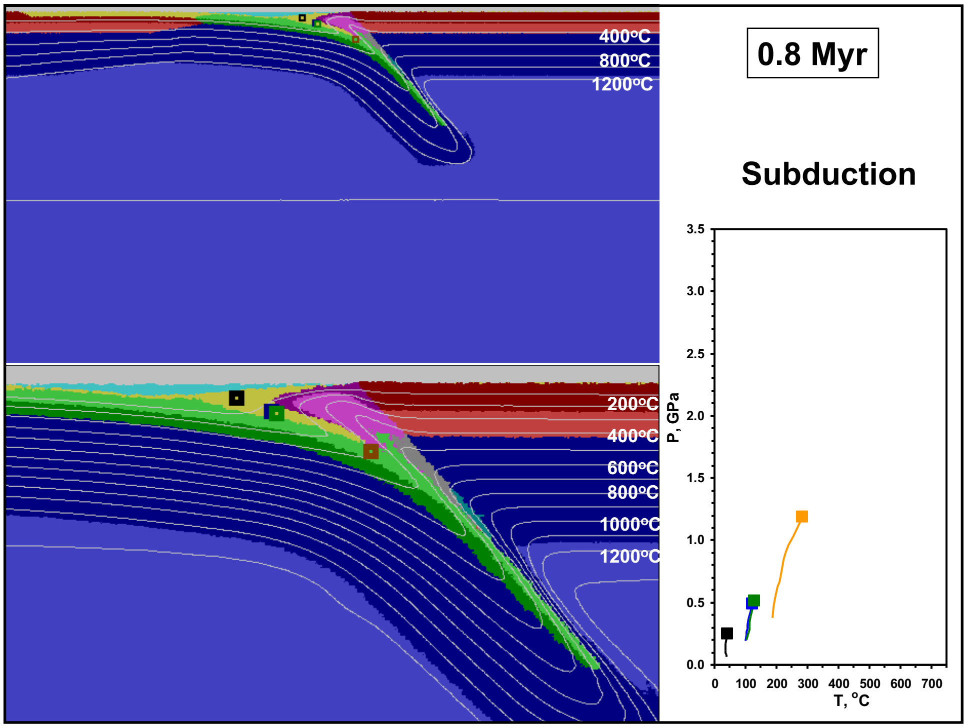
400°C
800°C
1200°C
0.8 Myr
Subduction
200°C
400°C
600°C
800°C
1000°C
1200°C
P, GPa
T, °C
3.5
3.0
2.5
2.0
1.5
1.0
0.5
0.0
0 100 200 300 400 500 600 700

55

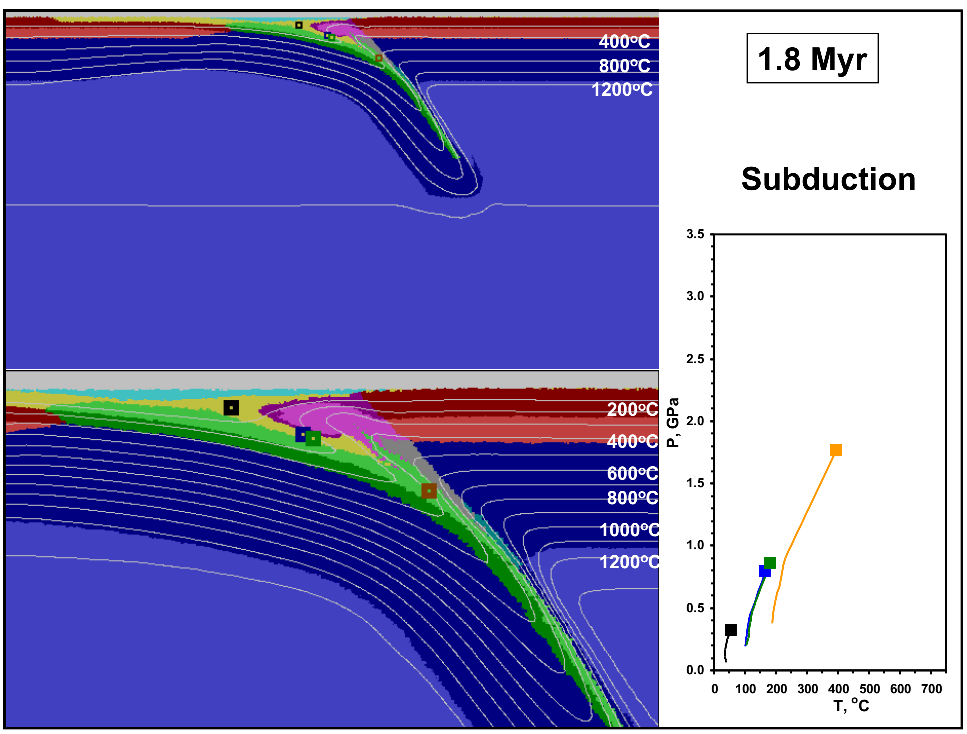
400°C
800°C
1200°C
1.8 Myr
Subduction
200°C
400°C
600°C
800°C
1000°C
1200°C
P, GPa
T, °C
3.5
3.0
2.5
2.0
1.5
1.0
0.5
0.0
0 100 200 300 400 500 600 700

56

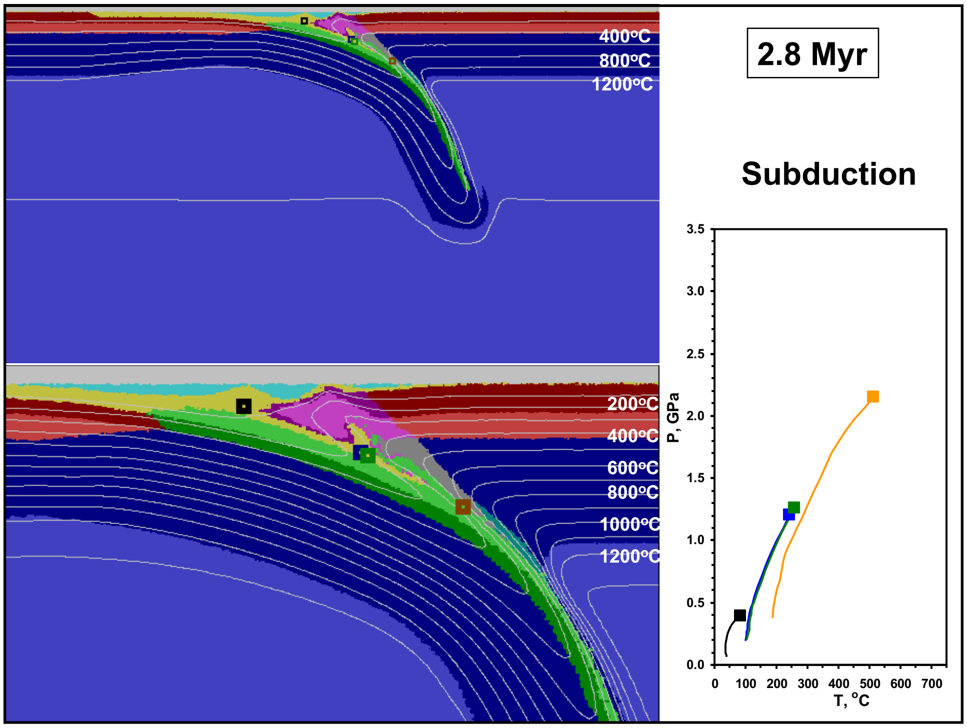

400ºC
800ºC
1200ºC
200ºC
400ºC
600ºC
800ºC
1000ºC
1200ºC
2.8 Myr
Subduction
P, GPa
T, °C

57

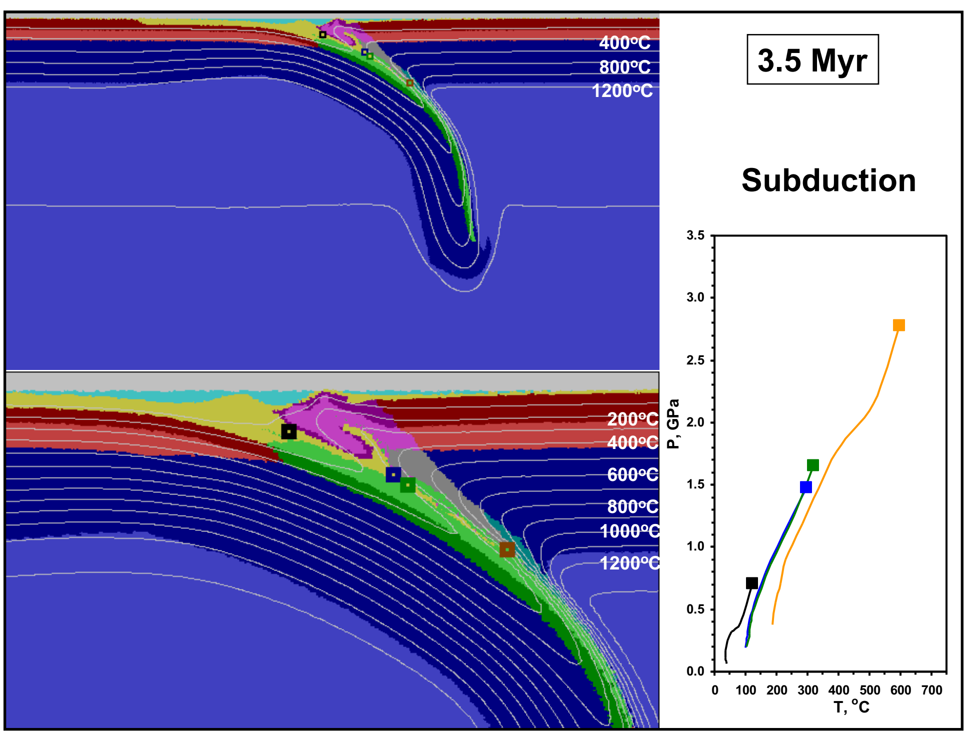

400ºC
800ºC
1200ºC
200ºC
400ºC
600ºC
800ºC
1000ºC
1200ºC
3.5 Myr
Subduction
P, GPa
T, °C

58

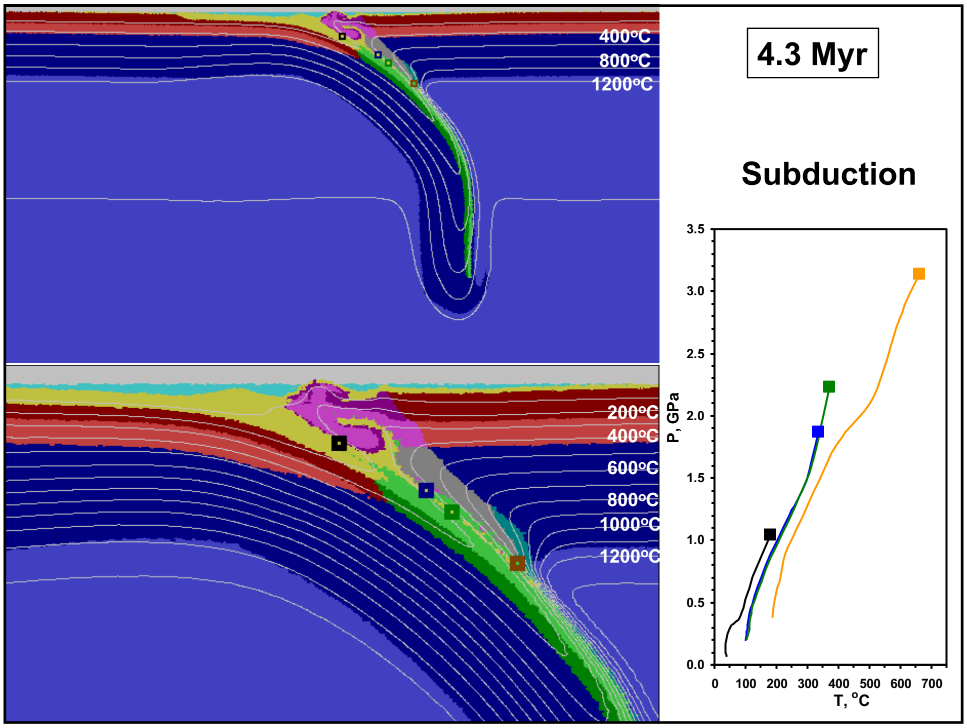
400ºC
800ºC
1200ºC
200ºC
400ºC
600ºC
800ºC
1000ºC
1200ºC
4.3 Myr
Subduction
P, GPa
T, °C
0.0
0.5
1.0
1.5
2.0
2.5
3.0
3.5
0
100
200
300
400
500
600
700

59

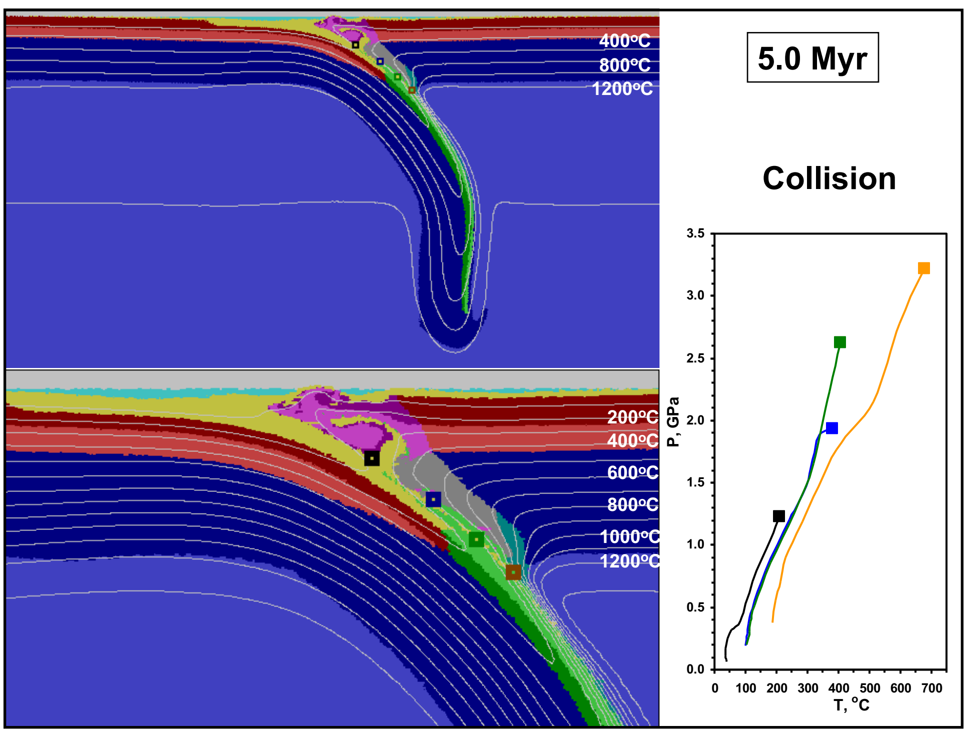
400ºC
800ºC
1200ºC
200ºC
400ºC
600ºC
800ºC
1000ºC
1200ºC
5.0 Myr
Collision
P, GPa
T, °C
0.0
0.5
1.0
1.5
2.0
2.5
3.0
3.5
0
100
200
300
400
500
600
700

60

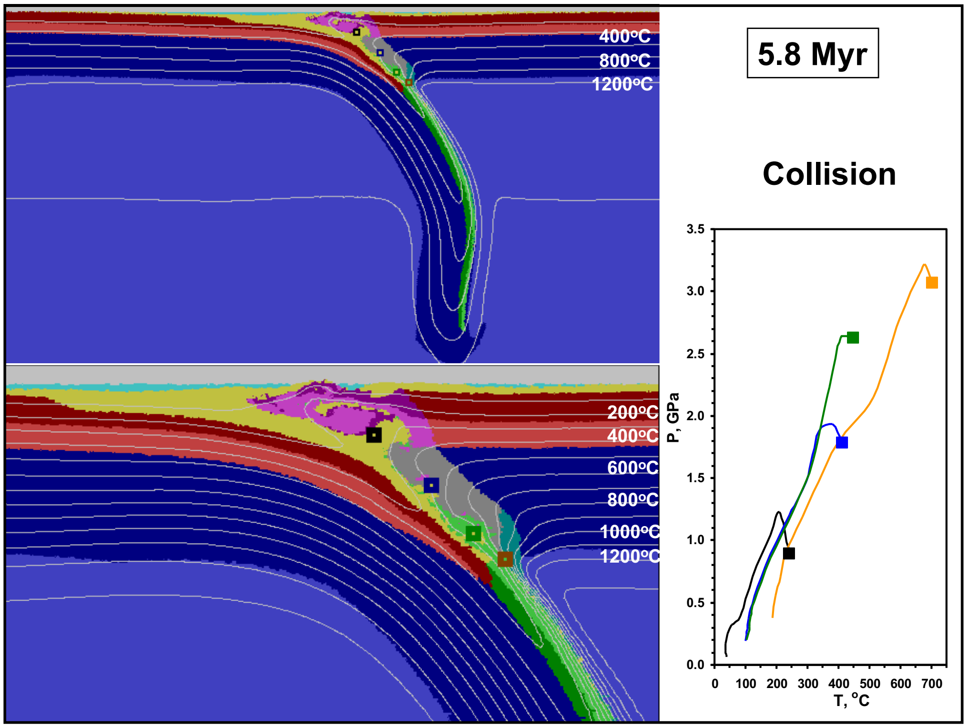
400ºC
800ºC
1200ºC
5.8 Myr
Collision
200ºC
400ºC
600ºC
800ºC
1000ºC
1200ºC
P, GPa
T, ºC
0.0 0.5 1.0 1.5 2.0 2.5 3.0 3.5
0 100 200 300 400 500 600 700

61

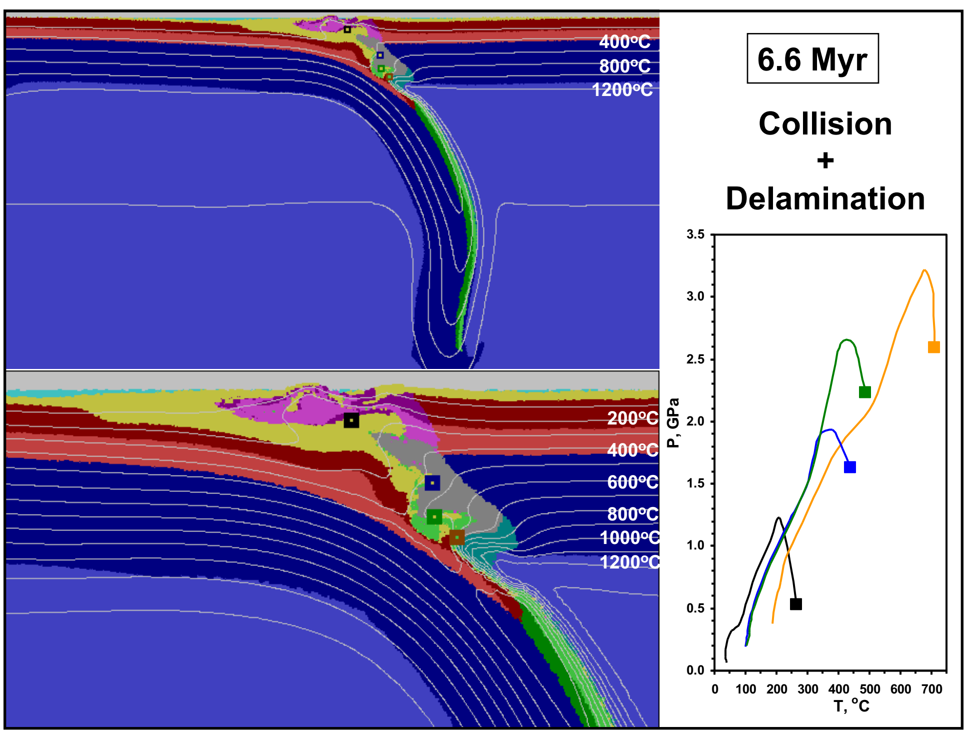
400ºC
800ºC
1200ºC
6.6 Myr
Collision
+
Delamination
200ºC
400ºC
600ºC
800ºC
1000ºC
1200ºC
P, GPa
T, ºC
0.0 0.5 1.0 1.5 2.0 2.5 3.0 3.5
0 100 200 300 400 500 600 700

62

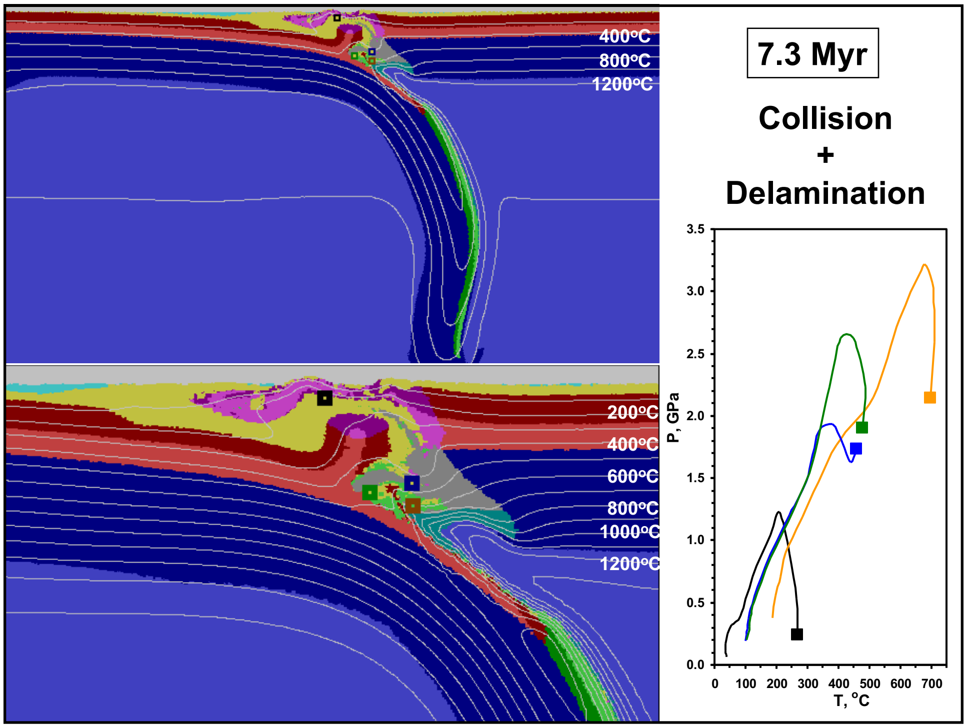

400ºC
800ºC
1200ºC
200ºC
400ºC
600ºC
800ºC
1000ºC
1200ºC
7.3 Myr
Collision
+
Delamination
P, GPa
T, °C

63

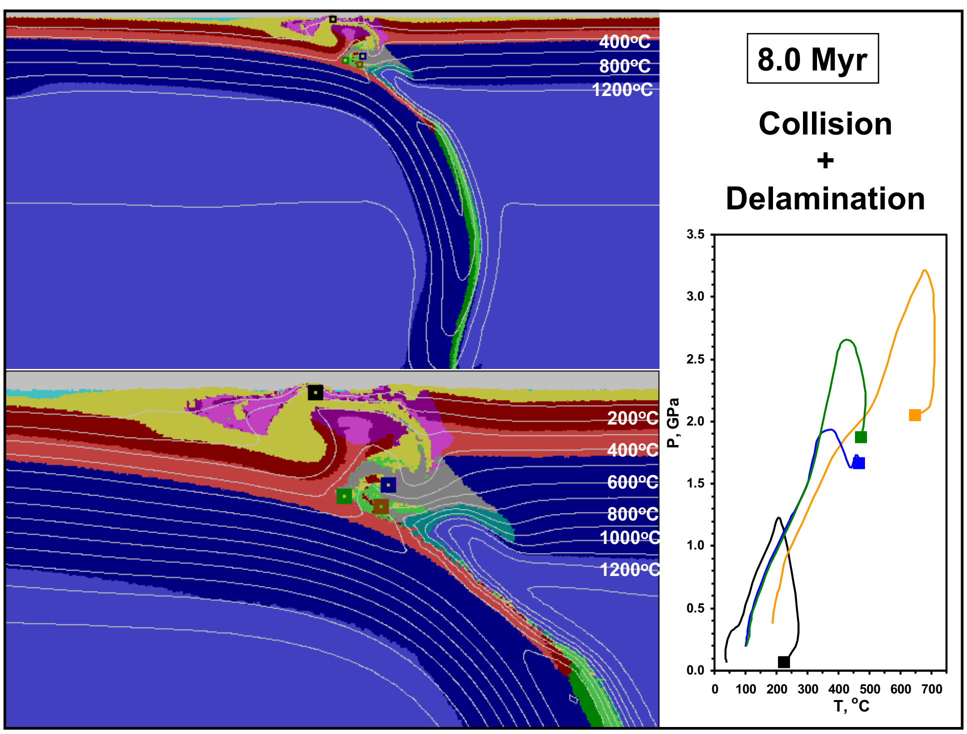

400ºC
800ºC
1200ºC
200ºC
400ºC
600ºC
800ºC
1000ºC
1200ºC
8.0 Myr
Collision
+
Delamination
P, GPa
T, °C

64

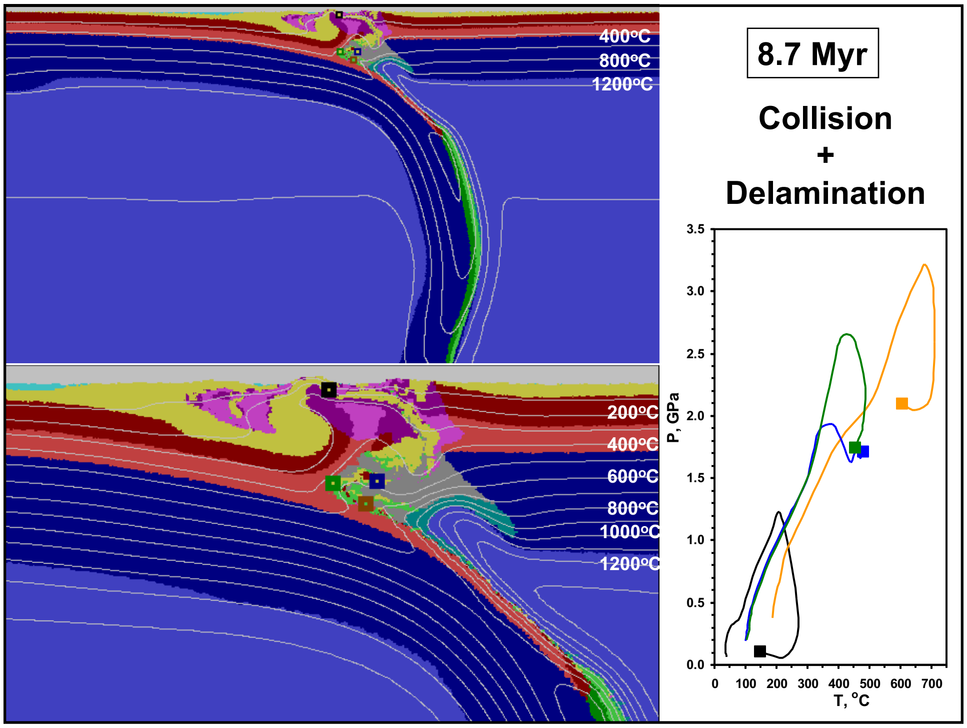
400ºC
800ºC
1200ºC
200ºC
400ºC
600ºC
800ºC
1000ºC
1200ºC
8.7 Myr
Collision
+
Delamination
P, GPa
T, °C
0.0
0.5
1.0
1.5
2.0
2.5
3.0
3.5
0
100
200
300
400
500
600
700

65

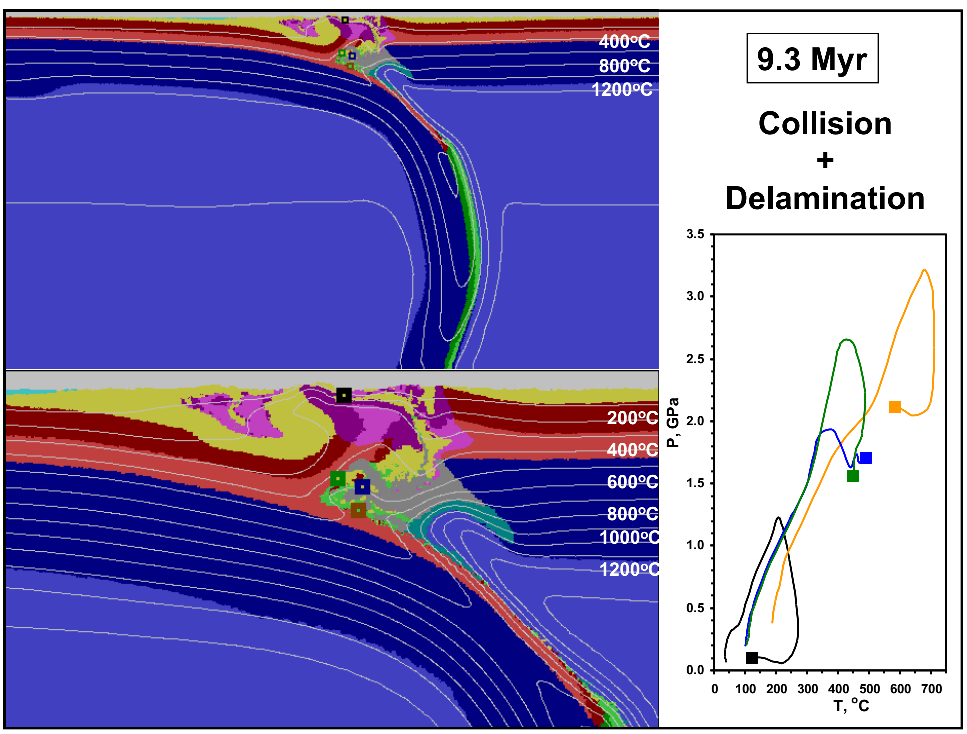
400ºC
800ºC
1200ºC
200ºC
400ºC
600ºC
800ºC
1000ºC
1200ºC
9.3 Myr
Collision
+
Delamination
P, GPa
T, °C
0.0
0.5
1.0
1.5
2.0
2.5
3.0
3.5
0
100
200
300
400
500
600
700

66

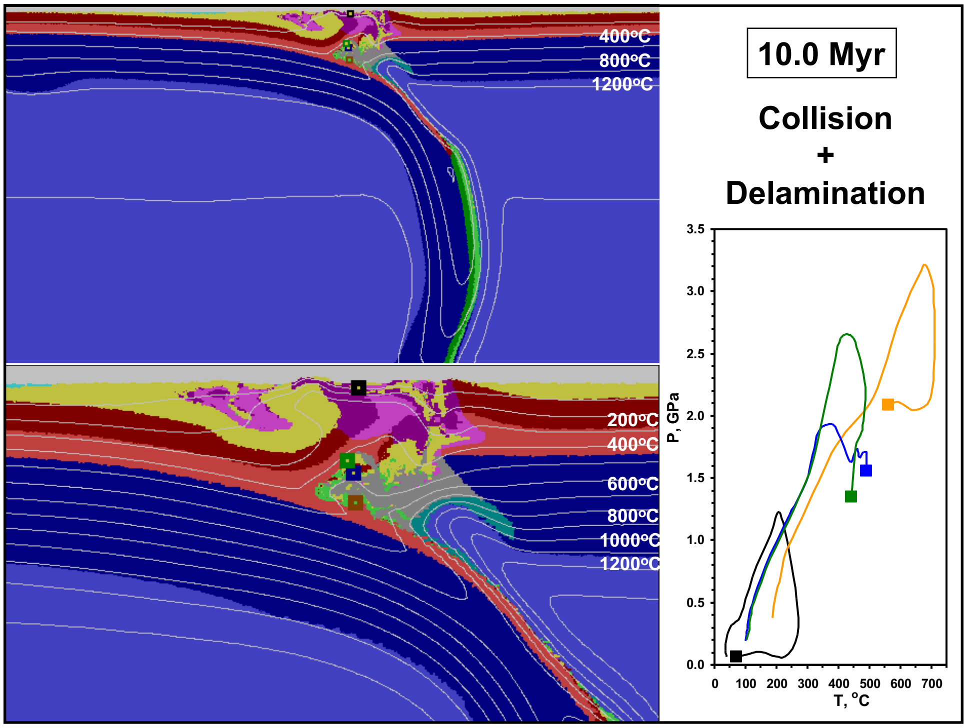
400°C
800°C
1200°C
200°C
400°C
600°C
800°C
1000°C
1200°C
10.0 Myr
Collision
+
Delamination
P, GPa
T, °C

67

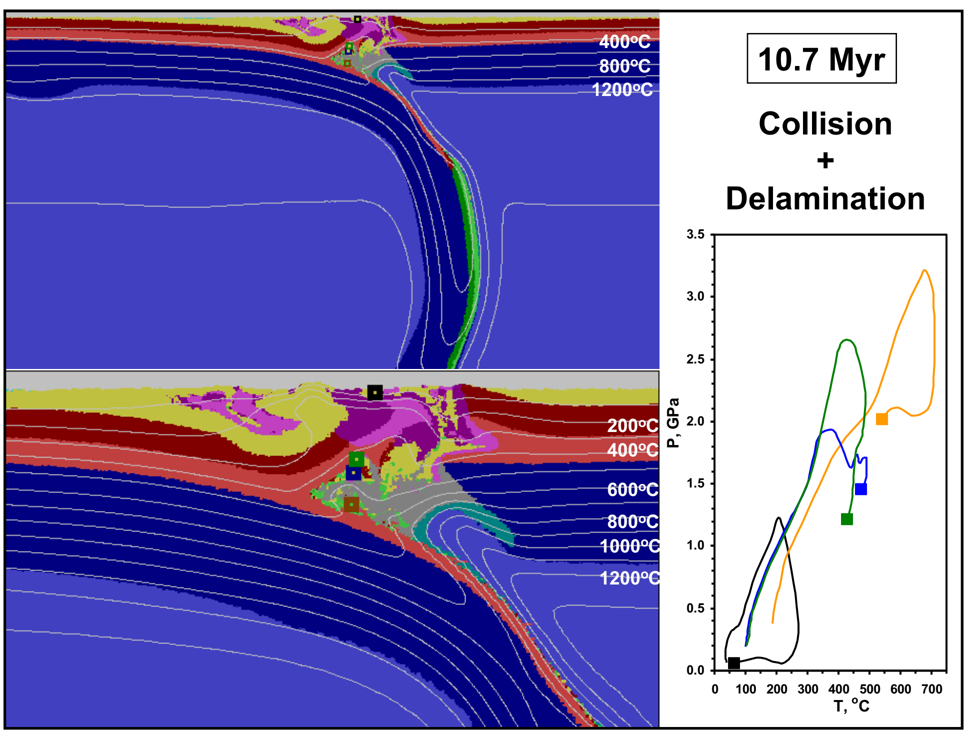
400°C
800°C
1200°C
200°C
400°C
600°C
800°C
1000°C
1200°C
10.7 Myr
Collision
+
Delamination
P, GPa
T, °C

68

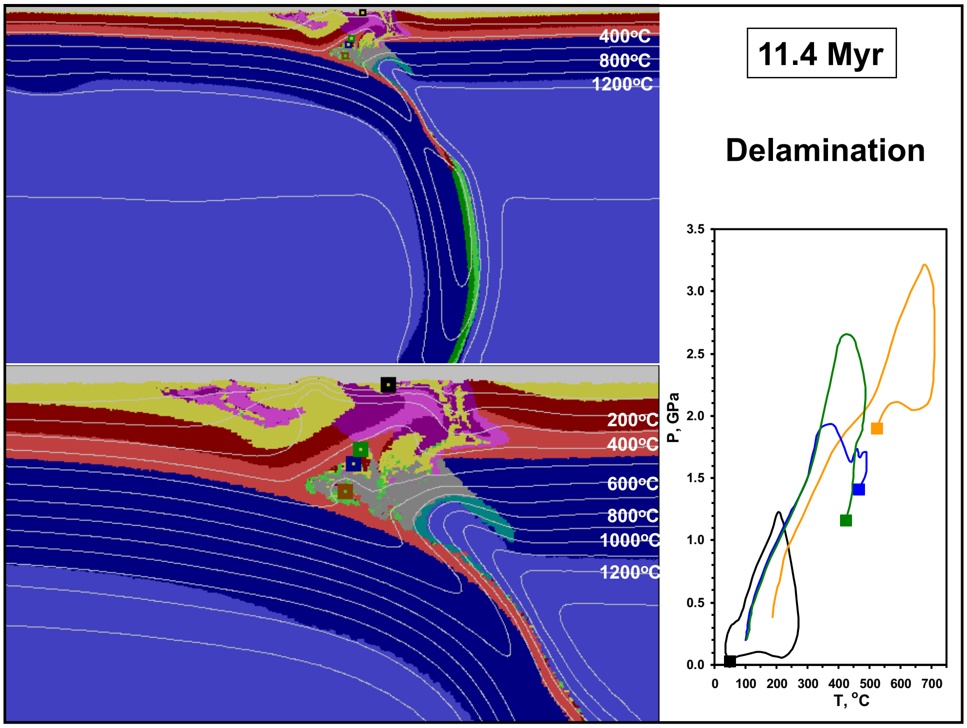
400ºC
800ºC
1200ºC
11.4 Myr
Delamination
200ºC
400ºC
600ºC
800ºC
1000ºC
1200ºC
P, GPa
T, °C

69

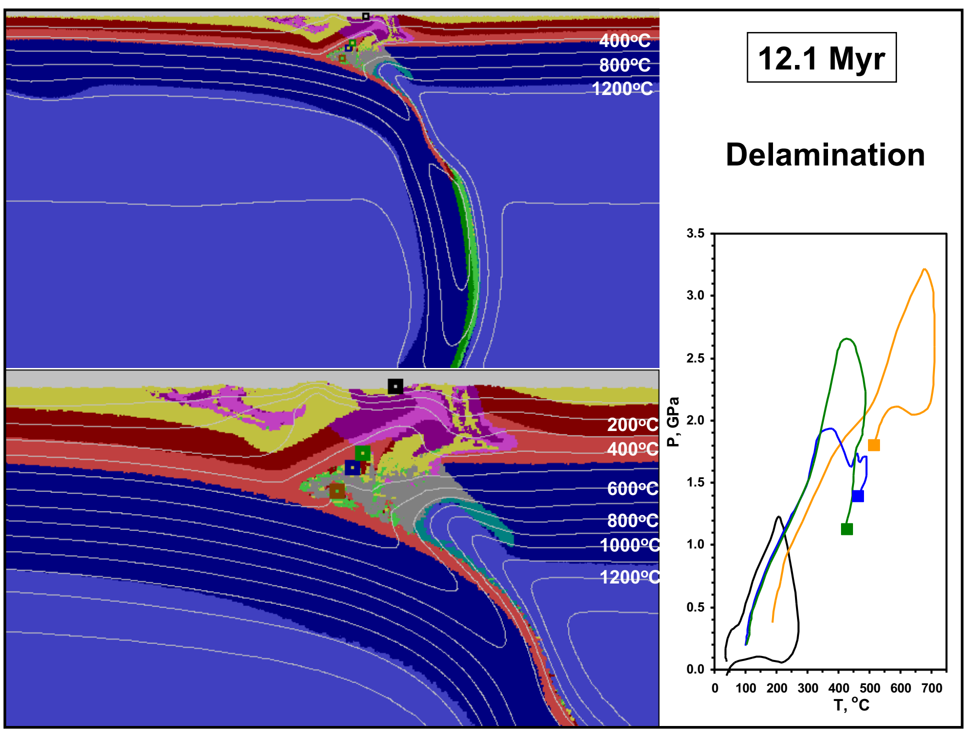
400ºC
800ºC
1200ºC
12.1 Myr
Delamination
200ºC
400ºC
600ºC
800ºC
1000ºC
1200ºC
P, GPa
T, °C

70

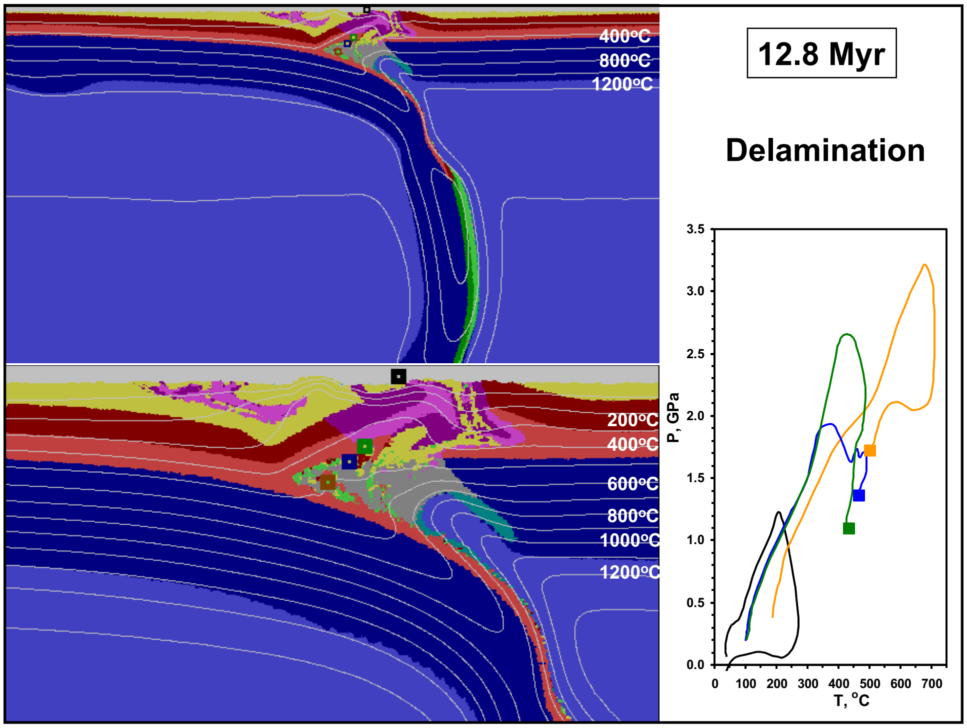
400ºC
800ºC
1200ºC
200ºC
400ºC
600ºC
800ºC
1000ºC
1200ºC
12.8 Myr
Delamination
P, GPa
T, °C
0.0
0.5
1.0
1.5
2.0
2.5
3.0
3.5
0
100
200
300
400
500
600
700

71

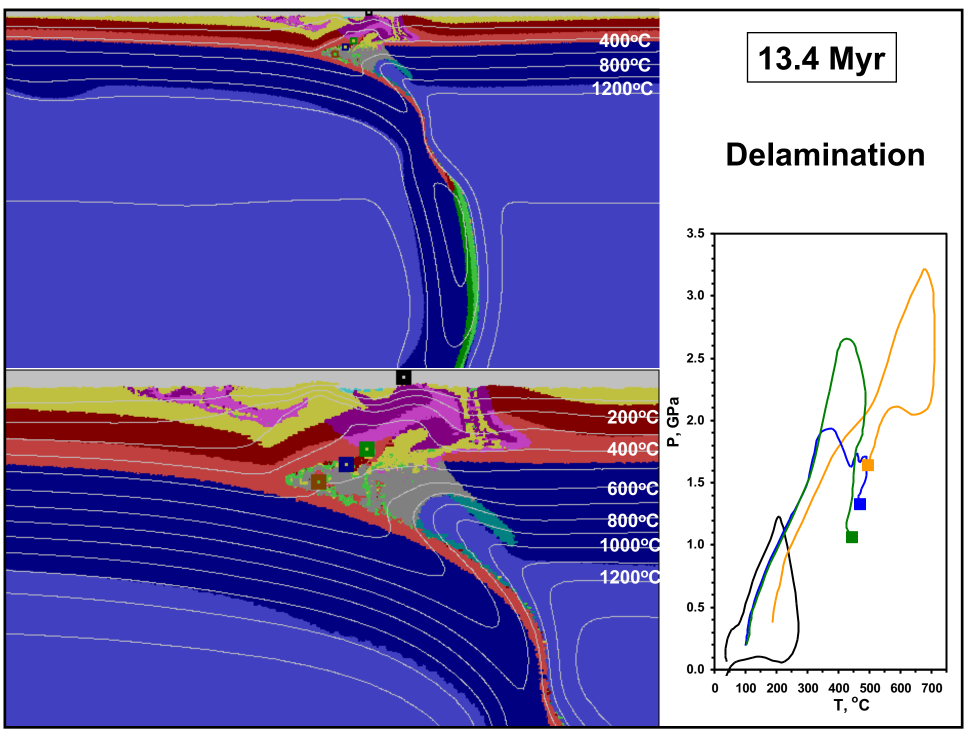
400ºC
800ºC
1200ºC
200ºC
400ºC
600ºC
800ºC
1000ºC
1200ºC
13.4 Myr
Delamination
P, GPa
T, °C
0.0
0.5
1.0
1.5
2.0
2.5
3.0
3.5
0
100
200
300
400
500
600
700

72

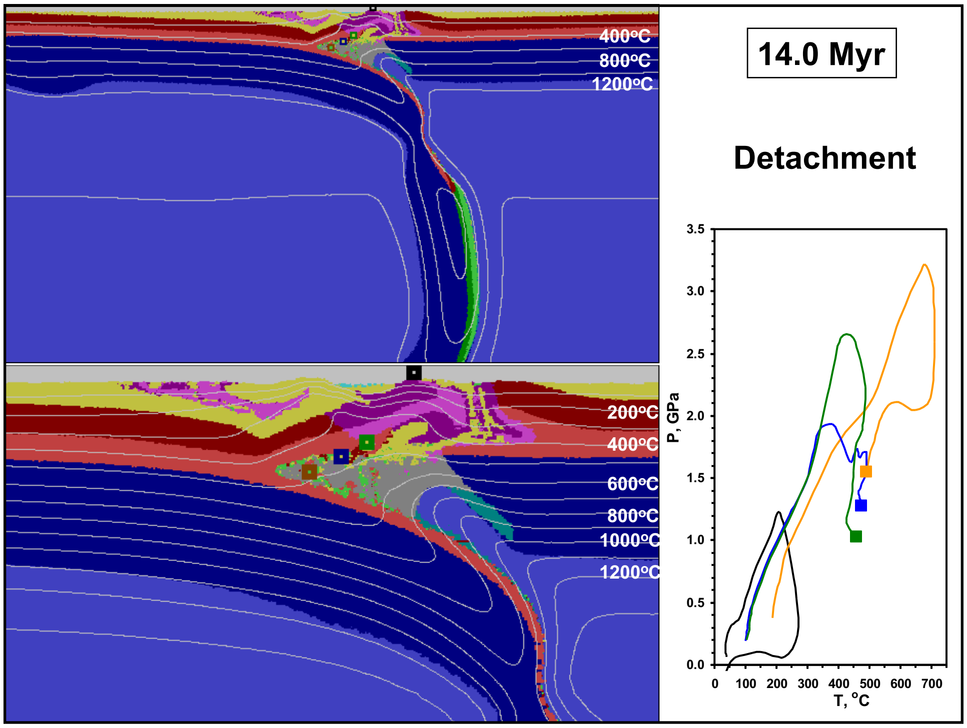
400ºC
800ºC
1200ºC
14.0 Myr
Detachment
200ºC
400ºC
600ºC
800ºC
1000ºC
1200ºC
P, GPa
T, °C
0.0
0.5
1.0
1.5
2.0
2.5
3.0
3.5
0
100
200
300
400
500
600
700

73

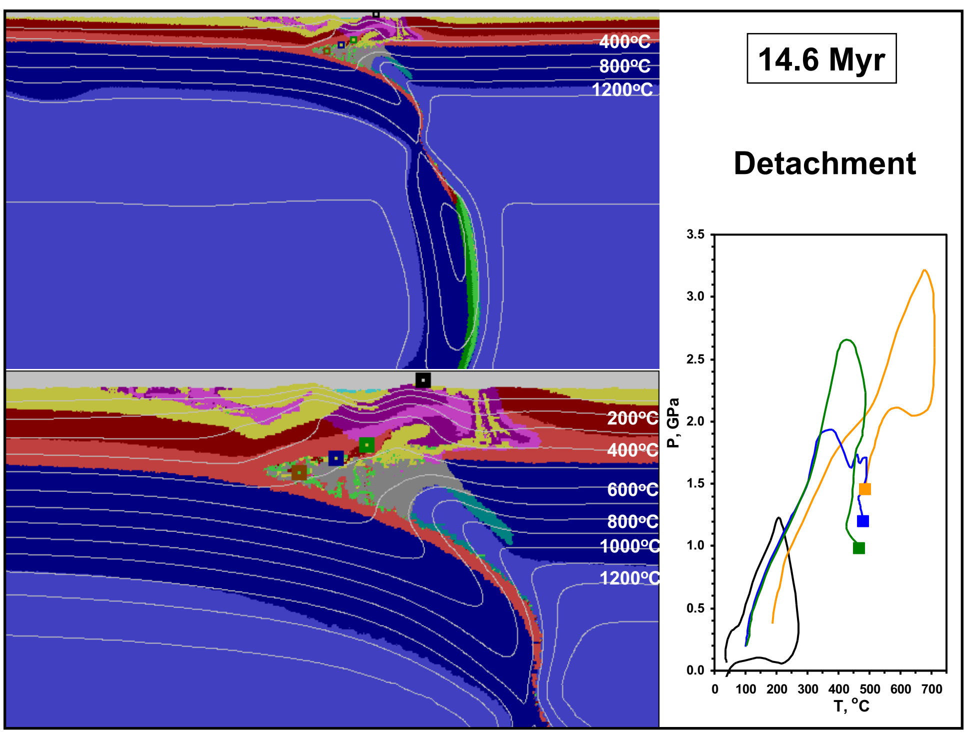
400ºC
800ºC
1200ºC
14.6 Myr
Detachment
200ºC
400ºC
600ºC
800ºC
1000ºC
1200ºC
P, GPa
T, °C
0.0
0.5
1.0
1.5
2.0
2.5
3.0
3.5
0
100
200
300
400
500
600
700

74

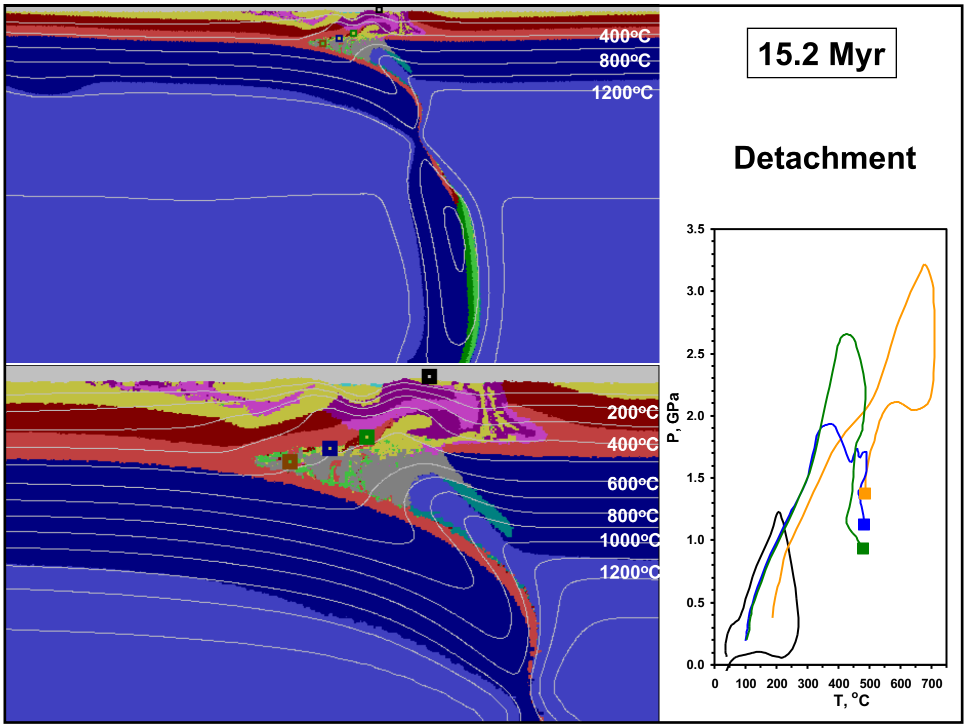
400°C
800°C
1200°C
200°C
400°C
600°C
800°C
1000°C
1200°C
15.2 Myr
Detachment
P, GPa
T, °C
0.0
0.5
1.0
1.5
2.0
2.5
3.0
3.5
0
100
200
300
400
500
600
700

75

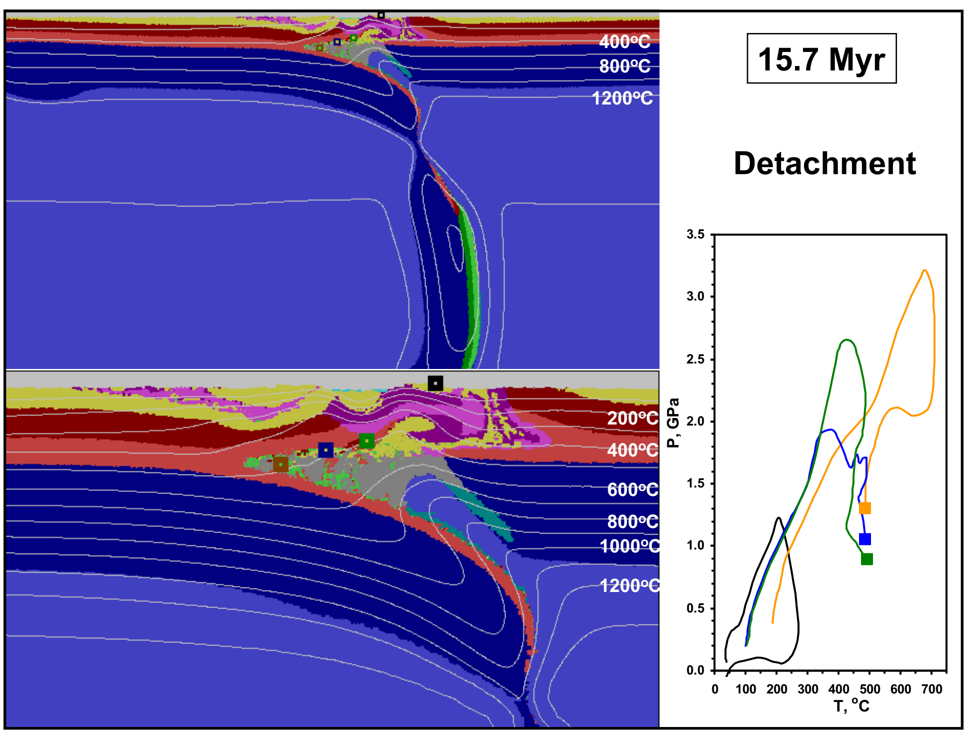
400°C
800°C
1200°C
200°C
400°C
600°C
800°C
1000°C
1200°C
15.7 Myr
Detachment
P, GPa
T, °C
0.0
0.5
1.0
1.5
2.0
2.5
3.0
3.5
0
100
200
300
400
500
600
700

76

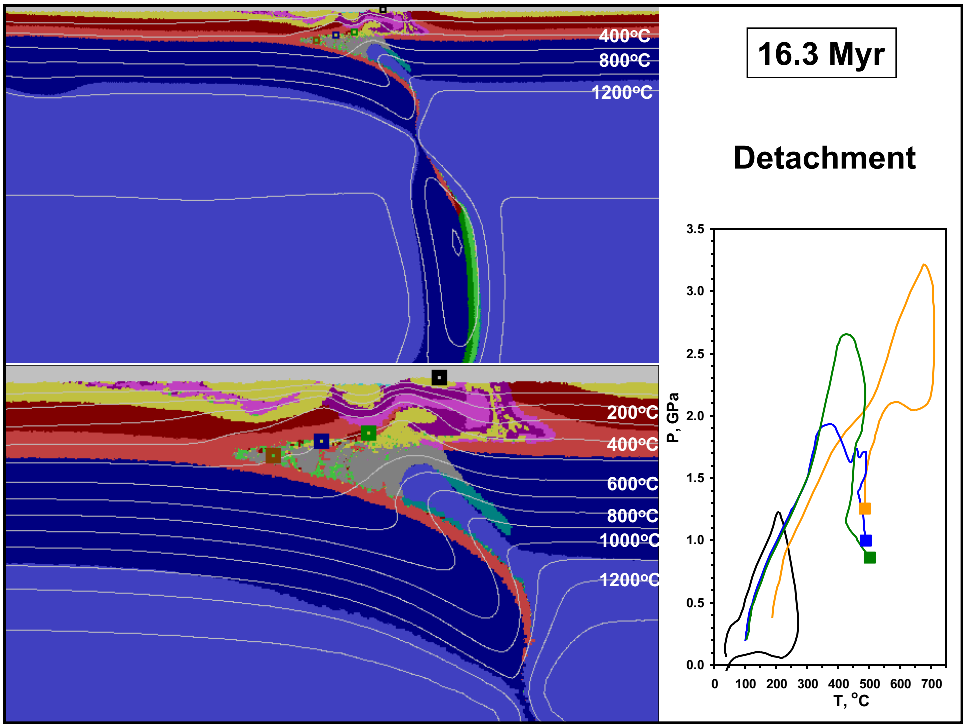
400°C
800°C
1200°C
200°C
400°C
600°C
800°C
1000°C
1200°C
16.3 Myr
Detachment
P, GPa
T, °C

77

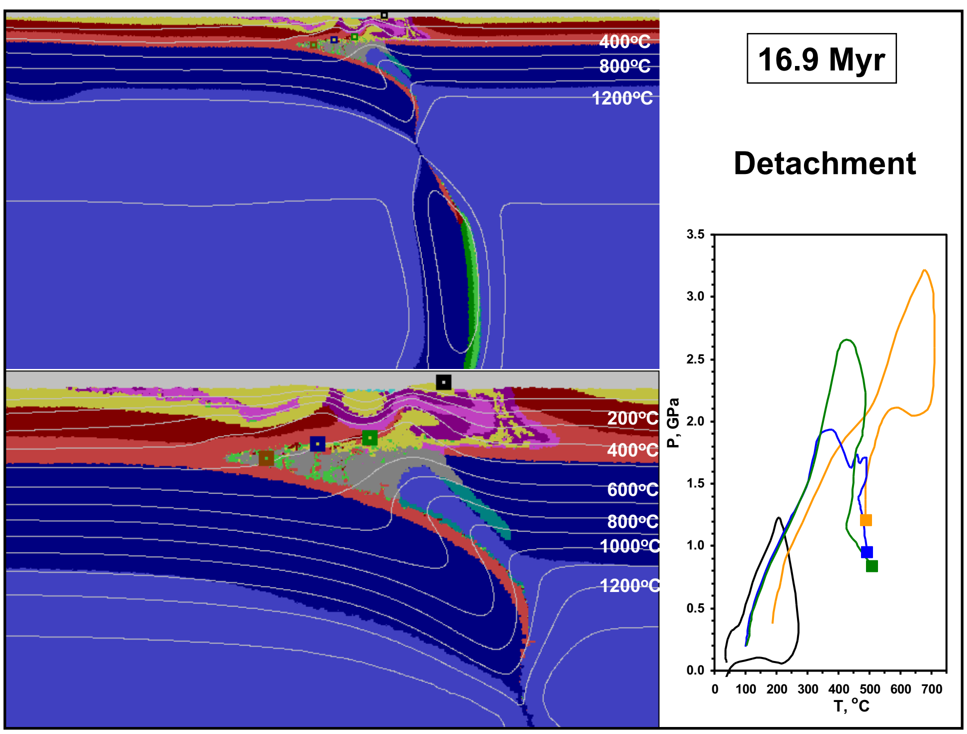
400°C
800°C
1200°C
200°C
400°C
600°C
800°C
1000°C
1200°C
16.9 Myr
Detachment
P, GPa
T, °C

78

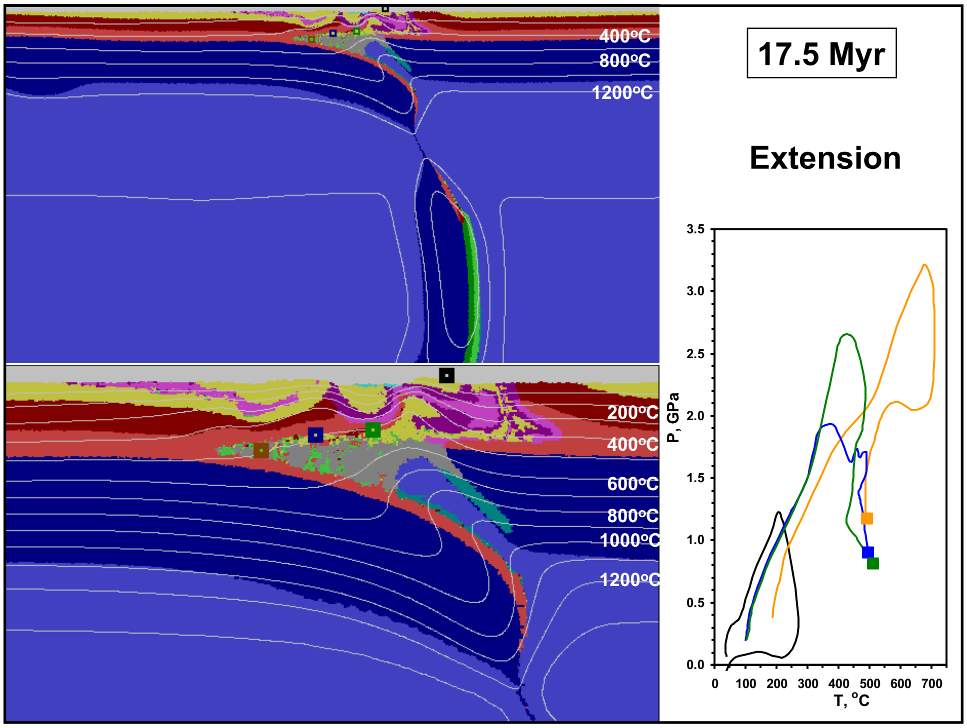

400ºC
800ºC
1200ºC
200ºC
400ºC
600ºC
800ºC
1000ºC
1200ºC
17.5 Myr
Extension
P, GPa
T, °C

79

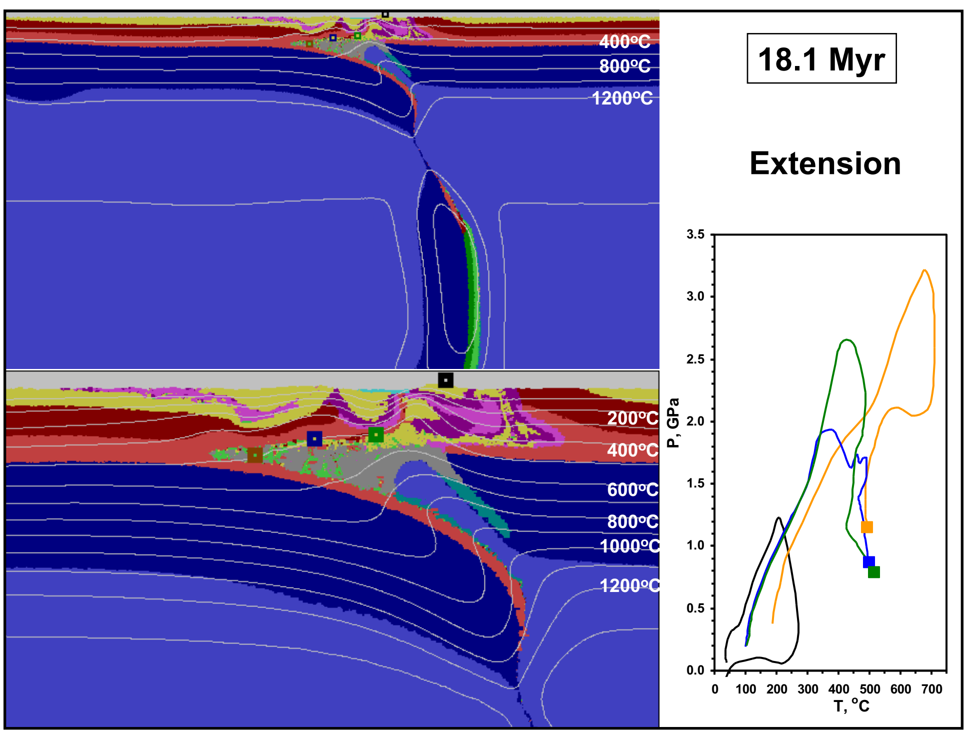

400ºC
800ºC
1200ºC
200ºC
400ºC
600ºC
800ºC
1000ºC
1200ºC
18.1 Myr
Extension
P, GPa
T, °C

80

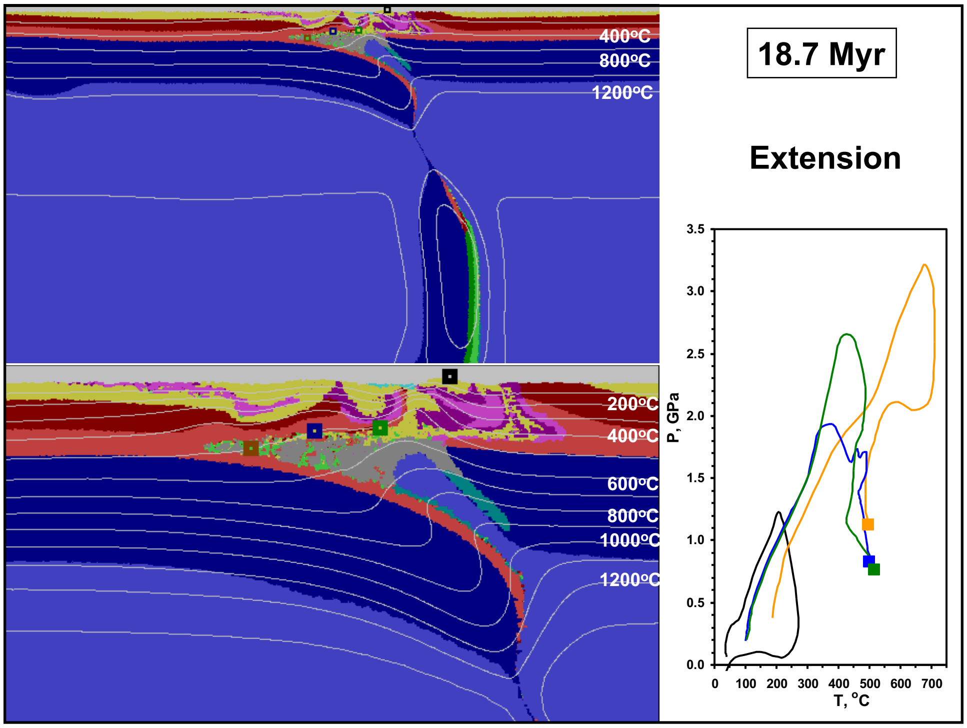
400ºC
800ºC
1200ºC
18.7 Myr
Extension
200ºC
400ºC
600ºC
800ºC
1000ºC
1200ºC
P, GPa
T, °C

81

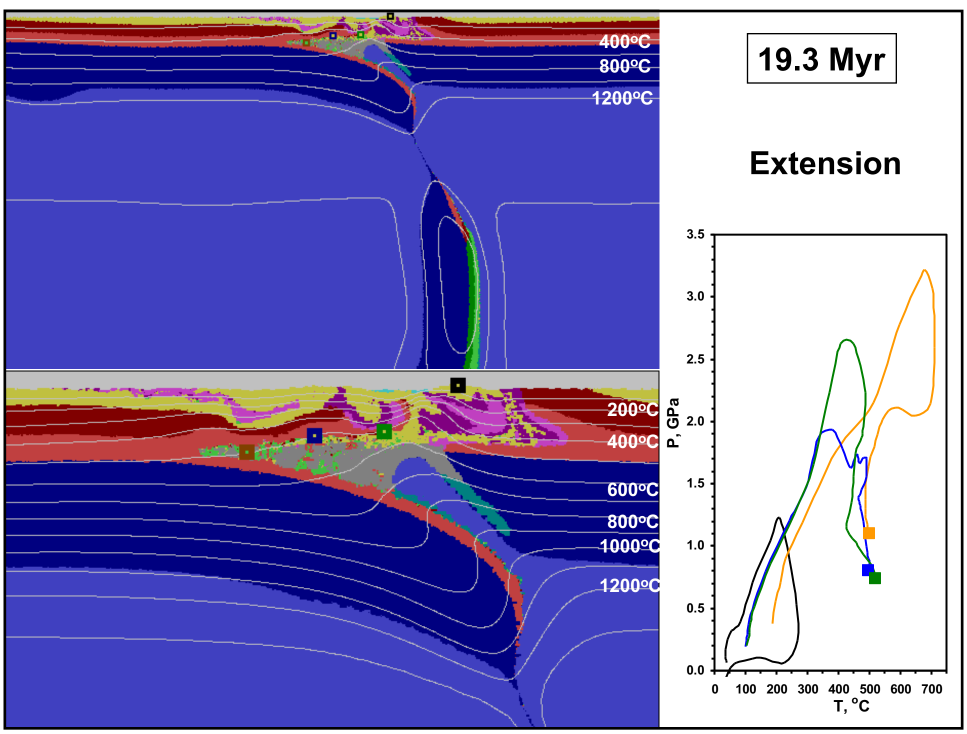
400ºC
800ºC
1200ºC
19.3 Myr
Extension
200ºC
400ºC
600ºC
800ºC
1000ºC
1200ºC
P, GPa
T, °C

82

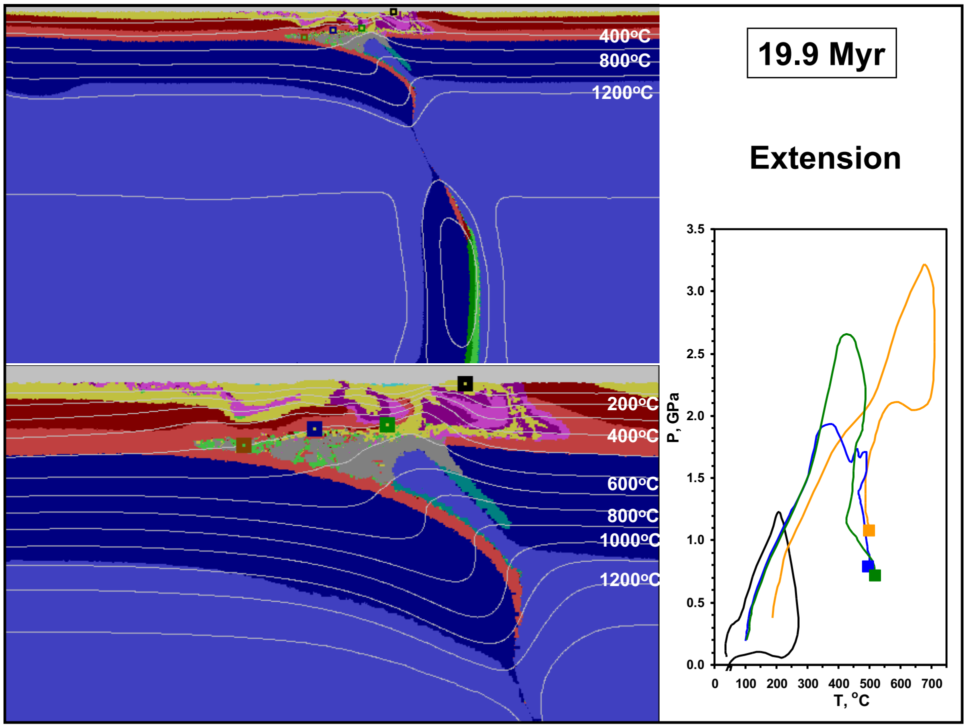
400ºC
800ºC
1200ºC
200ºC
400ºC
600ºC
800ºC
1000ºC
1200ºC
19.9 Myr
Extension
P, GPa
T, °C
0.0
0.5
1.0
1.5
2.0
2.5
3.0
3.5
0
100
200
300
400
500
600
700

83

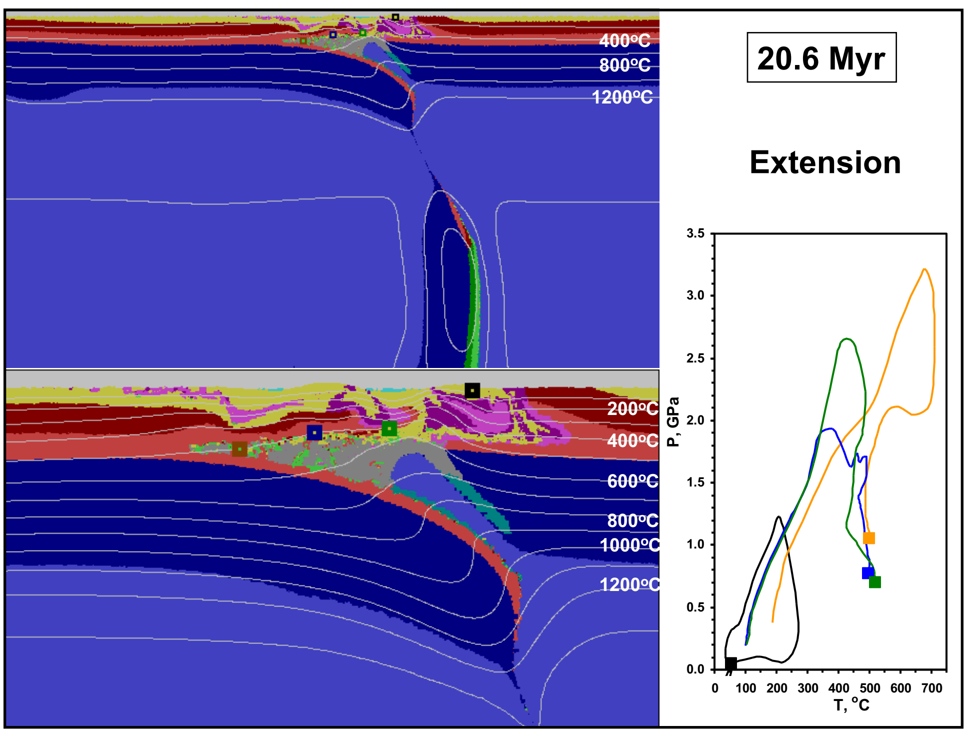
400ºC
800ºC
1200ºC
200ºC
400ºC
600ºC
800ºC
1000ºC
1200ºC
20.6 Myr
Extension
P, GPa
T, °C
0.0
0.5
1.0
1.5
2.0
2.5
3.0
3.5
0
100
200
300
400
500
600
700

84

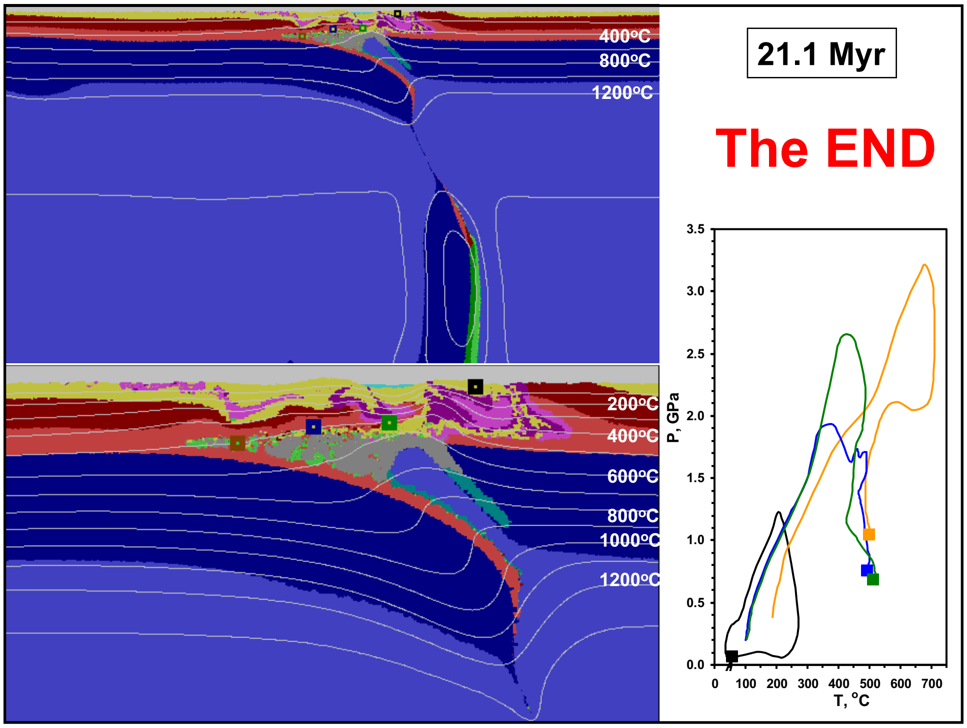

85

Dynamics of orogenic wedges and the uplift of high-pressure metamorphic rocks

J. P. PLATT *Department of Earth Sciences, Oxford University, Parks Road, Oxford 0X1 3PR, England*

ABSTRACT

Subduction-accretion complexes can be approximated as wedge-shaped continua with a rigid buttress behind and a subducting lithospheric slab beneath. Thick wedges undergoing prograde metamorphism have a negligible long-term yield strength and are likely to exhibit a complex nonlinear viscous rheology. Such a wedge will tend to deform internally until it reaches a stable configuration, in which the gravitational forces generated by the wedge geometry balance the traction exerted on its underside by the subducting slab. Accretion of material at the wedge front will lengthen the wedge and cause it to shorten internally to regain the stable geometry. This shortening will be expressed as late (out-of-sequence) thrusting, backthrusting, and folding. Conversely, underplating of sediment or crustal slices will thicken the wedge, which may need to extend internally to regain stability. Extension will cause listric normal faults that may merge downward into zones of ductile extension. Continued underplating at depth and compensating extension above provides a mechanism for bringing high-P/low-T metamorphic rocks to upper levels in the rear of the wedge, where they are commonly observed. Many major tectonic boundaries in convergent orogens (such as the Coast Range thrust in the Franciscan Complex, major nappe contacts in the Alps, and the contact between the Nevado-Filabride and Higher Betic nappe complexes in the Betic Cordillera) show abrupt increases in metamorphic grade downward across them. This is consistent with their origin or reactivation as uplift-related, extensional structures.

material is then detached at depth, it will be incorporated into a growing accretionary wedge and will be potentially available for subsequent exhumation. Compressional deformation alone, however, cannot bring rocks closer to the topographic surface. An additional process is needed, either to bring the high-P rocks upward relative to their surroundings or to remove material from above them. Possibilities include the buoyant rise of subducted slabs of crustal material relative to higher density mantle rocks (Ernst, 1971b, 1975, 1984; Platt, 1986); entrainment of blocks of high-P rocks in relatively low-density diapirs (England and Holland, 1979; Carlson, 1981; Moore, 1984) or in flowing mud-matrix mélanges (Cloos, 1982); or regional uplift driven by underplating of material at the base of the accretionary wedge, coupled with erosion at the surface (Platt, 1975; Rubie, 1984). None of these processes appears to adequately explain the tectonic setting and timing of uplift of regionally coherent metamorphic

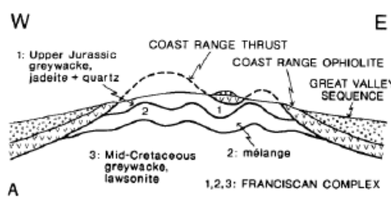

A

Geological Society of America Bulletin, v. 97, p. 1037–1053, 9 figs., September 1986.

86

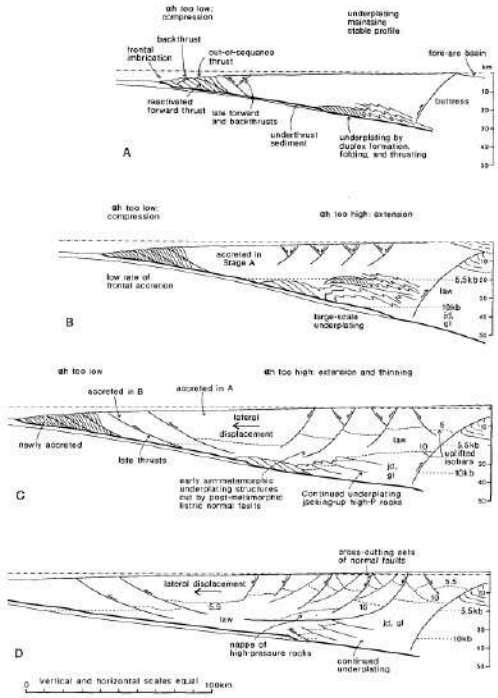

87

Tectonophysics 603 (2013) 79–88

Contents lists available at ScienceDirect

Tectonophysics

journal homepage: www.elsevier.com/locate/tecto

Review Article

Paradigms, new and old, for ultrahigh-pressure tectonism

Bradley R. Hacker [a,*], Taras V. Gerya [b]

[a] Earth Science, University of California, Santa Barbara, CA 93106, USA
[b] Geophysical Fluid Dynamics Group, Institute of Geophysics, Department of Earth Sciences, Swiss Federal Institute of Technology (ETH-Zurich), Sonneggstrasse, 5, 8092 Zurich, Switzerland

A R T I C L E I N F O

Article history:
Received 31 January 2013
Received in revised form 20 May 2013
Accepted 22 May 2013
Available online 4 June 2013

Keywords:
Ultrahigh pressure
Exhumation
Subduction
Relamination
Diapir

A B S T R A C T

Regional ultrahigh-pressure (UHP) metamorphic terranes exhibit a spectrum of lithological, structural and petrological characteristics that result from the geodynamic processes that formed and exhumed them. At least six geodynamic processes can be envisioned to have carried continental rocks to mantle depths: i) continental margin subduction, ii) microcontinent subduction, iii) sediment subduction, iv) intracontinental subduction, v) subduction erosion, and vi) foundering of a crustal root. Most of these processes have been investigated through numerical or analog models and most have been invoked for one or more specific occurrences of UHP rocks. At least six geodynamic processes can be envisioned to have exhumed UHP continental rocks: i) eduction, ii) microplate rotation, iii) crustal stacking, iv) slab rollback, v) channel flow, and vi) trans-mantle diapirs. Most of these processes have also been investigated through numerical or analog models and all have been invoked to explain the exhumation of at least one UHP terrane. More-detailed and systematic field investigations are warranted to assess the predictions of numerical models, and more-sophisticated and realistic numerical models are required to replicate and explain the petrological, structural, and chronological data obtained from UHP terranes.

88

Table 1
Geologic characteristics of terranes exhumed by different mechanisms.

	a) Structural	b) Petrological	c) Chronological	d) Length scale	e) Example
Eduction ("Andersen model")	• Relatively weakly deformed • No thrust fault at base	• Monotonic down-dip gradient in peak P & T	• Up to 10 Myr subduction & exhumation in models • Monotonic down-dip gradient in ages	• Thickness of educting lithospheric section	Western Gneiss region
Microplate rotation	• Rotation of lineations in space and time • Possible thrust fault at base with increasing offset from rotation axis	• P & T gradient with respect to rotation axis	• Not yet modeled • Age gradient with respect to rotation axis	• Thickness of rotation lithospheric section, unless diminished by basal thrust	Dabie Shan
Crustal stacking ("Chemenda model")	• Relatively coherent slab • Thrust fault at base above another crustal section	• Monotonic down-dip gradient in peak P & T	• Up to 20 Myr in models • Monotonic down-dip gradient in ages	• Crust	Dora Maira(?)
Slab rollback	• Microcontinent • Thrust fault at base	• Associated back-arc spreading	• 15 Myr in Mediterranean • Monotonic down-dip gradient in ages	• Microcontinent crust	Not yet(?) demonstrated for UHP rocks
Channel flow	• Nappes or strong mixing	• Mixing of domains of different pressures • Possible pressure cycling of individual domains	• A few Myr to tens of Myr in models • Mixing of domains with different ages	• Meters to kilometers	Unknown
Trans-mantle diapirs	• Radially symmetric structures • Dome within upper plate • No basal fault	• Significant local melting • Mixing of domains of different pressures • Concurrent magmatism	• Rapid (<1 Myr) ascents of diapirs over a period of tens of Myr	• 10–20 km diapir radius	N Qaidam

89

Formação de rochas UH*P*

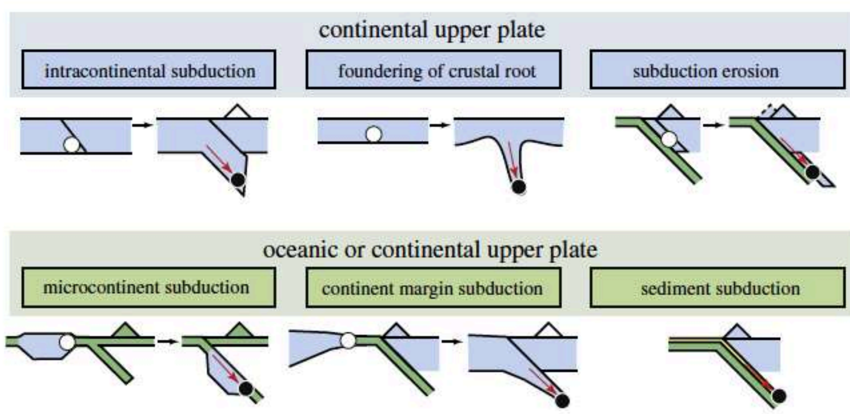

baseado em grandes terrenos dominados por rochas quartzo-feldspáticas
não leva em conta pequenas ocorrências de rochas máfica-ultramáficas

90

Forças que controlam subducção e exumação

- Forças tectônicas globais transmitidas por movimentos de placas

- Forças dos corpos derivadas da flutuabilidade (*buoyancy*) de rochas subductadas
  - afetada por *T*, *P*, composição da rocha e transformação de fases (reações metamórficas)
  - rochas continentais em profundidades mantélicas tem flutuabilidade positiva e têm tendência a serem exumadas, especialmente se são submetidas à fusão parcial

91

Mecanismos de exumação

- **Educção**

- exumação de uma placa subductada por reversão do movimento da placa com relativa pouca tensão interna

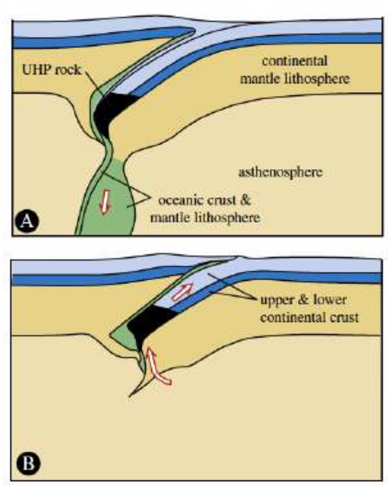

Fig. 2. Eduction, after Andersen et al. (1991) and Duretz et al. (2012). A) A continent attached to oceanic lithosphere follows the latter to UHP depth. At some point, slab pull exceeds slab strength, initiating necking. B) The positively buoyant portion of the subducting plate reverses direction and rebounds, exhuming the UHP rocks. If the continent is sufficiently strong, it undergoes little strain.

92

Mecanismos de exumação

- **Rotação de microplaca**

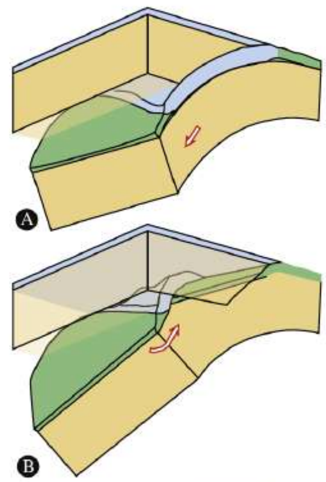

Fig. 3. Microplate rotation to exhume UHP rocks (after Hacker et al., 2000). If the changes in force that occur in response to continent subduction vary along the length of the subduction zone, these lateral gradients may drive plate rotation that exhumes UHP rocks.

93

Mecanismos de exumação

- Delaminação e empilhamento crustal acionados por flutuabilidade

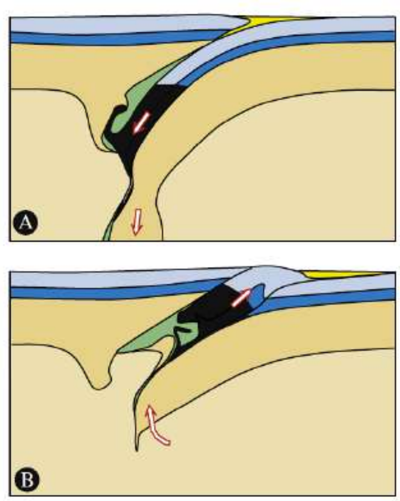

Fig. 4. Buoyancy-driven crustal delamination and stacking ("Chemenda" model) after Duretz and Gerya (2013). A weak buoyant layer atop a stronger negatively buoyant layer detaches where buoyancy exceeds slab pull, and extrudes upward as a semi-coherent sheet. The delaminated crust is thrust upward over the downgoing plate.

94

Mecanismos de exumação

- Reversão do movimento da placa (*slab rollback*)

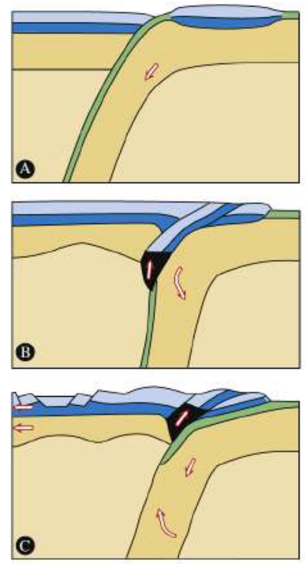

Fig. 5. Slab rollback (Brun and Faccenna, 2008). The buoyancy of a microcontinent slows slab rollback & steepens the slab. If the mafic lithosphere on either side of the microcontinent continues to roll back, a buoyant portion of the microcontinent may detach, allowing the retarded portion of the slab to roll quickly back, making room for the UHP continental crust to exhume and driving back-arc extension.

95

Mecanismos de exumação

- Fluxo de canal na subducção

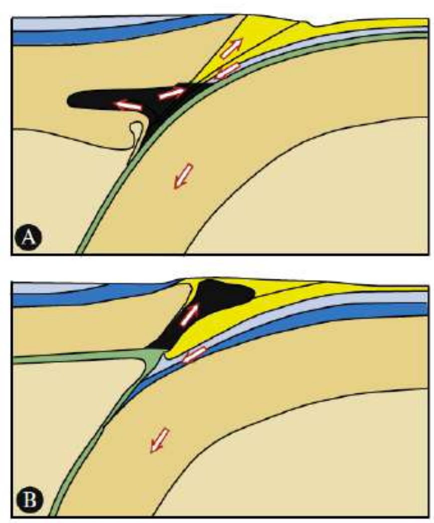

Fig. 6. Subduction channel flow (Li and Gerya, 2009). Crustal material subducted in a confined channel circulates, driven by traction along the base of the channel and the buoyancy of rocks in the channel. Material in the channel can be exhumed if: i) new material pushes old material up; ii) buoyancy in the channel exceeds traction; or iii) an indenter squeezes channel.

96

Mecanismos de exumação

- Diápiros trans-mantélicos

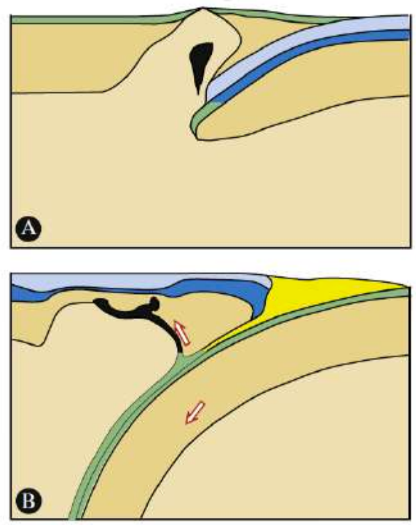

Fig. 7. Some UHP terranes might be coalesced material derived from subduction-sourced diapirs of sediment or material removed by subduction erosion (Gerya and Meilick, 2011; Little et al., 2011).

97

Relaminação (não-exumação)

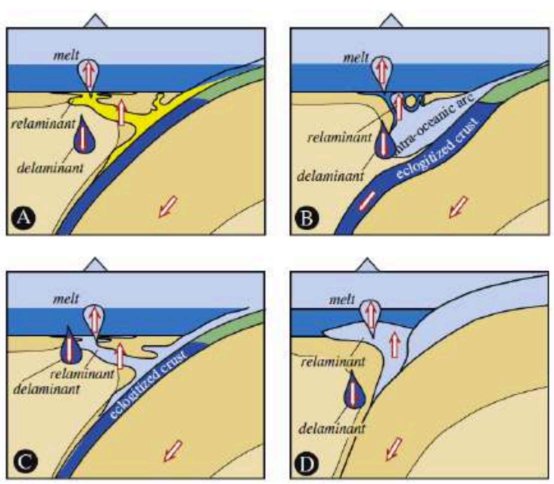

Fig. 8. Transfer of subducted crustal rock into the base of the upper plate is termed 'relamination'. A) Relamination of subducted sediment (Currie et al., 2007). B) Relamination of subducted intra-oceanic arc. C) Relamination of crust removed by subduction erosion (Stöckhert and Gerya, 2005). D) Relamination of subducted continental crust (Walsh and Hacker, 2004).

98

Resumo

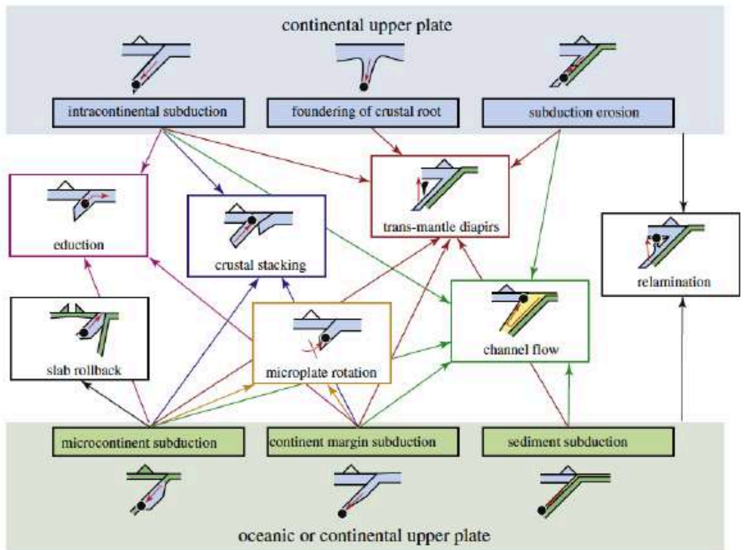

Fig. 9. Range of possible formation and exhumation mechanisms for UHP terranes.

99

Metamorfismo em Cinturões Envolvendo Colisão Continental

Trajetórias *P*-*T*-t e modelos termais
O **Metamorfismo Barroviano**

100

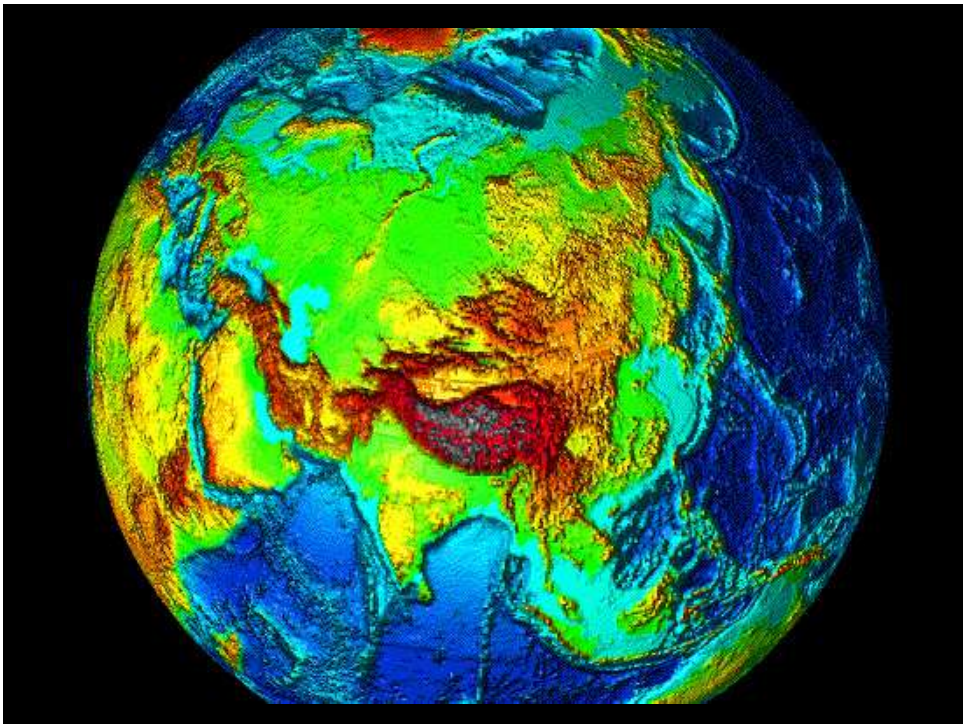

101

The influence of erosion upon the mineral facies of rocks from different metamorphic environments

P. C. ENGLAND & S. W. RICHARDSON

SUMMARY

Metamorphism of tectonically thickened continental crust or subducted sediment wedges is likely to take place in a thermal regime where temperature increases by conductive relaxation whilst concurrently pressure decreases by erosion of the pile. The mineral facies of rocks reaching the surface do not reflect any one geotherm through the pile but lie on a locus of P–T conditions, the metamorphic geotherm, which will generally be concave towards the temperature axis. Maximum pressures on the metamorphic geotherm are significantly less than maximum pressures experienced by rocks during the early stages of recrystallization. The metamorphic geotherm is polychronic, points at lower temperatures reflecting conditions earlier in the development than those at higher temperature; crustal melts are developed after low-medium temperature metamorphism and the amount of such melts could be significant.

Blueschists develop on the low temperature end of the metamorphic geotherm and are succeeded in exposure at the surface by greenschist- or amphibolite-facies rocks; the timescale for this process is consistent with the virtual absence of Precambrian blueschists. Crust thickened by addition of hot magma is likely to yield a metamorphic geotherm convex towards the temperature axis. Recognition of differently curving metamorphic geotherms can be used to assess the part played by magmatic activity in older metamorphic terrains.

Jl geol. Soc. Lond. vol. **134**, 1977, pp. 201–213,

102

O que controla o metamorfismo regional em cinturões colisionais?

- Fontes primárias de calor
  - elementos radioativos produtores de calor
  - calor emanado do manto
  - Outras fontes de calor – intrusões e astenosfera
- Mecanismos de transferência de calor
  - Condução é o mecanismo predominante no metamorfismo crustal
  - Advecção de magmas e fluidos pode contribuir
- Distribuição inicial dos elementos produtores de calor na crosta continental
  - A crosta continental é estratificada
    - crosta média superior é rica em rochas graníticas ricas em elementos produtores de calor
    - crosta inferior é formada por resíduo granulítico pobre em elementos produtores de calor

103

Geoterma

- Linha (ou superfície) que descreve a variação de *T* com a profundidade (ou *P*) na Terra
- De onde vem o calor?

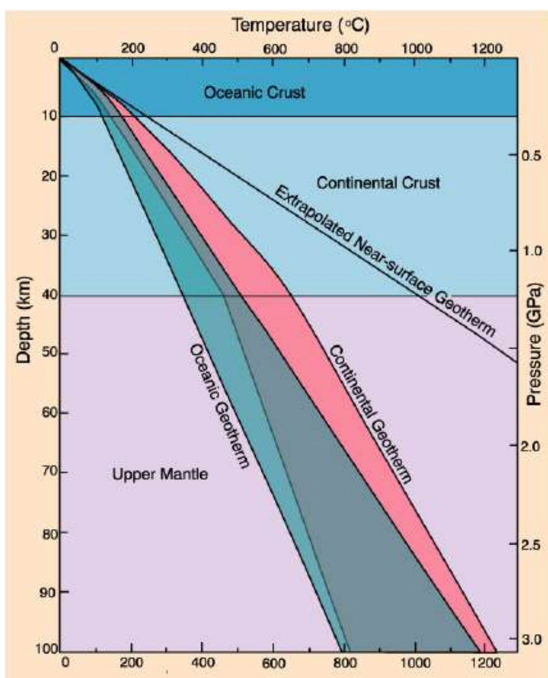

104

O que controla o metamorfismo regional em cinturões colisionais?

- Geometria do espessamento crustal e da colisão
  - Espessamento crustal homogêneo ou não
  - Espessamento homogêneo da litosfera
  - Colisão frontal ou oblíqua
- Taxas de erosão (outros processos de exumação)
  - Taxa de erosão constante
  - Extensão crustal e denudação por falhas
  - A erosão do orógeno (implica em restabelecimento de equilíbrio isostático) está dentro do intervalo entre 50 e 200 Ma
  - 2 a 5 mm.y^{-1}

105

Pressure–Temperature–Time Paths of Regional Metamorphism I. Heat Transfer during the Evolution of Regions of Thickened Continental Crust

by PHILIP C. ENGLAND[1] AND ALAN BRUCE THOMPSON[2]

[1]*Department of Geological Sciences, Harvard University, Cambridge, MA 02138 U.S.A.*
[2]*Institut für Mineralogie und Petrographie, ETH Zürich, CH 8092 Zürich, Switzerland*

(*Received 20 June 1982; in revised form 15 April 1984*)

ABSTRACT

The development of regional metamorphism in areas of thickened continental crust is investigated in terms of the major controls on regional-scale thermal regimes. These are: the total radiogenic heat supply within the thickened crust, the supply of heat from the mantle, the thermal conductivity of the medium and the length and time scales of erosion of the continental crust. The orogenic episode is regarded as consisting of a relatively rapid phase of crustal thickening, during which little temperature change occurs in individual rocks, followed by a lengthier phase of erosion, at the end of which the crust is at its original thickness. The principal features of pressure–temperature–time (*PTt*) paths followed by rocks in this environment are a period of thermal relaxation, during which the temperature rises towards the higher geotherm that would be supported by the thickened crust, followed by a period of cooling as the rock approaches the cold land surface. The temperature increase that occurs is governed by the degree of thickening of the crust, its conductivity and the time that elapses before the rock is exhumed sufficiently to be affected by the proximity of the cold upper boundary. For much of the parameter range considered, the heating phase encompasses a considerable portion of the exhumation (decompression) part of the *PTt* path. In addition to the detailed calculation of *PTt* paths we present an idealized model of the thickening and exhumation process, which may be used to make simple calculations of the amount of heating to be expected during a given thickening and exhumation episode and of the depth at which a rock will start to cool on its ascent path. An important feature of these *PTt* paths is that most of them lie within 50 °C of the maximum temperature attained for one third or more of the total duration of their burial and uplift, and for a geologically plausible range of erosion rates the rocks do not begin to cool until they have completed 20 to 40 per cent of the total uplift they experience. Considerable melting of the continental crust is a likely consequence of thickening of crust with an average continental geotherm. A companion paper discusses these results in the context of attempts to use metamorphic petrology data to give information on tectonic

***Journal of Petrology*,** 1984, **25** (4): 894-928

106

Modelo de England & Thompson (1984)

- Suposições termais
  - temperatura na superfície da Terra é constante
  - o fluxo de calor proveniente do manto é constante
  - produção do calor radiogênico é constante e abaixo de 15 km é zero
  - dentro da crosta a transferência de calor se dá por condução
  - o manto contribui com aproximadamente 50% do calor na crosta continental
- Com essas suposições o modelo gera valores de fluxo de calor dentro do intervalo medido na superficie terrestre (entre 0,045 e 0,075 Wm^{-2})

107

Modelo de England & Thompson (1984)

- Suposições mecânicas:
  - espessamento crustal:
    - ocorre por empurrões e só na crosta
    - é homogêneo e instantâneo
    - é homogêneo em toda a litosfera
  - durante os primeiros 20 Ma não ocorre movimentação vertical no orógeno (não há erosão)
  - denudação ocorre apenas por erosão, a qual é homogênea ao longo do tempo

108

TrajetóriasP-T-t

- O tempo relativo de três processos controla a forma da trajetória *P-T*-t ?
  - duração da colisão
  - duração do re-equilibrio termal da crosta (relaxamento termal)
  - duração da exumação (erosão)
- Trajetória *P-T* horária
- England & Richardson (1977):
  - duração da colisão - estágio mais rápido < 10 Ma
  - relaxamento termal e exumação – dezenas de Ma
  - erosão entre 50 e 200 Ma

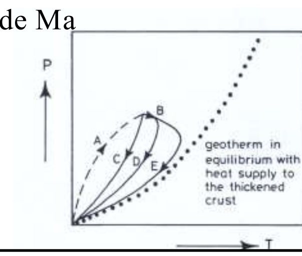

109

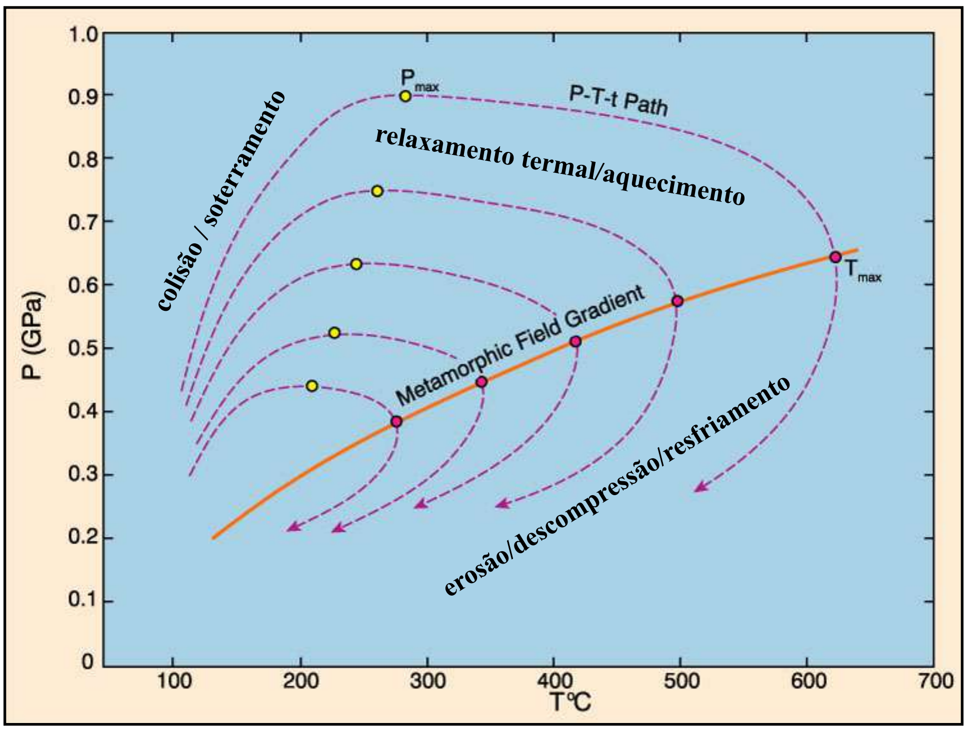

110

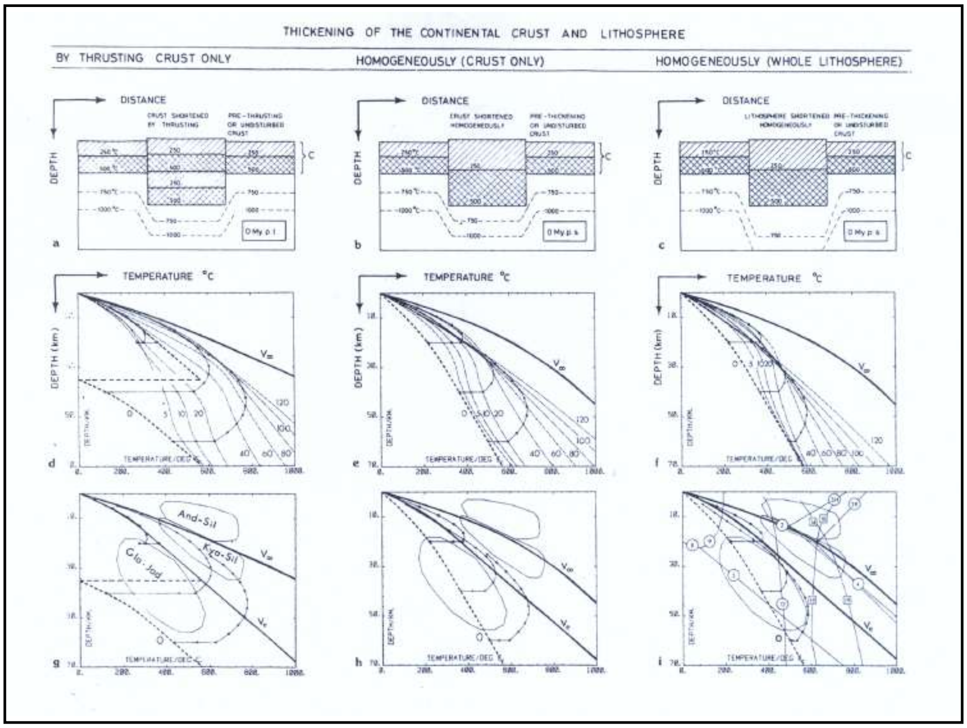
THICKENING OF THE CONTINENTAL CRUST AND LITHOSPHERE
BY THRUSTING CRUST ONLY
HOMOGENEOUSLY (CRUST ONLY)
HOMOGENEOUSLY (WHOLE LITHOSPHERE)
DISTANCE
DEPTH
TEMPERATURE °C
DEPTH (km)
And-Sil
Kya-Sil
Glo-Jad

111

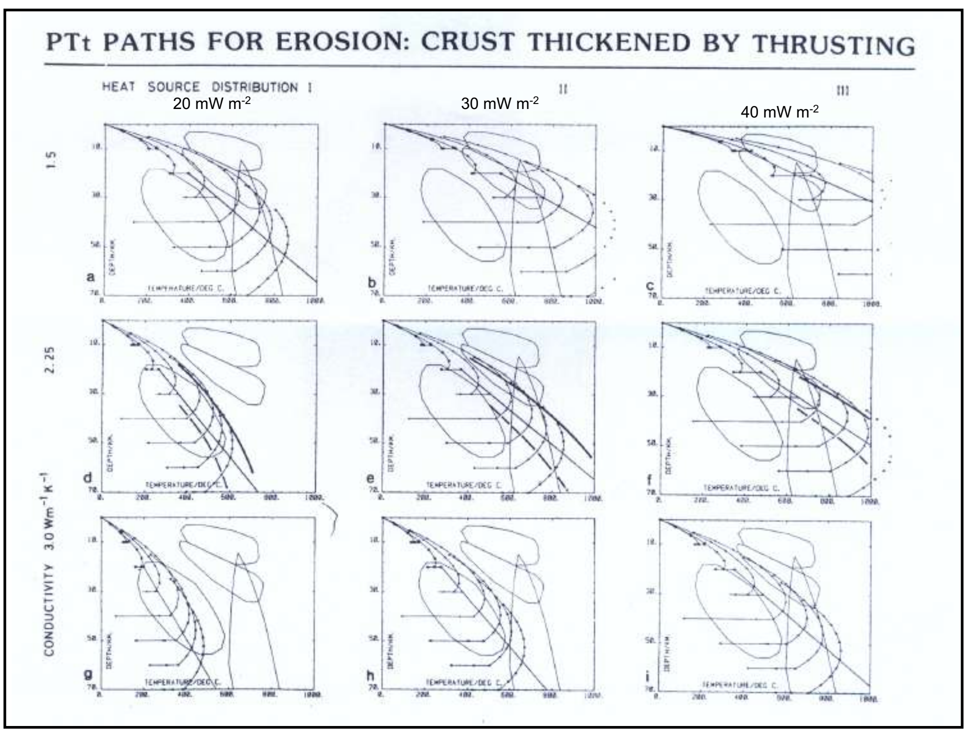
PTt PATHS FOR EROSION: CRUST THICKENED BY THRUSTING
HEAT SOURCE DISTRIBUTION I
II
III
20 mW m-2
30 mW m-2
40 mW m-2
1.5
2.25
CONDUCTIVITY 3.0 Wm-1 K-1
TEMPERATURE/DEG C.

112

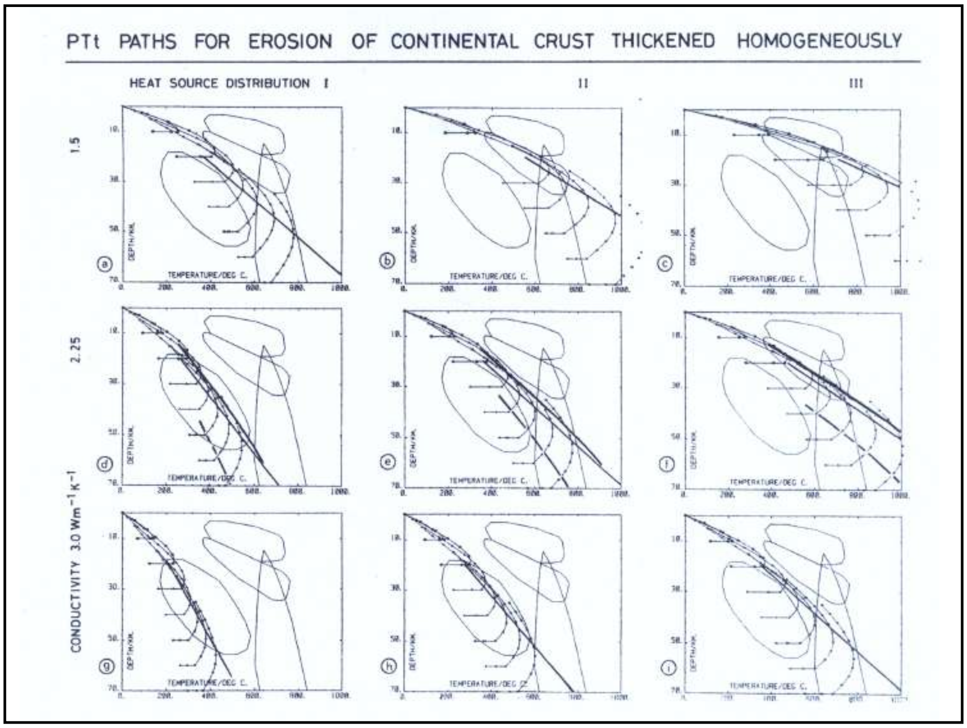
PTt PATHS FOR EROSION OF CONTINENTAL CRUST THICKENED HOMOGENEOUSLY
HEAT SOURCE DISTRIBUTION I
II
III
1.5
2.25
CONDUCTIVITY 3.0 Wm^{-1}K^{-1}
DEPTH/KM.
TEMPERATURE/DEG C.

113

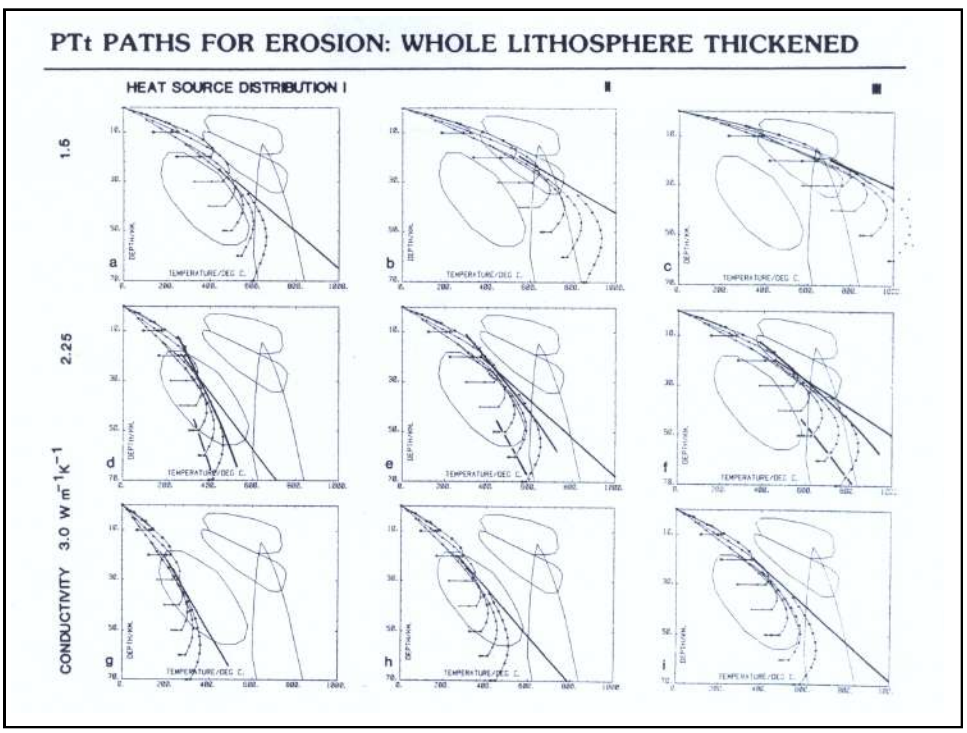
PTt PATHS FOR EROSION: WHOLE LITHOSPHERE THICKENED
HEAT SOURCE DISTRIBUTION I
1.6
2.25
CONDUCTIVITY 3.0 W m^{-1}K^{-1}
DEPTH/KM.
TEMPERATURE/DEG C.

114

Geoterma em cinturões colisionais

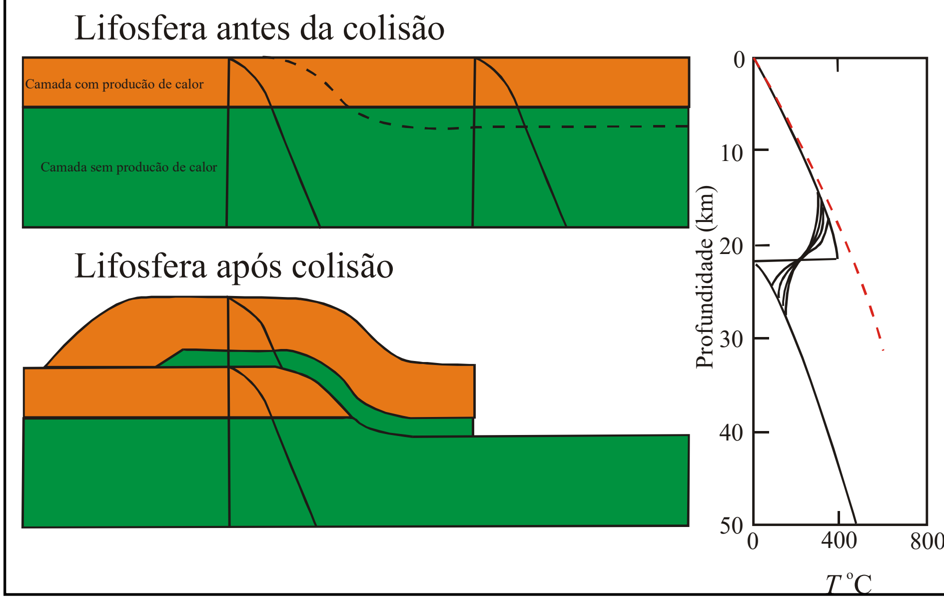

115

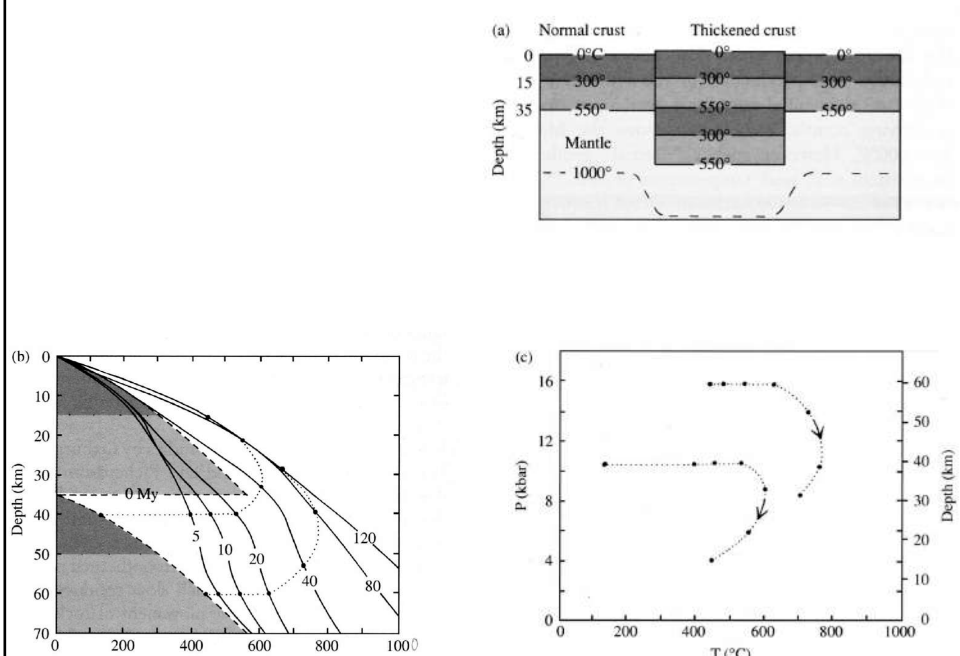

116

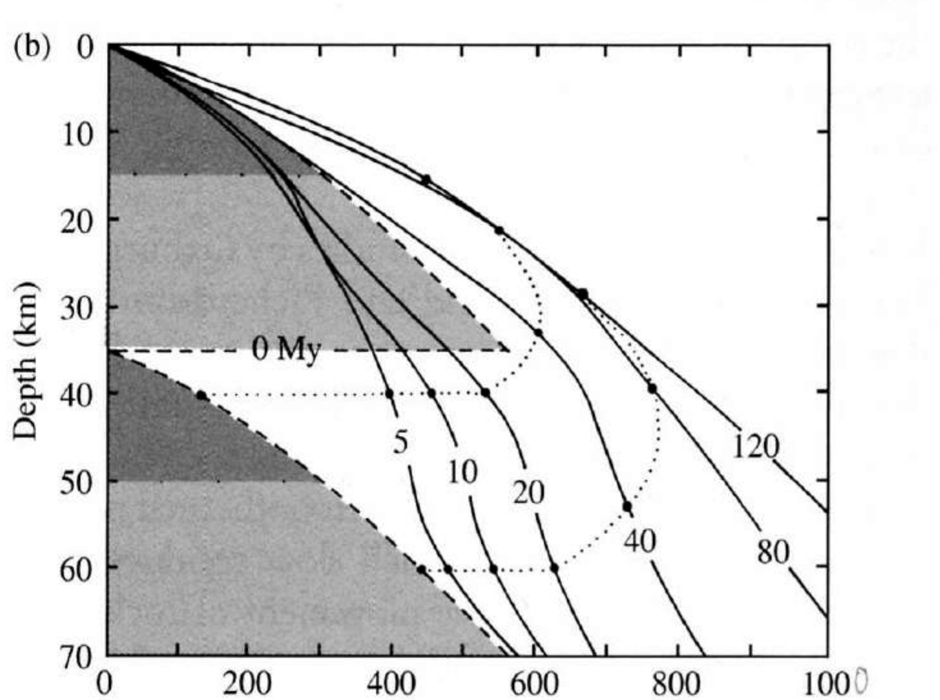

117

Trajetórias *P-T* horárias

- O relaxamento termal aumenta a *T* da rocha enquanto a erosão tende a diminuí-la
- P_{max} antece T_{max}(estágio de alta *P*)
- T_{max} é alcançada durante a descompressão
- Quanto mais rápido acontecer o início da erosão após a colisão, menor vai ser a diferença entre P_{max} e P_{pico} e menor vai ser T_{max}
- O pico termal pós-data o pico da deformação, resultado da colisão

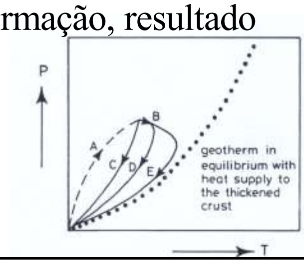

118

Trajetórias *P-T* horárias

- Metamorfismo barroviano (Ky-Sil) ocorre quando baixa condutividade térmica, alto fluxo de calor, baixa erosão (ou super-espessamento) ocorrem
- A pressão do pico metamórfico é entre 50 e 80% da pressão máxima atingida
- Quanto mais rápido for o aquecimento inicial, ou maior for o intervalo de tempo para começar a erosão, maior será a temperatura do pico metamórfico
- O metamorfismo depende da profundidade de soterramento, da taxa de aquecimento e da taxa de erosão

119

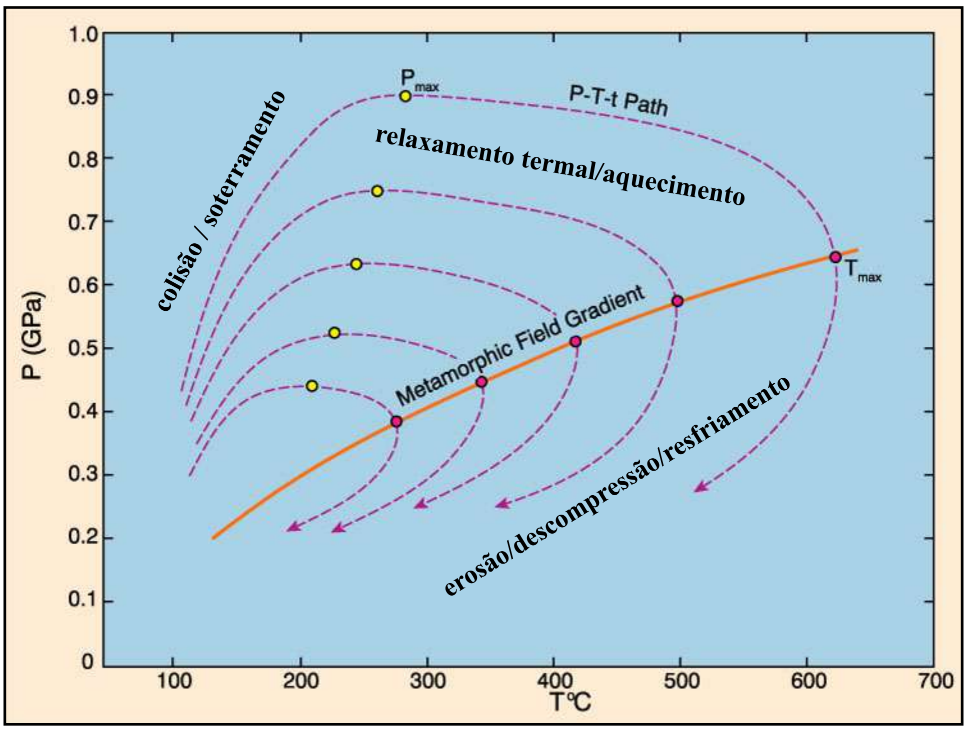

120

gradiente metamórfico de campo indica o tipo de
Série de Fácies (ou tipo bárico) do cinturão metamórfico

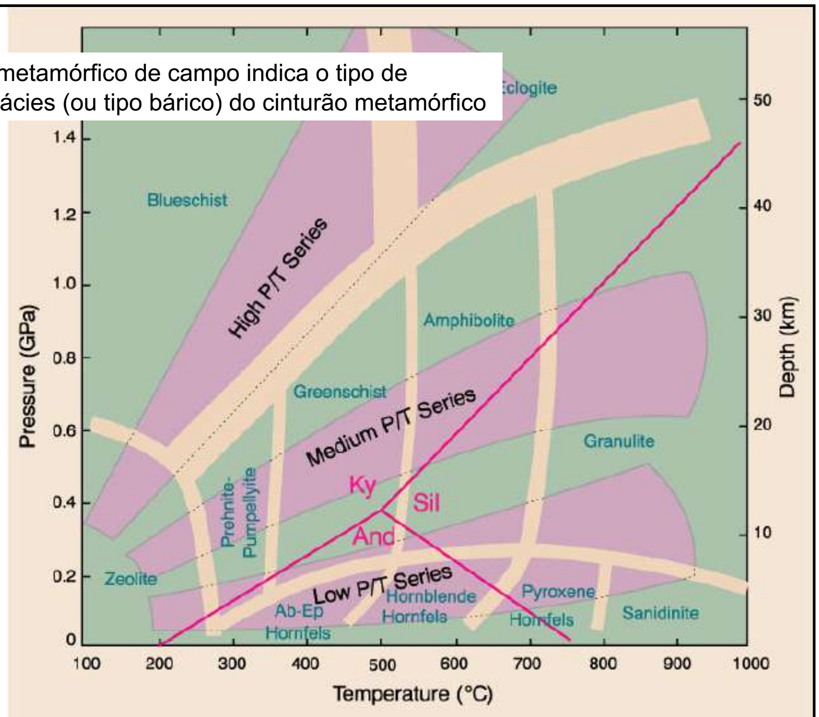

121

Int J Earth Sci (Geol Rundsch)
DOI 10.1007/s00531-016-1436-7

CrossMark

ORIGINAL PAPER

Pseudo- and real-inverted metamorphism caused by the superposition and extrusion of a stack of nappes: a case study of the Southern Brasília Orogen, Brazil

Rafael Gonçalves da Motta[1] **· Renato Moraes**[1]

Received: 4 March 2016 / Accepted: 14 December 2016

Abstract The Southern Brasília Orogen is a Neoproterozoic belt that occurs along the southernmost border of the São Francisco Craton where the Andrelândia Nappe System represents the subducted sedimentary domain and is divided into three allochthonous groups, of which the ages and *P–T* conditions of metamorphism are studied here. The basal unit, the Andrelândia Nappe, exhibits an inverted metamorphic pattern. The base of the structure, composed of staurolite, garnet, biotite, kyanite, quartz, and muscovite, marks the metamorphic peak, whereas at the top, the association of the metamorphic peak does not contain staurolite. The Liberdade Nappe, the middle unit, presents a normal metamorphic pattern; its base, close to the Andrelândia Nappe, shows paragneiss with evidence of in situ partial (622.3 ± 7.6 Ma). The upper unit, the Serra da Natureza Klippe, bears a typical high-pressure granulite mineral assemblage that is composed of kyanite, garnet, K-feldspar, rutile, and leucosome, as well as a metamorphic peak at 604.5 ± 6.1 Ma. This tectonic assembly, with inverted and non-inverted metamorphic patterns and generation of klippen structures, is consistent with exhumation models and a strong indentor located in the lower continental crust.

Keywords Brasília Orogen · High-pressure granulite · Inverted metamorphism · Metamorphic field gradient · Monazite dating · Exhumation model

122

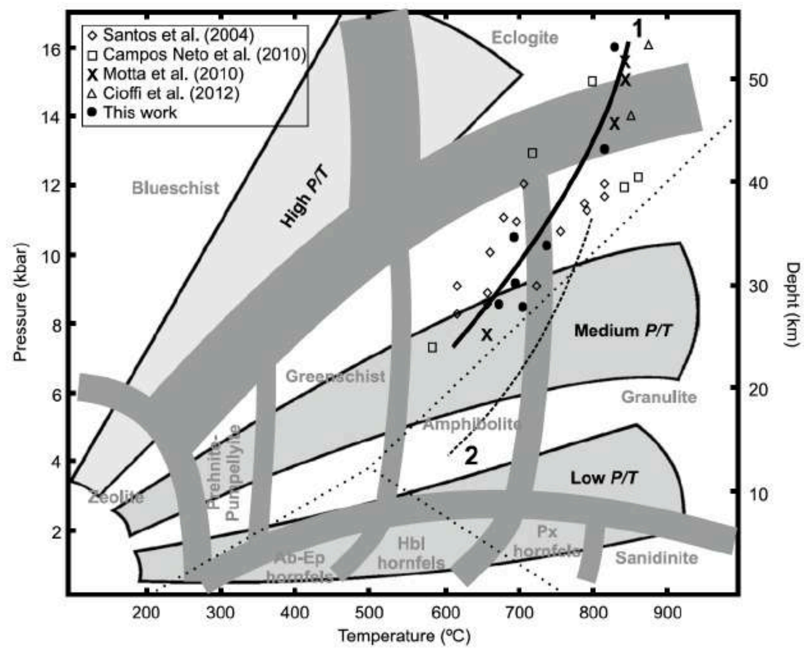

123

Precambrian Research 345 (2020) 105766

Contents lists available at ScienceDirect

Precambrian Research

journal homepage: www.elsevier.com/locate/precamres

ELSEVIER

Tectonic implications of juxtaposed high- and low-pressure metamorphic field gradient rocks in the Turvo-Cajati Formation, Curitiba Terrane, Ribeira Belt, Brazil

Bruna S. Ricardo*, Frederico M. Faleiros, Renato de Moraes, Oswaldo Siga Júnior, Ginaldo A.C. Campanha

Instituto de Geociências, Universidade de São Paulo, Rua do Lago, 562, CEP 05508-080 São Paulo, SP, Brazil

A R T I C L E I N F O

Keywords:
Detrital zircon U–Pb ages
Metamorphic field gradients
Paired metamorphic belts
Pseudosection modeling
Ribeira Belt
Neoproterozoic

A B S T R A C T

The Turvo-Cajati Formation (TCF) is an important unit forming the Curitiba Terrane, a major segment of the southern Ribeira Belt, SE Brazil. It is composed of rocks of greenschist (LTCF), amphibolite (MTCF) and granulite (HTCF) facies conditions. Previous studies in the HTCF indicate that the unit underwent extensive partial melting under high-pressure conditions (670–810 °C and 9.5–12 kbar), within the kyanite stability field. In this paper, a study of the metamorphic zoning within the LTCF and MTCF is undertaken using pseudosection modeling in the NCKFMASHTO and MnNCKFMASHTO model systems coupled with detrital zircon U–Pb geochronology. Four metamorphic zones are recognized for the LTCF and MTCF: biotite, garnet, staurolite and sillimanite zones, with predominance of sillimanite zone and pressures lower than 8 kbar, as staurolite breaks down straight to sillimanite, without formation of a kyanite zone. Pseudosections yielded metamorphic peak conditions of ~530–560 °C and ~6–7.5 kbar (garnet zone) and ~660–690 °C and ~6–7.5 kbar (sillimanite zone). The metamorphic field gradient is flat and of low to medium pressure, below the typical Barrovian-type baric regime, and different from the HTCF. Available petrological and geochronological data suggest that the TCF comprises a paired low-*P* and high-*P* metamorphic belt, associated with a major Ediacaran suture zone in the southern Ribeira Belt. Probability density plots from detrital zircon U–Pb ages indicate late-Cryogenian-Ediacaran arc-related and Rhyacian sources for all TCF sub-units. This scenario suggests that the TCF is made up of a collisional juxtaposition of an accretionary wedge (HTCF) and a back-arc basin (LTCF and MTCF) on the border of a microplate, which includes a Rhyacian basement microcontinent, the Atuba Complex. It is inferred the high metamorphic gradient recorded in the LTCF and MTCF was related with asthenospheric upwelling in the back-arc region, which also produced extensive partial melting in the Atuba Complex basement.

124

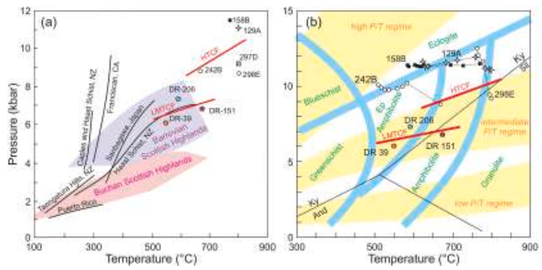

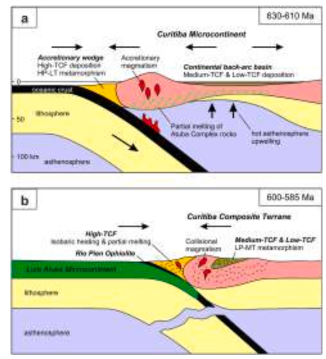

Fig. 15. Proposed model from the Curitiba Terrain evolution, based on TCF detailed study presented in this paper. (a) 630–610 Ma: Stage of subduction in the Curitiba Microcontinent, arc-development in Atuba Complex with partial melting, deposition in LMTCF and deposition followed by metamorphism type high-*P* and low-*T* in HTCF. Asthenospheric mantle upwelling in back-arc. (b) 600–585 Ma: Collision of the Curitiba Microcontinent and Luis Alves Microcontinent. metamorphism type low-*P* medium-*T* in LMTCF and isobaric heating and partial melting in HTCF.

125

Como formar granulitos, aquecer a crosta acima de 900 ° C e exumar a crosta inferior

126

Granulitos

Ambientes Tectônicos e Fontes de **Calor**

127

Ambientes Tectônicos e Fontes de Calor

- Granulitos gravam dois tipos principais de trajetórias *P-T*:
  - IBC – resfriamento isobárico
  - ITD – descompressão isotermal
- Trajetórias ITD são parte de trajetória *P-T* horária, implicando em colisão continental (colapso orogenético?)
- Trajetórias IBC implicam em resfriamento em crosta isostaticamente estável (**não** indicam trajetórias **anti-horárias**)

128

Trajetórias *P-T*

Complexo Anápolis-Itauçu
Complexo Barro Alto
Complexo Niquelândia

Seqüência Andrelândia

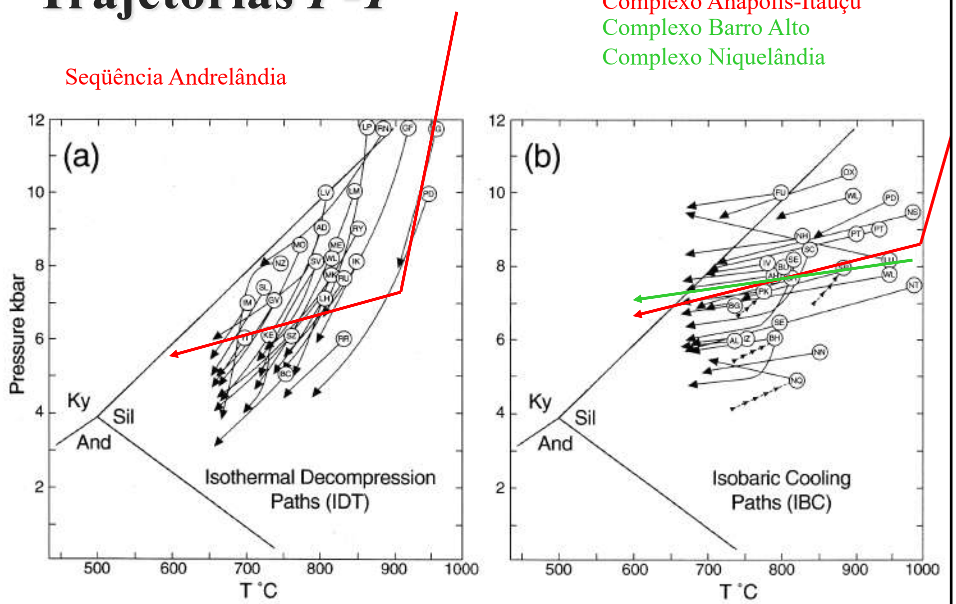

Harley, 1989

129

Origin and evolution of granulites in normal and thickened crusts

D. J. Ellis
Department of Geology, Australian National University
Canberra, ACT, Australia

ABSTRACT

Rocks buried in the upper part of a doubly thickened crust during orogeny can show prograde reactions with transitional features from lower grade rocks up to granulite facies. They can be exposed at the earth's surface within this one orogenic cycle. For example, the granulites exposed in British Columbia have concordant U/Pb zircon ages of 65–85 Ma. In contrast, rocks buried in the lower part of a thickened crust will crystallize granulites that typically show only retrograde relations with younger, lower grade rocks. At the cessation of orogeny, such rocks will undergo near-isobaric cooling from the peak metamorphism and can have very long residence times at the base of a crust of normal thickness. These granulites require a second orogeny to uplift and expose them at the surface. As an example, the Archean granulites of Enderby Land, Antarctica, were metamorphosed at 3070 Ma at 1000 °C at 8–10-kbar pressure. They then followed at least a 400 °C isobaric cooling path. They also had a prolonged residence time of 2000 m.y. near the base of the crust before uplift.

No doubt a continuum exists between these extremes, but it is proposed that many intermediate- and high-pressure granulites form in the lower parts of thickened crust and therefore require a two-stage cycle of tectonism to be uplifted and exposed at the earth's surface. Although most granulites probably form in thickened crust at active plate margins, underplating of normal (30–40-km thickness) crust by mantle melts during extension can also produce granulites. These granulites would also undergo isobaric cooling and require a later orogeny to expose them. An example is the Paleozoic Lachlan Fold Belt of eastern Australia, which has undergone only minor uplift since the major ultrametamorphism at about 400 Ma. However, isotopic, petrologic, and geochemical differences are to be expected between these extremes of granulite formation.

It is apparent from these observations that metamorphic rocks formed during an episode of tectonic or magmatic thickening of the crust can be exhumed by isostatic rebound during a single orogenic event. Furthermore, the minerals in such rocks can record depths of equilibration of 20–30 km and still be underlain by a similar, normal thickness of stable continental crust. This is commonly assumed to be the case for many Archean terranes and is probably true for many low-grade (greenschist-amphibolite) terranes. Windley (1981) listed examples of Phanerozoic granulites that have formed and have been uplifted in the one orogenic event.

The effects of uplift and erosion toward the end of the period of evolution of Archean structures are recorded by the occurrence of Late Archean or earliest Proterozoic cratonic cover formations resting unconformably on granites or metamorphic basement, the ages of which show that, in some instances at least, uplift had taken place within a few hundred million years of tectonic activity in the basement (Watson, 1976). In general, such basement consists of regional low-pressure greenschist-amphibolite, as in granite-greenstone terranes. However, I propose here that many granulites resided for very long periods at deep crustal levels before uplift and exposure. Many intermediate- to high-pressure granulites are not unconformably overlain by old cover formations, which could have been removed during later orogenies needed to excavate the underlying granulites.

The active processes of rapid uplift of thickened crust have been used as a model for the formation of many metamorphic series. In particular, many blueschist, greenschist, and amphibolite facies series can be satisfactorily explained by the influence of erosion on the upper half of a doubly thickened crust. In thickened continental crust the principal features of pressure-temperature-time (*P-T-t*) paths followed by rocks after burial are a period of thermal r

GEOLOGY, v. 15, p. 167–170 February 1987

130

Trajetórias *P-T*

Ellis, 1987, Geology

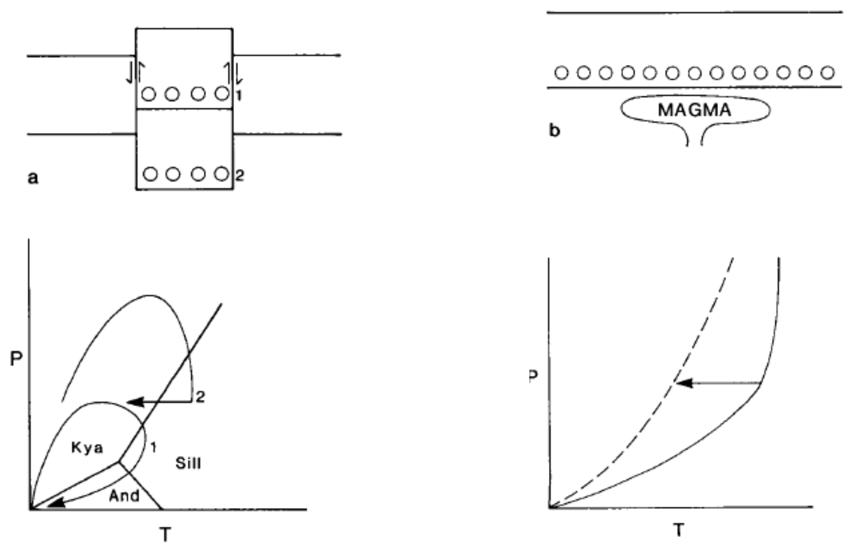

131

Delaminação do manto litosférico

- Colisão com duplicação da crosta
- Raiz mantélica do orógeno se torna muito espessa e instável
- Delaminação do manto litosférico é causada por erosão convectiva da astenosfera ou por gravidade
- Ocorre elevação da topografia

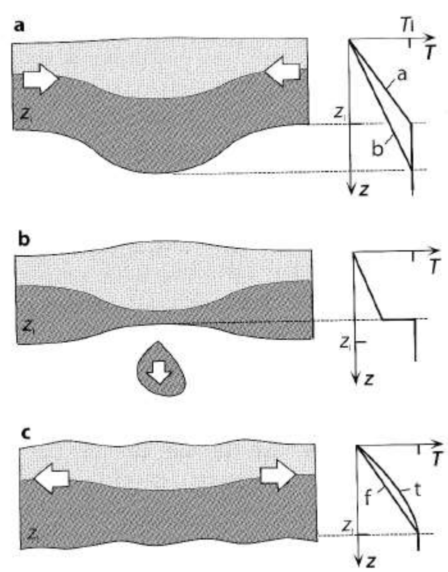

Stüwe (2002)
England (1993)

132

ELSEVIER

Tectonophysics 280 (1997) 171–184

TECTONOPHYSICS

Thermal evolution and exhumation in obliquely convergent (transpressive) orogens

Alan Bruce Thompson [a,*], Karel Schulmann [b], Josef Jezek [c]

[a] Department of Earth Sciences, ETH Zurich, Zurich CH-8092, Switzerland
[b] Department of Petrology and Structural Geology, Faculty of Science, Charles University, Albertov 6, Prague, Czech Republic
[c] Department of Applied Mathematics and Computer Science, Faculty of Science, Charles University, Albertov 6, Prague, Czech Republic

Received 20 March 1996; accepted 6 December 1996

Abstract

Most *P–T–t* path models to date have considered a linear erosion rate for exhumation from burial depth, related to isostatic readjustment of crustal thickness. A few have discussed extension-enhanced exhumation. Erosional exhumation can only restore lower crustal rocks from the thickened mountain root to their previous original depth in the pre-collisional crust. One major assumption of all models to date is that the compressive forces responsible for crustal thickening cease before elevation and erosion begins. However, compression is often still active, even if the crustal thickening has stopped. Further compression of the thickened and strongly deformed orogenic root is responsible for forceful exhumation–extrusion of softened rocks upwards. Hence, the rate of exhumation is related to the rate of convergence of colliding plates. Extrusional exhumation can elevate buried rocks to any depth depending on the action of fault-shear systems. In the extrusional exhamation models examined here, the ascending rocks cool faster because they approach the zero temperature surface conditions more rapidly than by isostatic erosion.The exhumation rate is also governed by the angle between the plate boundary and the displacement vector (α), implying that the convergent plate boundaries are regarded as complex transpressive systems in which the degree of obliquity can be expressed by the ratio of pure to simple shear components. A low ratio of pure/simple shear typical for wrench-dominated plate boundaries, implies long-distance

133

A.B. Thompson et al. / Tectonophysics 280 (1997) 171–184

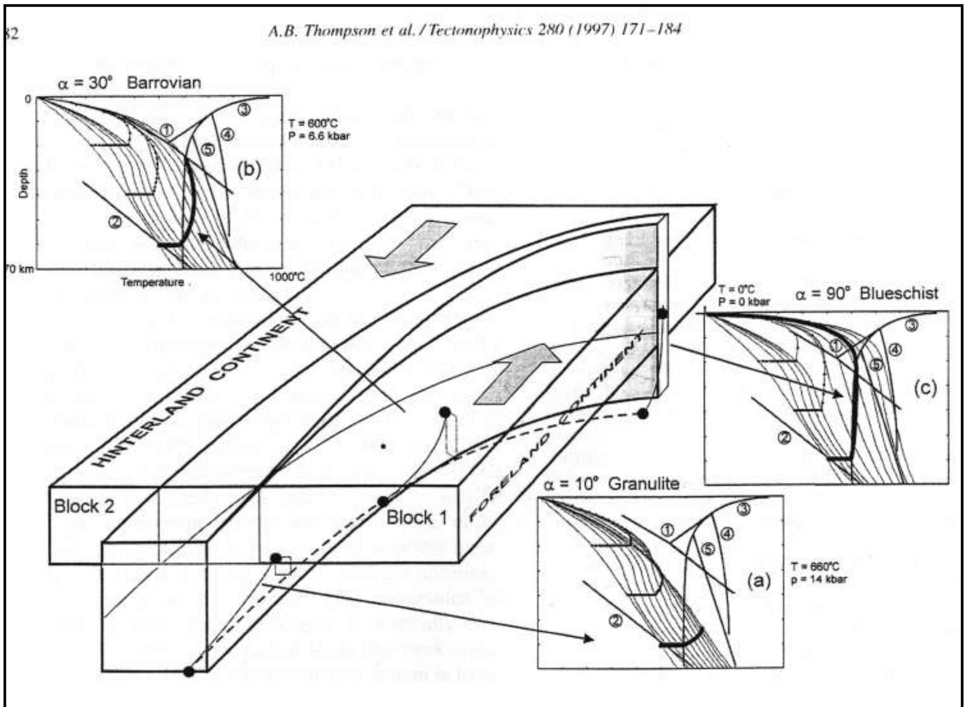

134

Subduction zone backarcs, mobile belts, and orogenic heat

Roy D. Hyndman, *Pacific Geoscience Centre, Geological Survey of Canada, P.O. Box 6000, Sidney, British Columbia V8L4B2, Canada,* and *School of Earth and Ocean Sciences, University of Victoria, Victoria, British Columbia V8W3P6, Canada, rhyndman@nrcan.gc.ca;* **Claire A. Currie,** *School of Earth and Ocean Sciences, University of Victoria, Victoria, British Columbia V8W3P6, Canada;* and **Stephane P. Mazzotti,** *Pacific Geoscience Centre, Geological Survey of Canada, P.O. Box 6000, Sidney, British Columbia V8L4B2, Canada*

ABSTRACT

Two important problems of continental tectonics may be resolved by recognizing that most subduction zone backarcs have hot, thin, and weak lithospheres over considerable widths. These are (1) the origin of long-lived active "mobile belts" contrasted to the stability of cratons and platforms, and (2) the origin ... hot backarc lithosphere, not from the orogenic deformation process itself.

INTRODUCTION

The model of plate tectonics with narrow plate boundaries provides an excellent first-order description of global tectonics. Plate tectonics also provides an elegant explanation for orogenic crustal shortening and thickening in

Figure 1. The North America Cordillera mobile belt. The high elevation and complex current tectonics illustrate the hot, weak, backarc lithosphere deformed by variable margin forces.

GSA Today: v. 15, no. 2, doi: 10:1130/1052-5173(2005)015<4:SZBMBA>2.0.CO;2

135

GEOSCIENCE CANADA Volume 42 2015 383

ANDREW HYNES SERIES: TECTONIC PROCESSES

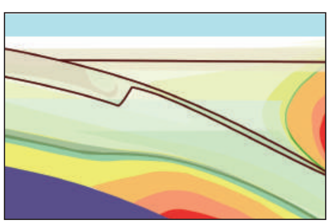

Tectonic Consequences of a Uniformly Hot Backarc and Why is the Cordilleran Mountain Belt High?

R.D. Hyndman

Pacific Geoscience Centre, Geological Survey of Canada and School of Earth and Ocean Sciences
University of Victoria
9860 W. Saanich Road, Sidney
British Columbia, V8L 4B2, Canada
Email: rhyndman@nrcan.gc.ca

concentrated in backarcs; (3) In the Cordillera there is widespread sporadic 'backarc' volcanism; (4) The high temperatures result in very low strength in the lower crust that allows lower-crust detachment; (5) The lower crust weakness facilitates large-scale crustal oroclines that may be independent of the upper mantle; (6) The lower crust in the Cordillera and other backarcs is in amphibolite- to granulite-facies conditions, ~800–900°C at the Moho; (7) In ancient backarcs globally, regional Barrovian metamorphism is concluded to be the result of high temperatures that predate the orogenic collision and deformation. No "heat of orogeny" is required. Following the termination of subduction, backarcs cool with a time constant of 300–500 m.y.

RÉSUMÉ

Pourquoi la chaîne de montagnes de la Cordillère nord-américaine est-elle si haute? On comprend qu'une croûte sur-épaisse puisse expliquer une grande élévation, mais voilà, la croûte de la Cordillère est mince. Il n'existe pas de racine crustale. Or, récemment, une conclusion importante s'est imposée, soit que cette haute élévation s'explique par l'expansion thermique plutôt que par l'existence d'une croûte sur-épaisse. L'élévation de la Cordillère n'est qu'une des conséquences d'une Cordillère uniformément chaude flottant sur une lithosphère mince, caractéristiques communes aux zones d'arrière-arc actuelles ou récentes. Quelques unes des autres conséquences de cette haute température, par opposition aux froids cratons adjacents, comprennent: (1) La Cordillère et d'autres zones d'arrières-arcs sont des zones chaudes et facilement déformables par les forces tectoniques ambiantes, contrairement aux cratons sta-

Geoscience Canada, v. 42, http://www.dx.doi.org/10.12789/geocanj.2015.42.078 pages 383–402

136

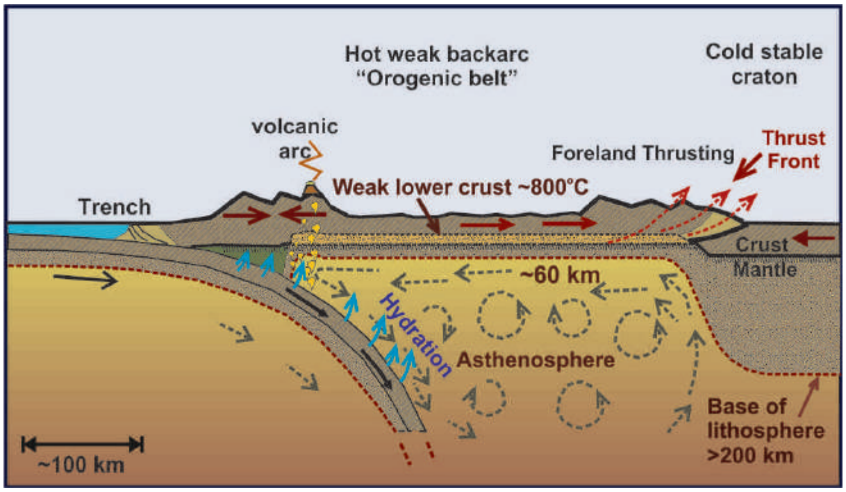

Figure 1. Cross-section of a subduction zone and backarc illustrating the hot and thin lithosphere and the inferred small-scale asthenosphere convection.

137

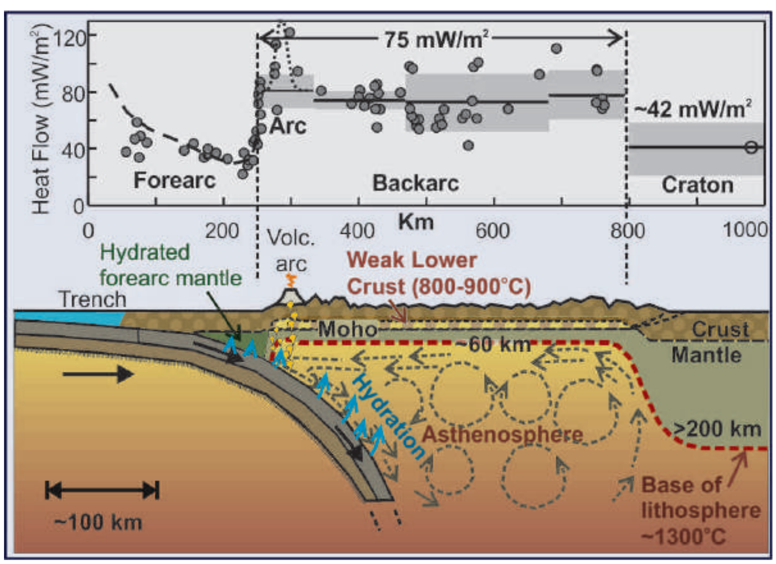

Figure 8. Heat flux data across the southern Canadian Cordillera showing the consistently high values relative to the adjacent craton, (e.g. Lewis et al. 1992). Corrections have been made for variations in upper crust radioactive heat generation that affect surface heat flow but have little effect on deep temperatures.

138

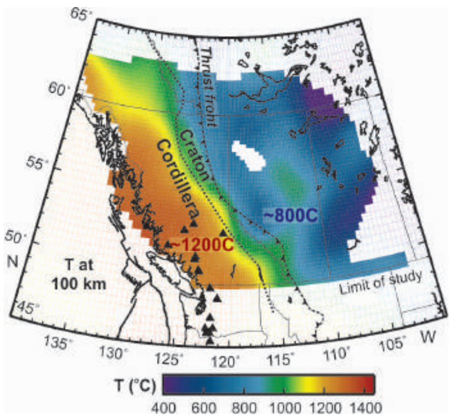

Figure 9. Temperatures at 100 km depth across the southern Canadian Cordillera (about 1200°C) and adjacent craton (about 800°C) estimated from mantle seismic velocities (after Hyndman et al. 2009).

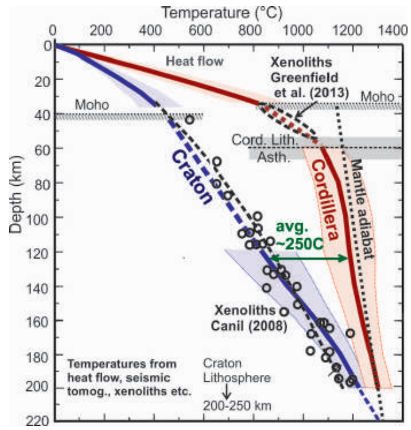

Figure 10. Average temperature-depth profile for the Canadian Cordillera and adjacent craton from heat flow, seismic tomography velocities (red and blue lines; variability, shaded areas), and xenoliths (black circles and dashed lines) (after Hyndman et al. 2009). There is a maximum difference between the Cordillera and the craton of about 400°C at 100 km and an average temperature difference to 220 km of about 250°C.

139

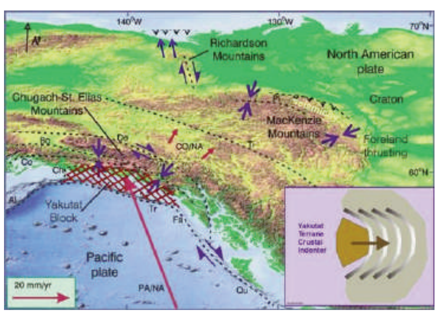

Figure 20. The Yakutat Terrane collision indenter in the Gulf of Alaska that drives the whole Cordilleran upper crust across the Cordillera to the active Mackenzie Mountains fold and thrust belt, and north to the fold and thrust belt of the Mackenzie River Delta (Mazzotti and Hyndman 2002; Leonard et al. 2008).

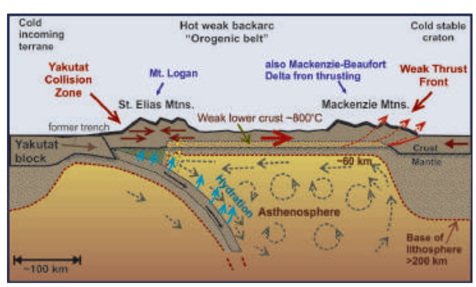

Figure 21. Model cross-section illustrating the current strain transfer across the northern Cordillera from the Yakutat collision zone to the Mackenzie Mountains that are overthrusting the craton (after Mazzotti and Hyndman 2002).

140

References:

Model HT-1:

Jamieson, R.A., Beaumont, C., Medvedev, S. & Nguyen, M.H. (2004) Crustal channel flows: 2. Numerical models with implications for metamorphism in the Himalayan-Tibetan orogen. *Journal of Geophysical Research* **109**, B06406, doi:10.1029/2003JB002811

Model HT-111:

Jamieson, R.A.**,** Beaumont, C. Nguyen, M.H. & Grujic, D. (2006) Provenance of the Greater Himalayan Sequence and associated rocks: Predictions of channel flow models. In"Channel flow, ductile extrusion, and exhumation of lower mid-crust in continental collision zones" (eds RD Law, L Godin, & M.P. Searle), *Geol. Soc. London Special Publication* 268, 165-182.

Model GO-3:

Jamieson, R.A.**,** Beaumont, C., Nguyen, M.H. & Culshaw, N.G. (2007) Synconvergent ductile flow in variable-strength continental crust: Numerical models with application to the western Grenville orogen, Tectonics, 26, TC5005, doi:10.1029/2006TC002036.

141

Model HT-1: Basic channel flow model

final conditions: t = 0 Ma (54 My elapsed model time)

MCT = base of extruded channel
STD = top of extruded channel

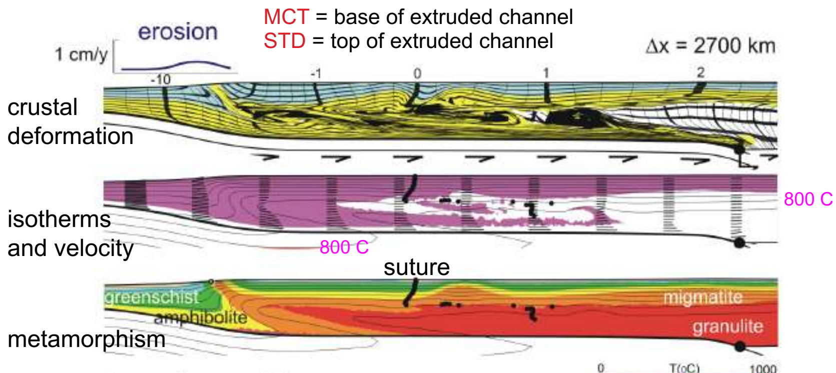

erosion starts: 30 Ma (slope x f(t) x g(x))

channel flow starts: 36-30 Ma

high-grade rocks exhumed: after 20 Ma

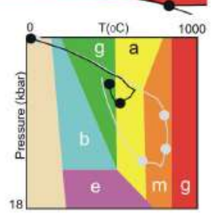

"facies" and P-T paths

142

HT1: *t = 54 Ma – 0 Ma* evolution of crustal deformation

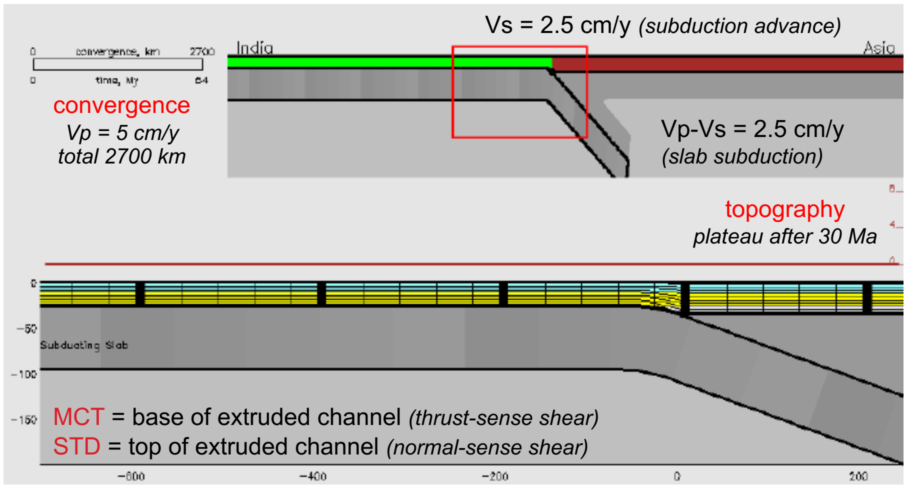

erosion (plateau flank)
starts 30 Ma
declines 15 Ma

channel flow (T ≥ 700°C)
starts 36-30 Ma
exhumed after 15 Ma

143

HT1: *t = 54 Ma – 0 Ma* evolution of metamorphic "facies"

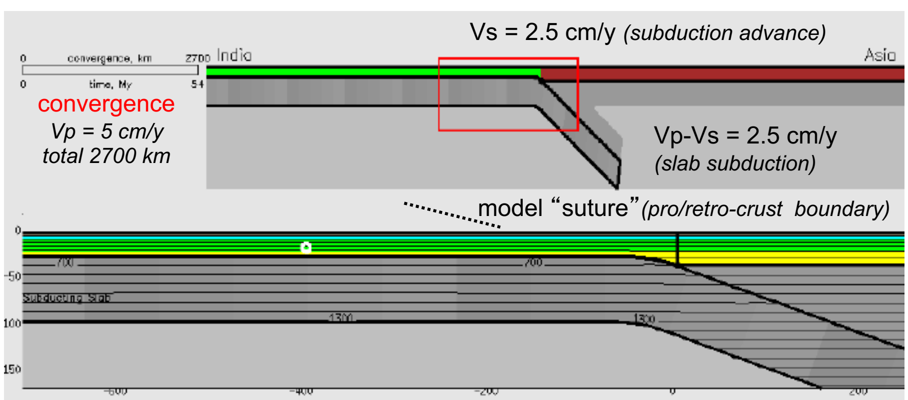

model "facies":
greenschist migmatite
amphibolite granulite
eclogite

Tmax and P@Tmax
(peak grade) at any stage

tracked points:
GHS
LHS
lower crust
P-T-t paths

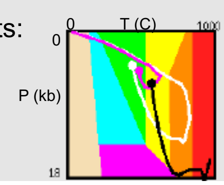

144

Model HT-111: Effect of weak upper crustal layer

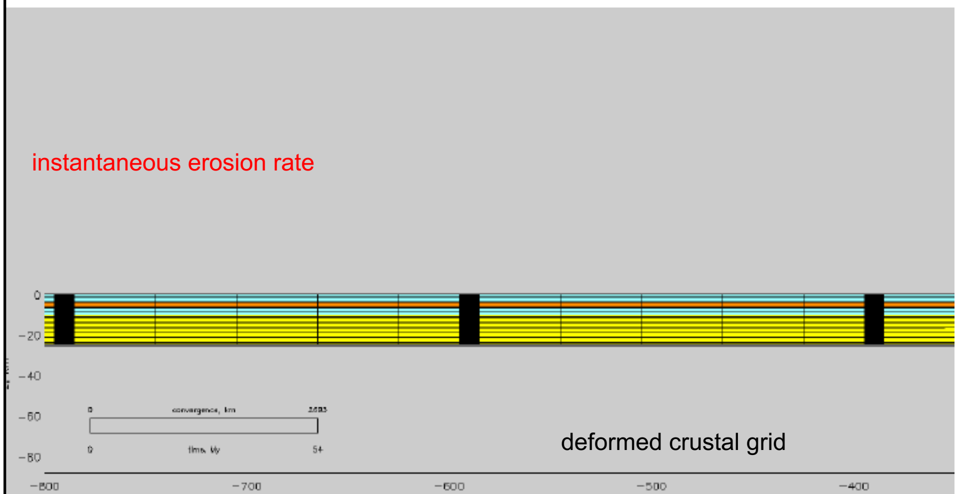

145

Model GO-3: Convergence with variable-strength lower crust

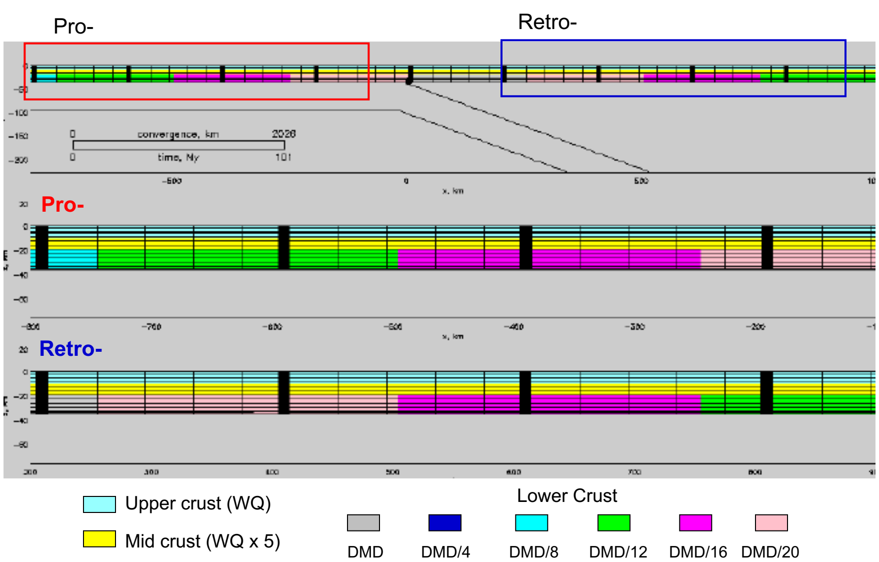

V_P = 2 cm/y V_S = 1 cm/y V_R = 0

146

How Does the Continental Crust Get Really Hot?

Chris Clark[1], Ian C. W. Fitzsimons[1], David Healy[2] and Simon L. Harley[3]

1811-5209/11/0007-0235$2.50 DOI: 10.2113/gselements.7.4.235

There is widespread evidence that ultrahigh temperatures of 900–1000 °C have been generated in the Earth's crust repeatedly in time and space. These temperatures were associated with thickened crust in collisional mountain belts and the production of large volumes of magma. Numerical modelling indicates that a long-lived mountain plateau with high internal concentrations of heat-producing elements and low erosion rates is the most likely setting for such extreme conditions. Preferential thickening of already-hot back-arc basins and mechanical heating by deformation in ductile shear zones might also contribute to elevated temperatures.

Keywords: metamorphism, ultrahigh temperature, heat production, mountain belt, thermal modelling

INTRODUCTION

Evidence for the pressure–temperature (*P–T*) conditions under which Earth's crust has generated large volumes of magma is provided by metamorphic rocks that represent

and pressures of 0.7 to 1.3 GPa. Brown (2006) proposed a revised upper pressure limit equivalent to a *P/T* gradient of 750 °C GPa^{-1}, close to the kyanite–sillimanite reaction boundary (Fig. 1a). The lower temperature limit of 900 °C is somewhat arbitrary, but it places the onset of UHT metamorphism beyond the conditions at which many crustal rocks start to melt, a process that represents a significant barrier to the attainment of higher temperatures.

Recognition of UHT metamorphism is problematic because few rocks develop diagnostic minerals at these conditions and widespread chemical equilibration during cooling makes temperature estimates based on mineral composition unreliable. Although rare

Clark et al., 2011

147

ITD & IBC

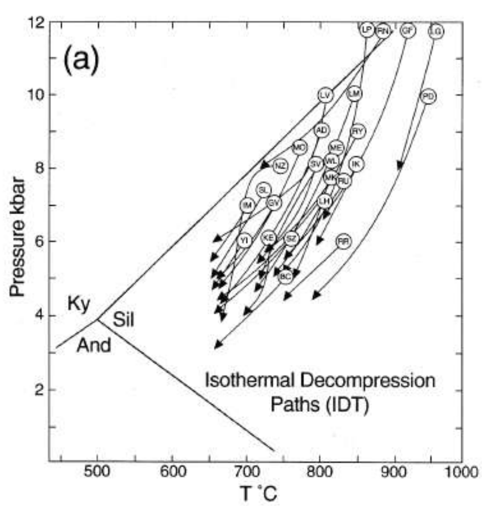

Harley, 1989

148

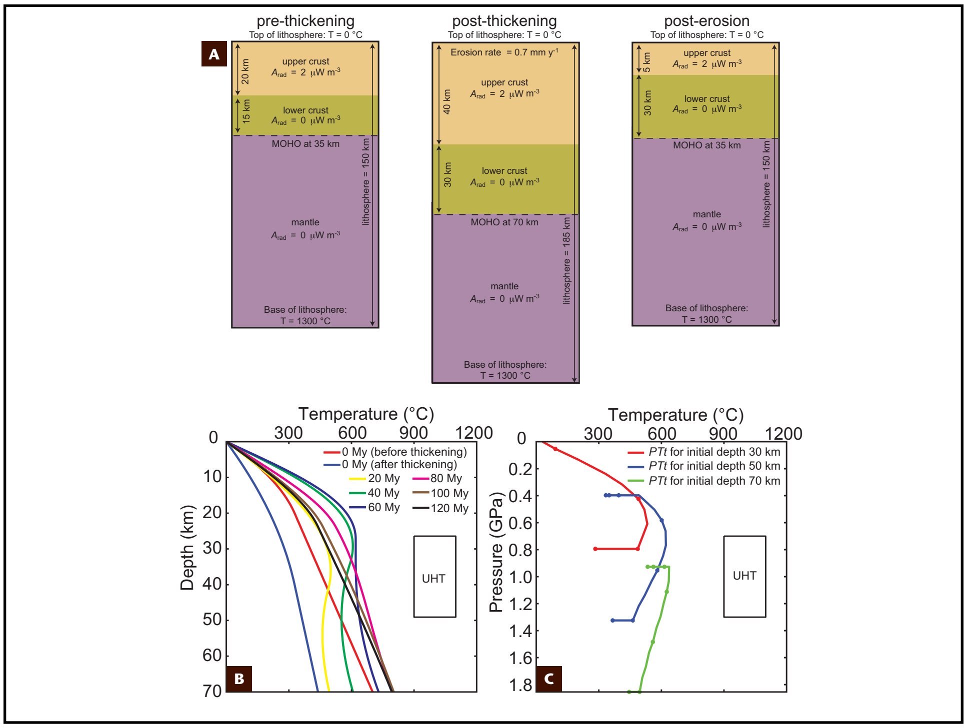

149

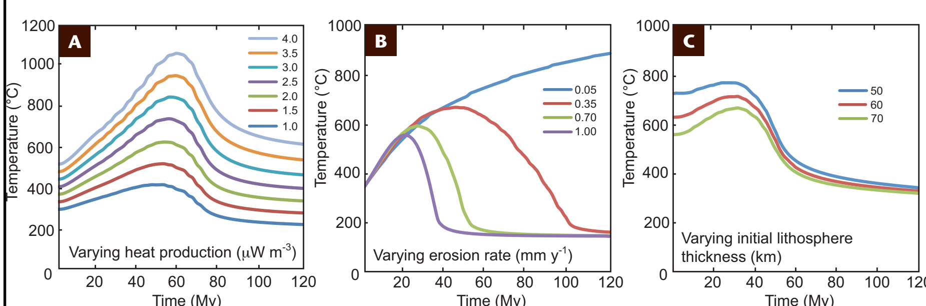

FIGURE 3 (A) T–t evolution of rocks at 40 km depth immediately after thickening for different values of upper crustal A_{rad}. All other parameters are identical to those in FIGURE 2. (B) T–t evolution of rocks at 40 km depth immediately after thickening for different erosion rates starting immediately after thickening. The upper crustal A_{rad} value is 3 μW m^{-3} and other parameters are identical to those in FIGURE 2. (C) T–t evolution of rocks buried to 40 km depth by thickening of a back-arc basin with varying initial lithospheric thickness. The crustal geometry is as in FIGURE 2, but the upper crustal A_{rad} value is 1.5 μW m^{-3} and the total lithospheric thickness is 50, 60 or 70 km. Instantaneous homogenous deformation doubles the thickness of both crust and lithosphere, and is followed immediately by erosion at 0.7 mm y^{-1}.

150

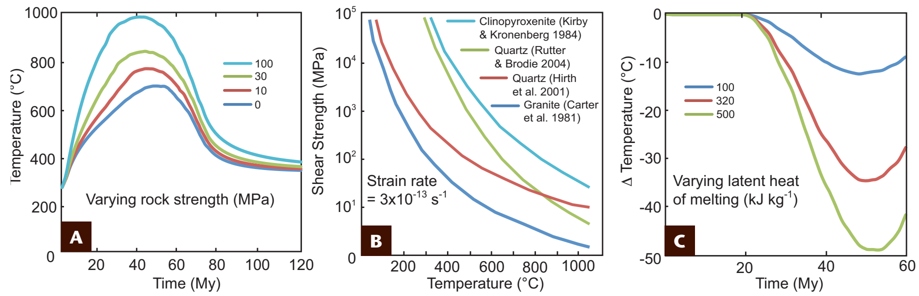

Figure 4 (**A**) T–t evolution of rocks buried to 40 km by instantaneous stacking of one 35 km thick crustal block on top of another along a 3 km wide shear zone that generates heat for four different rock strengths (τ). The initial geometry and A_{rad} values are from Figure 2A. The shear zone is active for 50 My, with a velocity of 3 cm yr^{-1}(shear strain rate = 3×10^{-13} s^{-1}). Values of τ are taken as constant at temperatures below 750 °C, but are set to zero at higher T to simulate melt weakening. Erosion at 0.7 mm y^{-1} starts 20 My after thickening. (**B**) Plot of shear strength against T for different rock types undergoing dislocation creep at a strain rate of 3×10^{-13} s^{-1} (after Nabelek et al. 2010), showing that rock strength decreases markedly on heating. (**C**) T–t evolution of rocks buried to 40 km by homogeneous thickening for three values of latent heat of melting (L). ΔT is the difference between the actual T for a selected value of L and T obtained if $L = 0$. The model set-up is from Figure 2, apart from the upper-crustal A_{rad} value (3.5 µW m^{-3}). We assume that the consumption of L increases linearly with melt fraction over the melting interval, and melt fraction increases linearly with T according to the best-fit line through the experimental data for natural metapelite. Latent heat is also released on cooling in our model, reducing retrograde cooling rates, but this is less realistic given that melt crystallization is not a simple reversal of melting and that some partial melt will escape to higher crustal levels.

151

UHT – de onde vem o calor?

- As fontes de calor não foram entendidas
- As rochas que perderam fundido são mais suscetíveis a alcançarem condições UHT
- Alta concentração de elementos produtores de calor, com colisão continental, fechamento de bacias back-arc ou calor astenosférico são ambientes favoráveis
- Trajetórias ITD ocorrem quando as forças tectônicas de convergência não suportam o potencial gravitacional da cadeia de montanhas

152

Journal of Mineralogical and Petrological Sciences, Volume 111, page 50–72, 2016

A matter of time: The importance of the duration of UHT metamorphism

Simon L. Harley

School of Geosciences, University of Edinburgh, James Hutton Road, Edinburgh EH9 3FE, U.K.

The duration of granulite (G) and ultra-high temperature (UHT) conditions in regional metamorphism is critical to arguments regarding the tectonic settings of granulites and their relationships to Supercontinent assembly. Analysis of zircon geochronology integrated with trace element (REE) constraints on the timing of zircon growth or modification and evidence for metamorphic temperatures from Ti-in-zircon reveals that zircon can form episodically at or near the metamorphic peak in long-lived UHT granulites. This reflects the segregation, transfer and stagnation or trapping of melts which leads to local melt-rock interactions that promotes zircon crystallisation. In contrast, although rutile can retain UHT information in short duration ('fast') G-UHT terrains it is afflicted by Zr loss in long duration ('slow') terrains and yields temperatures significantly lower than those preserved by zircons formed in the same G-UHT events. An assessment of the age-duration evidence from several well-documented G-UHT terrains reveals that most are 'slow', having durations of UHT, Δt_{900}, in the range 30–100 Myr. Some UHT terrains previously considered to be short-lived ($\Delta t_{900} < 10$ Myr) have longer durations of UHT in the light of recent geochronology and hence are also classed as 'slow'. Of the models proposed to account for UHT metamorphism, the 'large hot orogen' (LHO) model for collisional orogeny provides the best setting for the formation of such 'slow' UHT granulites. LHO models can account not only for the *P-T* paths, which can range from UHT with near-isothermal decompression (UHT-ITD) through to decompression-cooling and UHT followed by near-isobaric cooling (UHT-IBC), but also for residence times under UHT conditions. The Napier Complex, the Earth's premier UHT terrain, probably formed as trapped deep crust in the hot underbelly of a late-Archaean LHO. Shorter duration UHT and near-UHT granulites also exist, mostly with Δt_{900} less than 10 Myr. A number of these are likely to have formed as a consequence of severe lithospheric thinning and crustal extension accompanied by voluminous magmatism, which could occur in arc and back-arc settings affected by subduction roll-back or, as advocated by previous workers, continental arcs undergoing extension. However, attaining long-lived UHT conditions in these settings is unlikely unless the crust has inherently high radioactive heat production in addition to the transient heat added during extension and magmatism.

Keywords: Ultrahigh temperature (UHT) metamorphism, U-Pb geochronology, Zircon, Monazite, Large Hot Orogen, Napier Complex

153

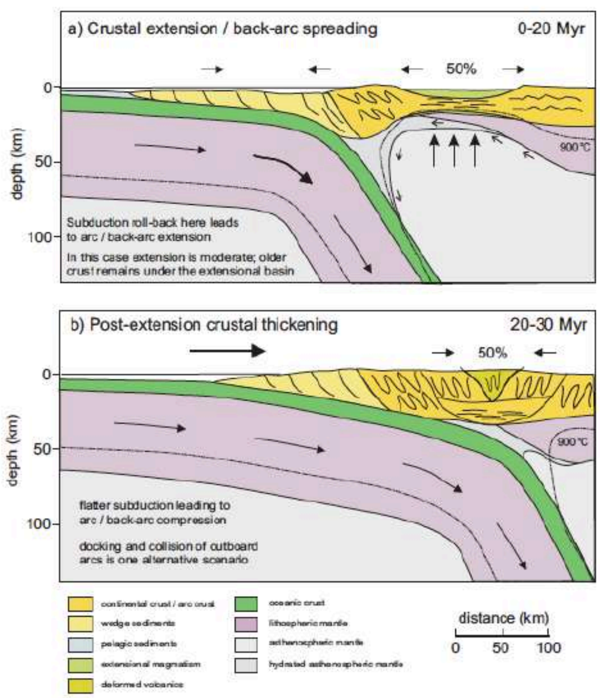

154

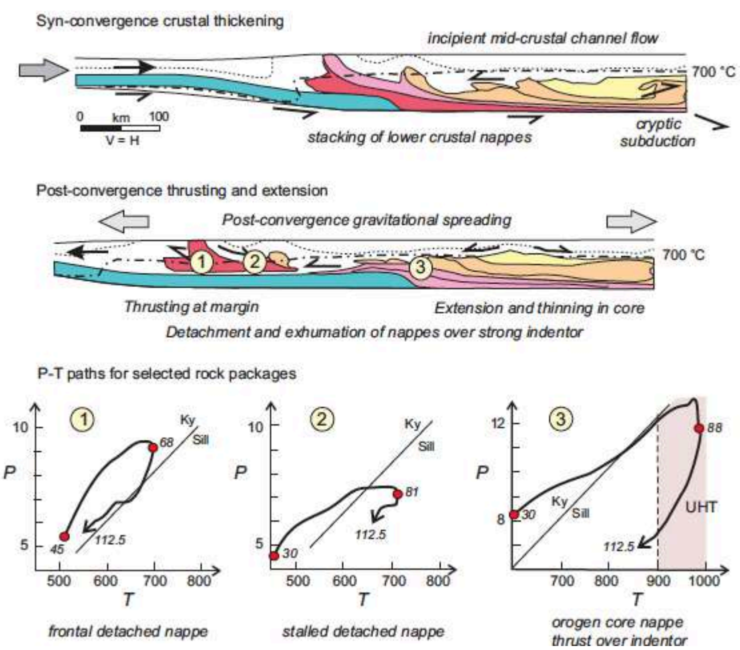
Syn-convergence crustal thickening
incipient mid-crustal channel flow
700 °C
0 km 100
V = H
stacking of lower crustal nappes
cryptic subduction
Post-convergence thrusting and extension
Post-convergence gravitational spreading
700 °C
Thrusting at margin
Extension and thinning in core
Detachment and exhumation of nappes over strong indentor
P-T paths for selected rock packages
frontal detached nappe
stalled detached nappe
orogen core nappe thrust over indentor
Ky
Sill
UHT
P
T

155

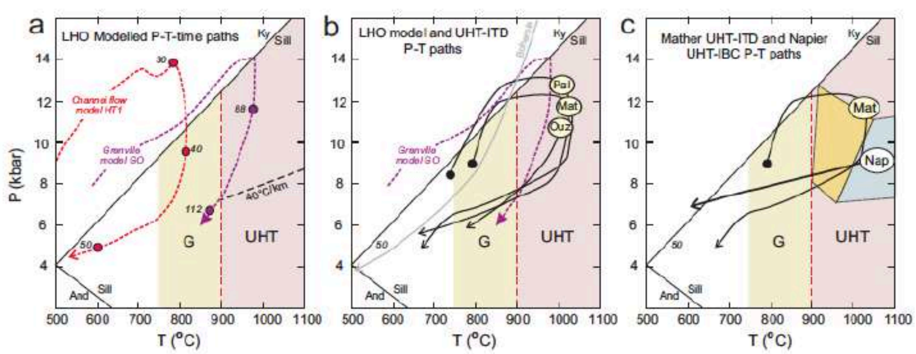
a LHO Modelled P-T-time paths
Channel flow model HT1
Grenville model GO
40°C/km
b LHO model and UHT-ITD P-T paths
Pal
Mat
Ouz
c Mather UHT-ITD and Napier UHT-IBC P-T paths
Nap
G
UHT
Ky
Sill
And
P (kbar)
T (°C)

156

Conclusões

- Metamorfismo em condições da fácies G e G-UHT ocorrem em intervalos de tempo relativamente curtos ~10 My até 30 a 100 My
- Ambientes favoráveis podem ocorrer em bacias tipo *back arc* ou arcos com extensão, envolvendo magmatismo e, nesses casos, não deve ocorrer metamorfismo muito prolongado
- O metamorfismo prolongado deve estar associado à colisão continental em orógenos grandes e super quentes

157

American Mineralogist, Volume 103, pages 181–196, 2018

INVITED CENTENNIAL ARTICLE

Secular change in metamorphism and the onset of global plate tectonics

MICHAEL BROWN[1,*] AND TIM JOHNSON[2]

[1]Laboratory for Crustal Petrology, Department of Geology, University of Maryland, College Park, Maryland 20742, U.S.A.
[2]Department of Applied Geology, The Institute for Geoscience Research (TIGeR), Curtin University, Perth, Western Australia 6845, Australia

ABSTRACT

On the contemporary Earth, distinct plate tectonic settings are characterized by differences in heat flow that are recorded in metamorphic rocks as differences in apparent thermal gradients. In this study we compile thermal gradients [defined as temperature/pressure (*T*/*P*) at the metamorphic peak] and ages of metamorphism (defined as the timing of the metamorphic peak) for 456 localities from the Eoarchean to Cenozoic Eras to test the null hypothesis that thermal gradients of metamorphism through time did not vary outside of the range expected for each of these distinct plate tectonic settings. Based on thermal gradients, metamorphic rocks are classified into three natural groups: high d*T*/d*P* [>775 °C/GPa, mean ~1110 °C/GPa (n = 199) rates], intermediate d*T*/d*P* [775–375 °C/GPa, mean ~575 °C/GPa (n = 127)], and low d*T*/d*P* [<375 °C/GPa, mean ~255 °C/GPa (n = 130)] metamorphism. Plots of *T*, *P*, and *T*/*P* against age demonstrate the widespread occurrence of two contrasting types of metamorphism—high d*T*/d*P* and intermediate d*T*/d*P*—in the rock record by the Neoarchean, the widespread occurrence of low d*T*/d*P* metamorphism in the rock record by the end of the Neoproterozoic, and a maximum in the thermal gradients for high d*T*/d*P* metamorphism during the period 2.3 to 0.85 Ga. These observations falsify the null hypothesis and support the alternative hypothesis that changes in thermal gradients evident in the metamorphic rock record were related to changes in geodynamic regime. Based on the observed secular changes, we postulate that the Earth has evolved through three geodynamic cycles since the Mesoarchean and has just entered a fourth. Cycle I began with the widespread appearance of paired metamorphism in the rock record, which was coeval with the amalgamation of widely dispersed blocks of protocontinental lithosphere into supercratons, and was terminated by the progressive fragmentation of the supercratons into protocontinents during the Siderian–Rhyacian (2.5 to 2.05 Ga). Cycle II commenced with the progressive reamalgamation of these protocontinents into the supercontinent Columbia and extended until the breakup of the supercontinent Rodinia in the Tonian (1.0 to 0.72 Ga). Thermal gradients of high d*T*/d*P* metamorphism rose around 2.3 Ga leading to a thermal maximum in the mid-Mesoproterozoic, reflecting insulation of the mantle beneath the quasi-integral continental lithosphere of Columbia, prior to the geographical reorganization of Columbia into Rodinia. This cycle coincides with the age span of most anorogenic magmatism on Earth and a scarcity of passive margins in the geological record. Intriguingly, the volume of preserved continental crust of Mesoproterozoic age is low relative to the Paleoproterozoic and Neoproterozoic Eras. These features are consistent with a relatively stable association of continental lithosphere between the assembly of Columbia and the breakup of Rodinia. The transition to Cycle III during the Tonian is marked by a steep decline in the thermal gradients of high d*T*/d*P* metamorphism to their lowest value and the appearance of low d*T*/d*P* metamorphism in the rock record. Again, thermal gradients for high d*T*/d*P* metamorphism show a rise to a peak at the end of the Variscides during the formation of Pangea, before another steep decline associated with the breakup of Pangea and the start of a fourth cycle at ca. 0.175 Ga. Although the mechanism by which subduction started and plate boundaries evolved remains uncertain, based on the widespread record of paired metamorphism in the Neoarchean we posit that plate tectonics was established globally during the late Mesoarchean. During the Neoproterozoic there was a change to deep subduction and colder thermal gradients, features characteristic of the modern plate tectonic regime.

Keywords: *P*-*T*-age of metamorphism, thermal gradients, subduction, geodynamic cycles, blueschist, eclogite; Invited Centennial article; Review article

158

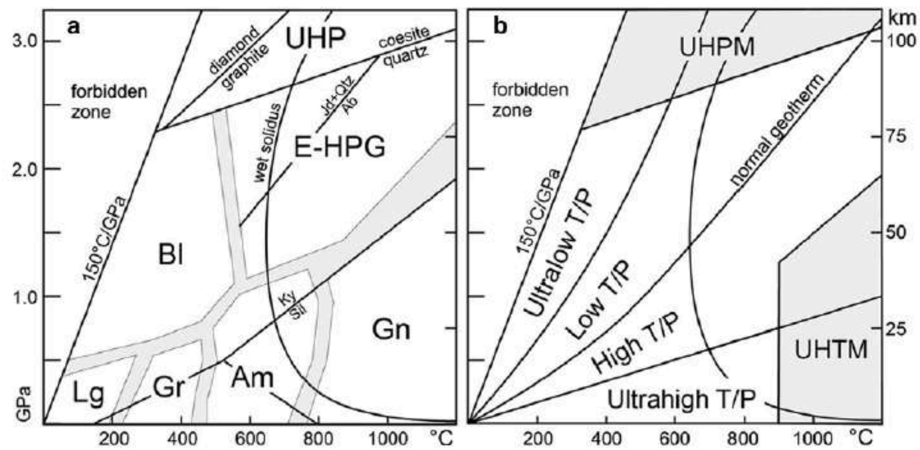

Brown, 2014, GeosciencesFrontiers

159

Gradiente termal (d*T*/d*P*)

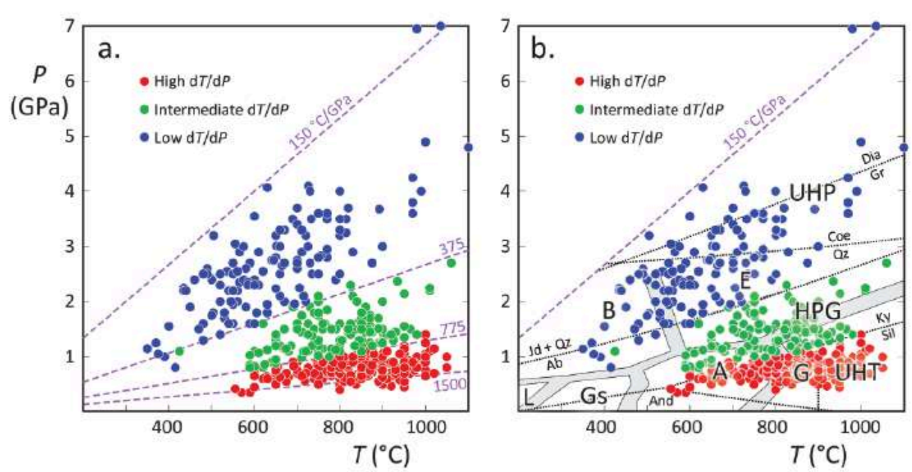

high dT/dP [>775 ° C/GPa, mean ~1110 ° C/GPa (n = 199)
intermediate dT/dP [775–375 ° C/GPa, mean ~575 ° C/GPa (n = 127)]
low dT/dP [<375 ° C/GPa, mean ~255 ° C/GPa (n = 130)]

160

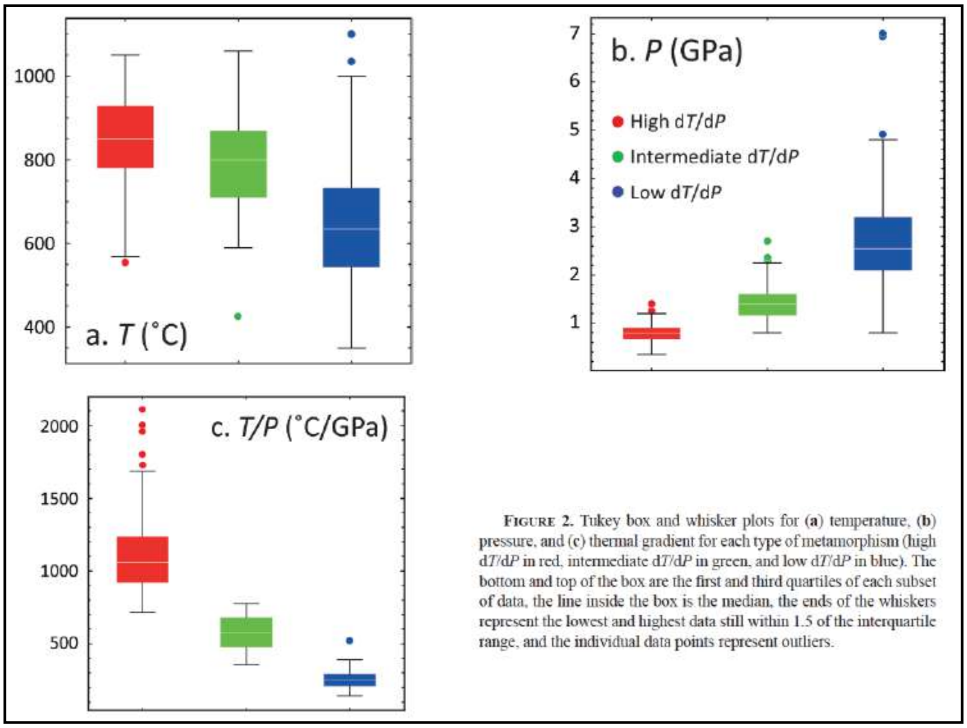

FIGURE 2. Tukey box and whisker plots for (a) temperature, (b) pressure, and (c) thermal gradient for each type of metamorphism (high dT/dP in red, intermediate dT/dP in green, and low dT/dP in blue). The bottom and top of the box are the first and third quartiles of each subset of data, the line inside the box is the median, the ends of the whiskers represent the lowest and highest data still within 1.5 of the interquartile range, and the individual data points represent outliers.

161

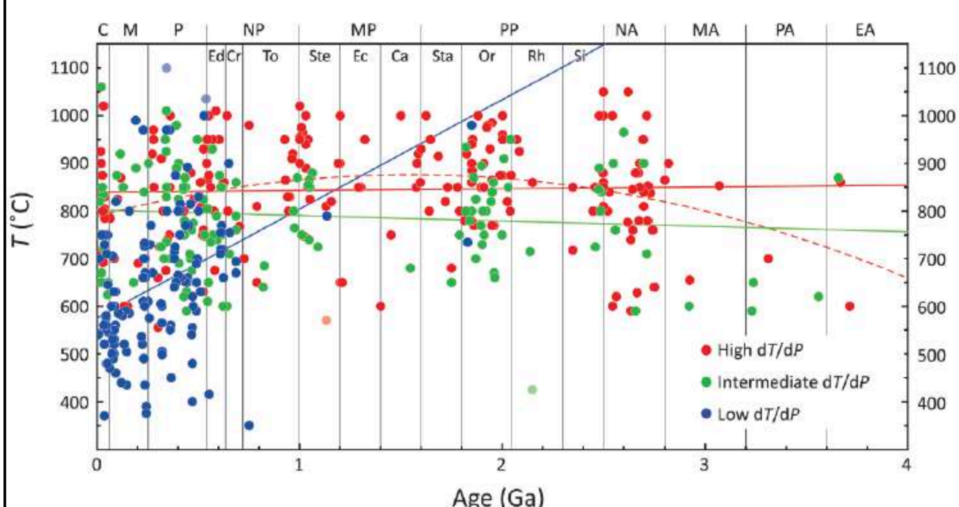

FIGURE 3. Metamorphic temperature for 456 localities (Supplementary Data Table[1]) grouped by type plotted against age. The three types of metamorphism are high dT/dP in red, intermediate dT/dP in green and low dT/dP in blue. The solid lines show linear regressions of the data by type whereas the dashed line shows a second-order polynomial regression for the high dT/dP type (second-order polynomial regressions for the intermediate and low dT/dP types are similar to the linear regressions).

162

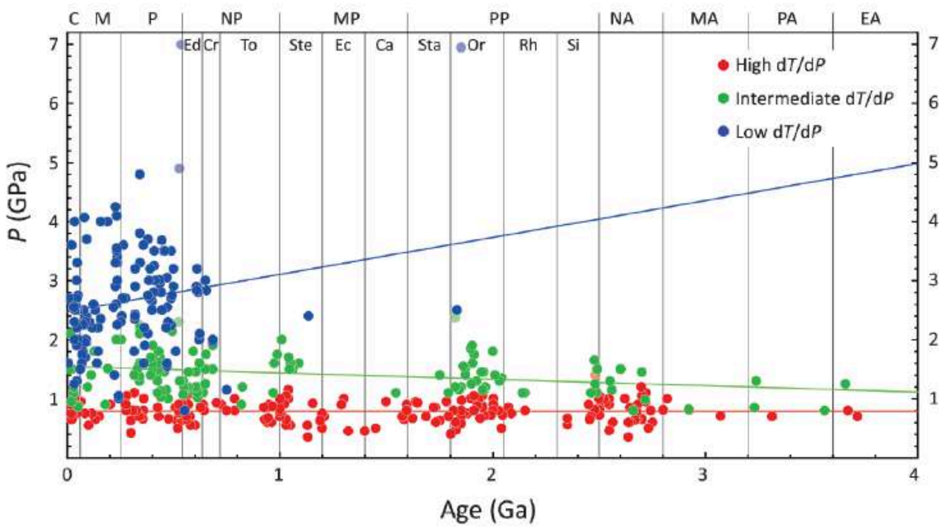

FIGURE 4. Metamorphic pressure for 456 localities (Supplementary Data Table[1]) grouped by type plotted against age. The three types of metamorphism are high d*T*/d*P* in red, intermediate d*T*/d*P* in green, and low d*T*/d*P* in blue. The solid lines show linear regressions of the data by type (second-order polynomial regressions for the three types are similar to the linear regressions).

163

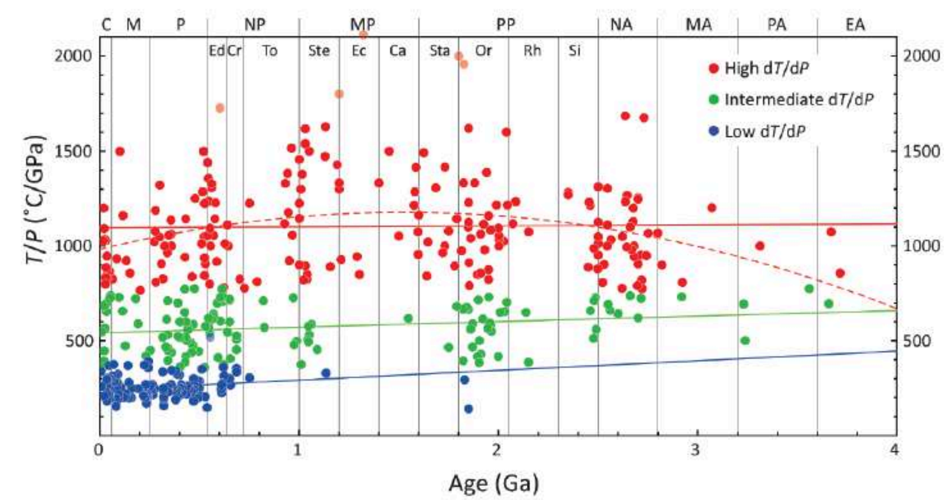

FIGURE 5. Metamorphic thermal gradient (*T*/*P*) for 456 localities (Supplementary Data Table[1]) grouped by type plotted against age. The three types of metamorphism are high d*T*/d*P* in red, intermediate d*T*/d*P* in green, and low d*T*/d*P* in blue. The solid lines show linear regressions of the data by type, whereas the dashed line shows a second-order polynomial regression for the high d*T*/d*P* type (second-order polynomial regressions for the intermediate and low d*T*/d*P* types are similar to the linear regressions).

164

Caledoniano
Variscidis
Altaides
amalgamação da Laurasia e Gondwana para formação do Pangea

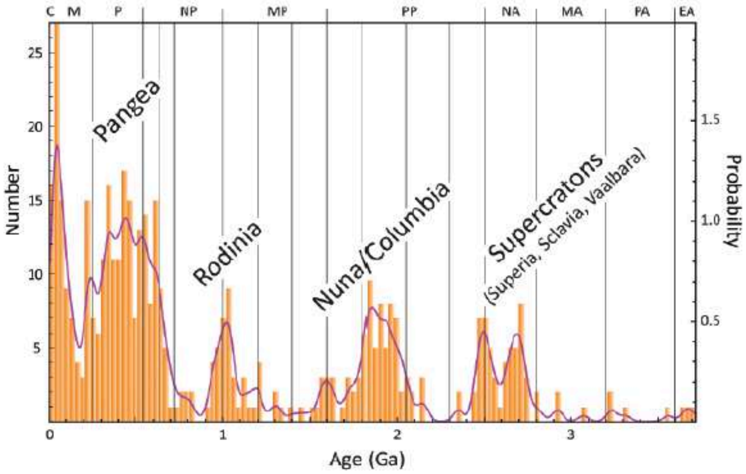

FIGURE 7. Histogram and probability curve for the age of metamorphism for the 456 localities used in this study (Supplementary Data Table[1]).

165

Localização de terrenos UHT

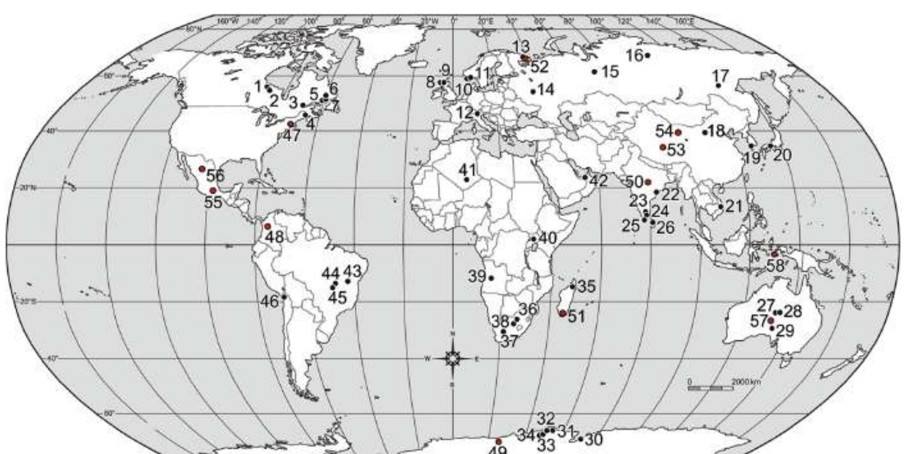

Figure 2. World map of exposed ultrahigh temperature metamorphic rocks (including xenoliths in some cases). The red filled circles denote newly found localities and localities not included in Kelsey (2008). The black filled circles represent localities reported in Kelsey (2008). See Table 1 herein and table 1 in Kelsey (2008) for the studies conducted for each locality.

Kelsey & Hand, 2014

166

Distribuição de idades rochas UHT

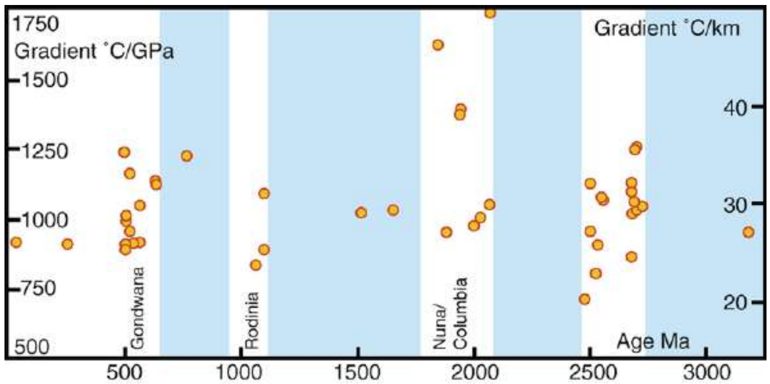

Kelsey 2008

167

Baixa d*T*/d*P*, zonas de subducção e trajetórias *P-T*

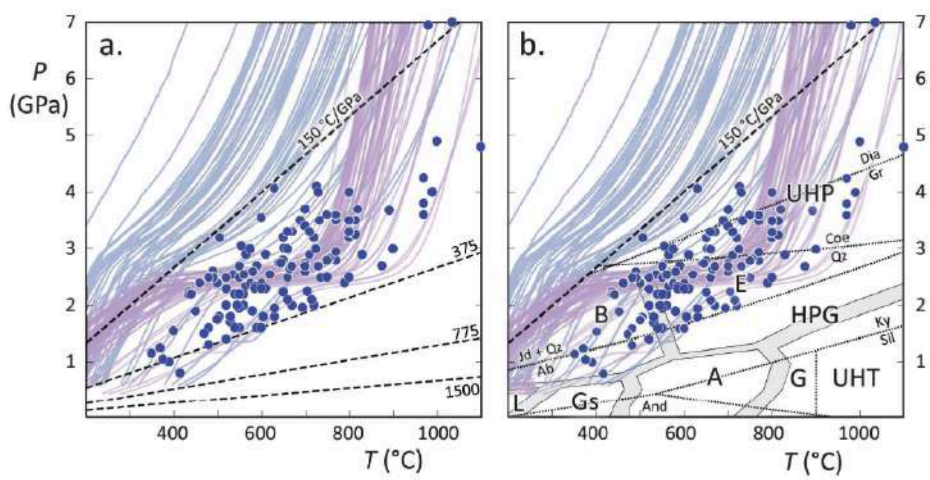

FIGURE 8. *P-T* conditions for low d*T*/d*P* metamorphism compared to subduction zone *P-T* paths for close to the top of the subducting slab (150 m depth; purple) and close to the Moho (6.5 km depth; blue) for active subduction zones (Syracuse et al. 2010; updated by P. van Keken, personal communication 2016). The fields for the four representative thermal gradients (**a**) and the standard metamorphic facies (**b**) are from Figure 1.

168

Idade *vs*. gradiente termal

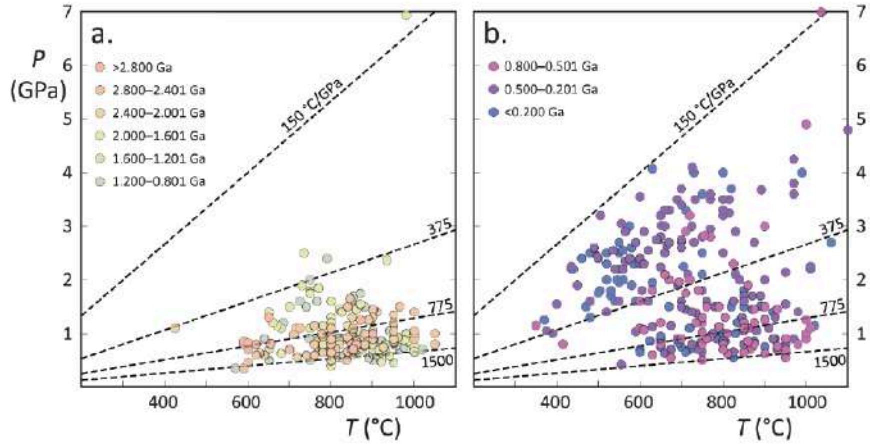

FIGURE 9. *P-T* conditions of metamorphism for 456 localities (Supplementary Data Table[1]) grouped by age. (**a**) >0.800 Ga grouped as follows >2.800, 2.800–2.401, 2.400–2.001, 2.000–1.601, 1.600–1.201, and 1.200–0.801 Ga, and (**b**) <0.800 Ga grouped as follows 0.800–0.501, 0.500–0.201, and <0.200 Ga, with four representative thermal gradients for reference from Figure 1a.

169

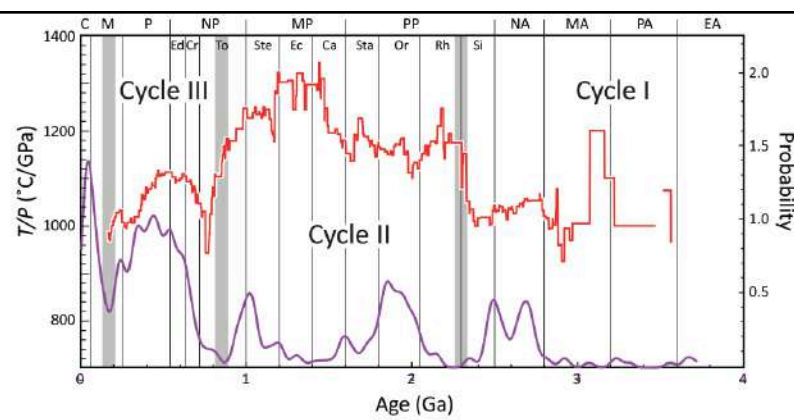

FIGURE 10. Moving mean of the thermal gradient for high d*T*/d*P* metamorphism (from Fig. 6) and probability curve for the age distribution of metamorphism (from Fig. 7). The three cycles are discussed in the text.

Ciclo 1 – começam os 2 tipos contrastantes de metamorfismo
- amalgamação de terrenos litosféricos continentais em supercratons
- manto começa a esfriar e o fluxo de calo total da superfície excede a produção interna de calor

170

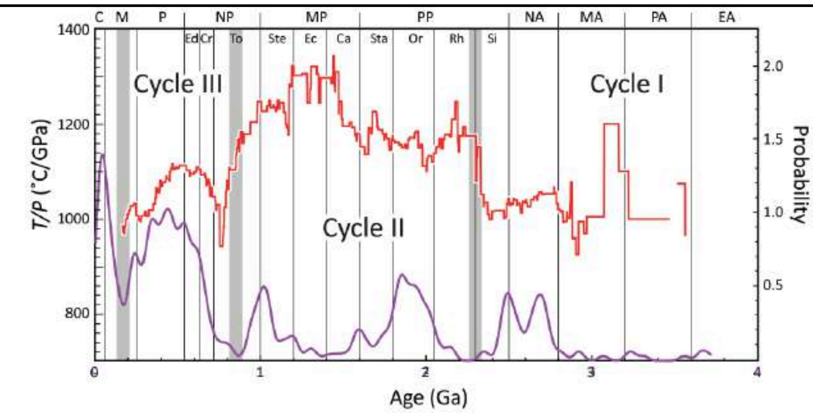

FIGURE 10. Moving mean of the thermal gradient for high dT/dP metamorphism (from Fig. 6) and probability curve for the age distribution of metamorphism (from Fig. 7). The three cycles are discussed in the text.

Ciclo 2 – re-amalgamação dos protocontinentes em supercontinentes (Columbia/Nuna no Paleoproterozoico Médio e depois Rodinia no Toniano)

- gradiente termal alto dT/dP chega ao máximo no Mezoproterozoico
- 1.9 – 1.0 magmatismo anorogênico

171

Rodinia reconstruction

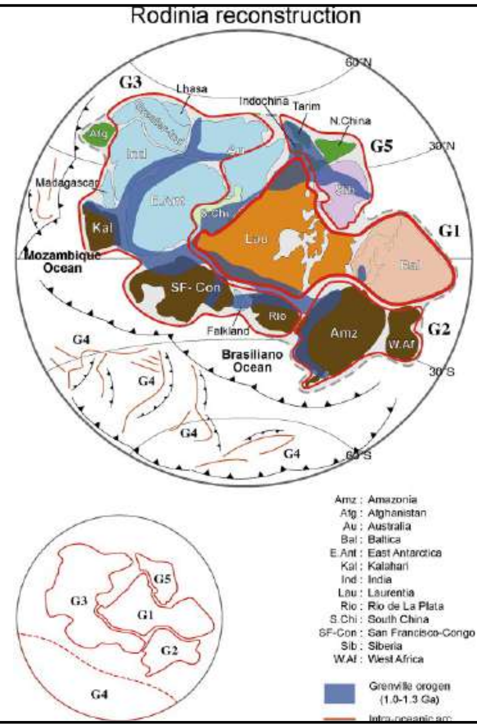

Rino et al., 2008

172

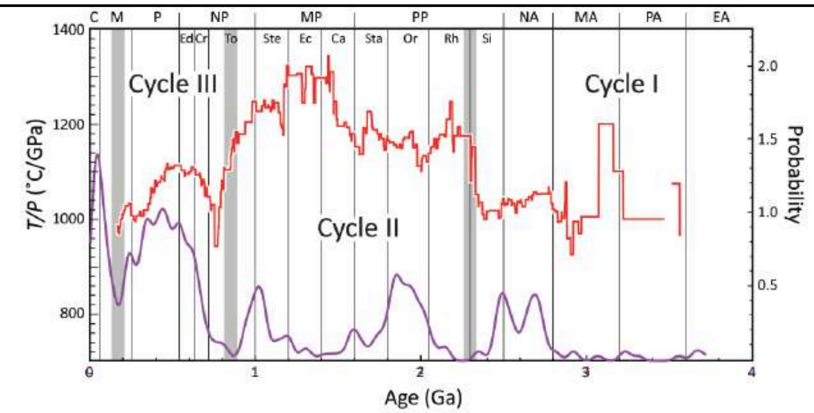

FIGURE 10. Moving mean of the thermal gradient for high d*T*/d*P* metamorphism (from Fig. 6) and probability curve for the age distribution of metamorphism (from Fig. 7). The three cycles are discussed in the text.

Ciclo 3 – os gradientes termais diminuem a partir do Toniano com aparecimento comum de metamorfismo de baixo d*T*/d*P* (xisto azul, eclogito e UHP)

- começo da subducção profunda, com resfriamento do manto

173

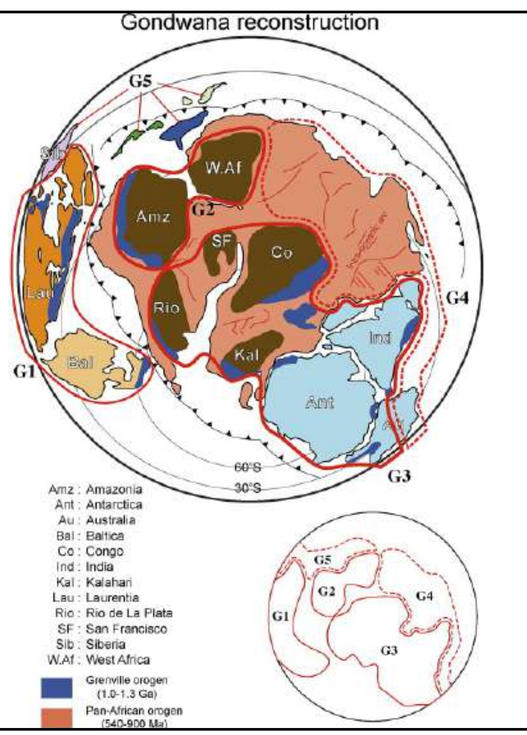

Rino et al., 2008

174

“Paleopangea-Late Neoproterozoic”

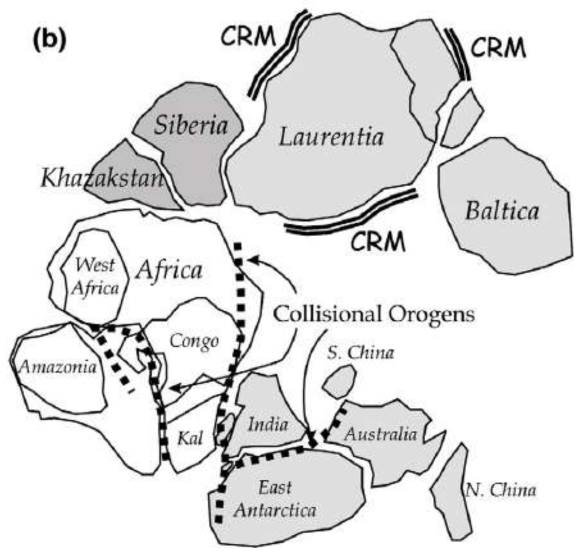

Meert, 2012

175

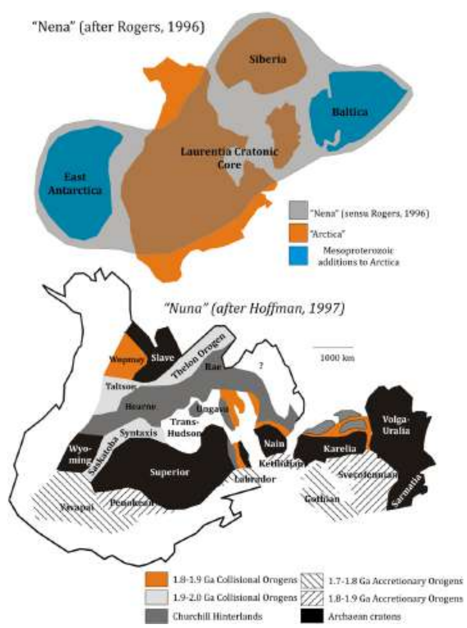

Fig. 5. (a) The “*Nena*” *sensu* Rogers (1996) configuration including Siberia and the Laurentian nuclei (*Arctica* of Rogers, 1996) coupled to Baltica and Antarctica. (b) The “Nuna” configuration of Hoffman (1997) with a tight fit between Baltica and Laurentia. This is equivalent to Gower et al.'s (1990) “*Nena*” reconstruction.

Meert, 2012

176

Referências

Brown , M. & Johnson, T.E. , 2018. Secular change in metamorphism and the onset of global plate tectonics. American Mineralogist, 103 (2): 181–196

Brown, M. 2014, The contribution of metamorphic petrology to understanding lithosphere evolution and geodynamics. Geosciences Frontiers, Volume 5, Issue 4, 553-569.

Chemenda, A., Lallemand, S, Bokun, A. 2000. Strain partitioning and interplate friction in oblique subduction zones: Constraints provided by experimental modeling. JOURNAL OF GEOPHYSICAL RESEARCH, VOL. 105, NO. B3, PAGES 5567-5581

Clark, C.; Fitzsimons, I.C.W.; Healy, D. ; Harley, S.I. 2011. How Does the Continental Crust Get Really Hot? Elements, 7 (4): 235–240.

Ellis, D.J. (1987). Origin and evolution of granulites in normal and thickened crusts. Geology 15, 167-170.

England, P.C. 1994. Convective removal of thermal boundary layer of thickened continental lithosphere: a brief summary of causes and consequences with special reference to the Cenozoic tectonics of the Tibetean Plateau and surrounding regions. Tectonophisics 223, 67-73.

England, P.C. & Richardson, S.W. 1977. The influence of erosion upon the mineral facies of rocks from different metamorphic environments. Journal Geolological Society London, 134: 201 - 213.

England, P.C. & Thompson, A.B. 1984. Pressure-Temperature-time path of regional metamorphism I. Het transfer during evolution of regions of thickened continental crust. Journal of Petrology, 25 (4): 894 - 928.

Hacker, B.R, Abers, G.A. Peacock, S.M. 2003. Subduction factory 1. Theoretical mineralogy, densities, seismic wave speeds, and H2O contents. Journal of Geophysical Research, **108**, NO. B1, 2029, doi:10.1029/2001JB001127

Hacker, B.R., Gerya, T.V. 2013. Paradigms, new and old, for ultrahigh-pressure tectonism. Tectonophysic, 603: 79-88.

Harley, S.L. 2016. A matter of time: The importance of the duration of UHT metamorphism. ournal of Mineralogical and Petrological Sciences,111: 50–72.

Harley, S.L 1989. The origins of granulites: a metamorphic perspective. Geological Magazine, 126 (3): 215 - 247.

Hyndman R.D., Currie C.A., Mazzotti S.P. 2005. Subduction zone backarcs, mobile belts, and orogenic heat. Geological Society of America Today, 15(2):4-10.

Jamieson, R.Amont, C., Medvedev, S. & Nguyen, M.H. (2004) Crustal channel flows: 2. Numerical models with implications for metamorphism in the Himalayan-Tibetan orogen. Journal of Geophysical Research109, B06406, doi:10.1029/2003JB002811

Kelsey, D.E. & Hand, M. 2015. On ultrahigh temperature crustal metamorphism: Phase equilibria, trace element thermometry, bulk composition, heat sources, timescales and tectonic settings. Geoscience Frontiers. 6(3): 311-356.

Meert, J.G. 2012. What's in a name? The Columbia (Paleopangaea/Nuna) supercontinent. Gondwana Research 21: 987–993.

Miyashiro, A. 1961. Evolution of Metamorphic Belts. Journal of Petrology, Vol. 2 , Part 3 , pp. 277-311.

Motta, R. G. & Moraes, R. 2017. Pseudo- and real-inverted metamorphism caused by superposition and extrusion of a stack of nappes: example of the Southern Brasília Orogen, Brazil. *International Journal of Earth Sciences*, 106(7): 2407–2427.

Ricardo, B.S., Faleiros, F.M., **Moraes, R**., Siga Júnior, O., Campanha, G.A.C. 2020. Tectonic implications of juxtaposed high- and low-pressure metamorphic field gradient rocks in the Curitiba Terrane, Ribeira Belt, Brazil. *Precambrian Research. 345: 105766*
https://doi.org/10.1016/j.precamres.2020.105766

Rino, S.,Kon, Y.,Sato, W.,Maruyama, S.,Santosh, M. ,Zhao, D. 2008. The Grenvillian and Pan-African orogens: World's largest orogenies through geologic time, and their implications on the origin of superplume. Gondwana Research 14: 51–72.

Stüwe, K. (2002). Geodynamics of the Lithosphere: An Introduction. Springer.

Thompson, A.B. & England, P.C. 1984. Pressure-Temperature-time paths of regional metamorphism II. Their inference and interpretation using mineral assemblages in metamophic rocks. Journal of Petrology. 25: 929 - 955.

Thompson, A.B., Schulmann, K., Jezek, J. 1997. Thermal Evolution and exhumation in obliquely convergent (transpressive) orogens. Tectonophysics, 280: 171-184.

Turner, F.J. 1981. Metamorphic Petrology - mineralogical, field and tectonic aspects, 2nd ed. McGraw-Hill, Nova York.

177